NASA CR-165, 400

NASA CR-165400
PWA-5594-152

NASA

ENERGY EFFICIENT ENGINE
HIGH-PRESSURE TURBINE SINGLE CRYSTAL VANE
AND BLADE FABRICATION TECHNOLOGY REPORT

by

Dr. Anthony F. Giamei,
Richard W. Salkeld and Charles W. Hayes

UNITED TECHNOLOGIES CORPORATION
Pratt & Whitney Aircraft Group
Commercial Products Division

Prepared for

PRATT & WHITNEY AIRCRAFT GROUP
Commercial Products Division

East Hartford, Connecticut 06108

In response please refer to:
WBG:MEK:1676Q - E1M3
LC-81-99

August 31, 1981

To: National Aeronautics and Space Administration
Lewis Research Center
21000 Brookpark Road
Cleveland, OH 44135

Attention: Mr. Carl C. Ciepluch, Mail Stop 301-4

Subject: Energy Efficient Engine High Pressure Turbine Single Crystal
Vane and Blade Fabrication Technology Report (PWA-5594-152)

Reference: Contract No. NAS3-20646

Enclosures: 20 copies of the subject report

In accordance with the requirements of the referenced contract, we are pleased
to submit 20 copies of the subject report.

Sincerely yours,

UNITED TECHNOLOGIES CORPORATION
Pratt & Whitney Aircraft Group
Commercial Products Division

W.B. Gardner
Program Manager

cc: Administrative Contracting Officer
Air Force Plant Representative Office
Pratt & Whitney Aircraft Group
East Hartford, CT 06108

N81-77512#

1.REPORT NO. NASA CR-165400	2. GOVERNMENT AGENCY	3.RECIPIENT'S CATALOG NO.
4.TITLE AND SUBTITLE Energy Efficient Engine High-Pressure Turbine Single Crystal Vane and Blade Fabrication Technology Report		5. REPORT DATE July 1981
		6. PERFORMING ORG. CODE
7.AUTHOR(S) Dr. Anthony F. Giamei, Richard W. Salkeld, Charles W. Hayes		8. PERFORMING ORG. REPT. NO. PWA-5594-152
9.PERFORMING ORG. NAME AND ADDRESS UNITED TECHNOLOGIES CORPORATION Pratt & Whitney Aircraft Group Commercial Products Division		10. WORK UNIT NO.
		11. CONTRACT OR GRANT NO. NAS3-20646
12. SPONSORING AGENCY NAME AND ADDRESS National Aeronautics and Space Administration Lewis Research Center 21000 Brookpark Road, Cleveland, Ohio 44135		13. TYPE REPT./PERIOD COVERED Contractor Report
		14. SPONSORING AGENCY CODE

16. ABSTRACT

The objective of the High-Pressure Turbine Fabrication Program was to demonstrate the application and feasibility of Pratt & Whitney Aircraft-developed two-piece, single crystal casting and bonding technology on the turbine blade and vane configurations required for the high-pressure turbine in the Energy Efficient Engine.

During the first phase of the program, casting feasibility was demonstrated. Several blade and vane halves were made for the bonding trials, plus solid blades and vanes were successfully cast for materials evaluation tests. Specimens exhibited the required microstructure and chemical composition.

Bonding feasibility was demonstrated in the second phase of the effort. Bonding yields of 75 percent for the vane and 30 percent for the blade were achieved, and methods for improving these yield percentages were identified. A bond process was established for PWA 1480 single crystal material which incorporated a transient liquid phase (TLP®) interlayer. Bond properties were substantiated and sensitivities determined. Tooling die materials were identified, and an advanced differential thermal expansion tooling concept was incorporated into the bond process.

Material evaluation indicated that longitudinal tensile properties met or exceeded yield strength and ultimate tensile strength design minimum levels over a range of temperatures from 593°C (1100°F) to 1093°C (2000°F) so long as the required crystallographic orientation was achieved in the castings. Vane stress-rupture lives were lower than typical PWA 1480 data at all test conditions.

17. KEY WORDS (SUGGESTED BY AUTHOR(S)) Single crystal casting, Single crystal bonding, Transient liquid phase bonding, Single crystal material Energy Efficient Engine	18. DISTRIBUTION STATEMENT Subject to the restriction of Clause 66 of NASA Contract NAS3-20646, "FEDD DATA CLAUSE"

19. SECURITY CLASS THIS (REPT) UNCLASSIFIED	20. SECURITY CLASS THIS (PAGE) UNCLASSIFIED	21. NO. PGS	22. PRICE *

* For sale by the National Technical Information Service, Springfield, VA 22161

N81-77512#

FOREWORD

The Energy Efficient Engine Component Development and Integration Program is
being conducted under parallel National Aeronautics and Space Administration
contracts to Pratt & Whitney Aircraft Group and General Electric Company. The
overall project is under the direction of Mr. Carl C. Ciepluch. Mr. John W.
Schaefer is the NASA Assistant Project Manager for the Pratt & Whitney
Aircraft effort under NASA Contract NAS3-20646, and Mr. Michael Vanco is the
NASA Project Engineer responsible for the portion of the project described in
this report. Mr. William B. Gardner is manager of the Energy Efficient Engine
Project at Pratt & Whitney Aircraft Group.

TABLE OF CONTENTS

LIST OF ILLUSTRATIONS

LIST OF ILLUSTRATIONS (Cont'd.)

LIST OF ILLUSTRATIONS (Cont'd.)

LIST OF TABLES

1.0 SUMMARY

The objective of the High-Pressure Turbine Fabrication Program was to demonstrate the application and feasibility of Pratt & Whitney Aircraft developed two-piece single crystal casting and bonding technology on the turbine blade and vane configurations specifically required by the single-stage high-pressure turbine designed for the Energy Efficient Engine.

A two-phase effort was formulated to achieve this objective. The purpose of the first phase was to demonstrate the feasibility of casting the single crystal, two-piece blade and vane configurations. The purpose of the second phase was to demonstrate the feasibility of transient liquid phase* bonding of these complex two-piece airfoil shapes.

During the casting phase of this effort, casting feasibility was demonstrated and several blade and vane halves were made for the bonding trials. In addition, solid blades and vanes were successfully cast and heat treated for use in the materials evaluation tests. All cast specimens exhibited the required microstructure and chemical composition. Single unit mold technology was found to enhance thermal gradient control and crystal growth while permitting lower mold temperatures, which alleviated internal ceramic breakdown of the mold material. Seeding of the PWA 1480 single crystal material was determined to be necessary in order to assure epitaxial growth and to provide the required primary and secondary crystalline orientation.

During the bonding phase, bonding feasibility was demonstrated and, at the existing state of bonding process refinement, bonding yields of 75 percent for the vane and 30 percent for the blade were shown to be reasonable. Methods for improving on these yield percentages were identified. A bond process was established for PWA 1480 single crystal material which incorporated a transient liquid phase (TLP®) interlayer, 1232°C (2250°F) bond temperature, and full heat treatment after bonding. Bond properties (i.e., stress-rupture, isothermal low cycle fatigue equivalent to parent metal) were substantiated and bond sensitivity to crystallographic misorientation was determined. Bond tooling die materials compatible with casting materials were identified and an advanced differential thermal expansion tooling concept utilizing multi-directional loading was incorporated into the process.

Material evaluation of specimens machined from solid blade and vane castings indicated that blade and vane longitudinal tensile properties met or exceeded yield strength and ultimate tensile strength design minimum levels over a range of temperatures from 593°C (1100°F) to 1093°C (2000°F) so long as the required crystallographic orientation was achieved in the castings. Vane stress-rupture lives were lower than typical PWA 1480 data at all test conditions, but are expected to improve with improved casting quality.

*Transient Liquid Phase is a registered trademark of United Technologies Corporation

2.0 INTRODUCTION

The objective of the National Aeronautics and Space Administration (NASA) Energy Efficient Engine Development and Integration program is to develop, evaluate, and demonstrate the technology for achieving lower installed fuel consumption and lower operating costs in future commercial turbofan engines. NASA has set minimum goals of 12 percent reduction in thrust specific fuel consumption, 5 percent reduction in direct operating cost, and 50 percent reduction in performance degradation for the Energy Efficient Engine (flight engine) relative to the JT9D-7A reference engine. In addition, environmental goals on emissions (the proposed Environmental Protection Agency 1981 regulation) and noise (1978 Federal Aviation Regulation 36 standards) have been established.

The objective of the High-Pressure Turbine Fabrication Program was to demonstrate the feasibility of Pratt & Whitney Aircraft developed two-piece single crystal casting and bonding technology on the turbine blade and vane configurations specifically required by the single-stage high-pressure turbine designed for the Energy Efficient Engine.

This casting and bonding feasibility demonstration program encompassed three major areas: component design, tooling design and fabrication, and actual vane and blade fabrication trials. In the component design effort, specific requirements were applied to the Energy Efficient Engine vane and blade based on company sponsored casting and bonding technology and previous Pratt & Whitney Aircraft two-piece component experience. Secondly, advanced tooling approaches were applied to the Energy Efficient Engine component geometries and tooling was fabricated. Finally, a series of casting and bonding trials were conducted on actual Energy Efficient Engine hardware to establish optimum procedures and demonstrate casting and bonding feasibility. Based on these trials, optimum cast and bond processing conditions and tooling configurations were selected.

The program effort was divided into a casting phase and a bonding phase. The purpose of the casting program was to: (1) evaulate the casting feasibility of single crystal vane and blade configurations required for the Energy Efficient Engine, (2) cast blades and vanes for the bonding trials and document mechanical properties, (3) verify the reproducibility of casting vane and blade geometries and (4) define optimum precast and casting parameters for producing the experimental blades and vanes required.

Concurrent with the casting phase of the program, a joining effort was undertaken to demonstrate the feasibility of bonding the cast vane and blade halves into integral components. The purpose of the bonding program was to (1) evaluate the feasibility of transient liquid phase (TLP®) bonding the Energy Efficient Engine vane and blade configurations, (2) verify the reproducibility of transient liquid phase bonding the Energy Efficient Engine blade and vane component geometries, (3) provide verification of single crystal microstructure at bond joint, and (4) define specific transient liquid phase bonding procedures for the fabrication of these components.

The following sections of this report describe, in detail, the efforts and results associated with the casting and bonding phases of this program. A brief description of the technical challenges posed by the complex blade and vane geometries precedes the program technical effort section.

3.0 TECHNOLOGY CHALLENGE

To meet its performance and cost goals, the Energy Efficient Engine High Pressure Turbine Component comprises a single-stage design with high AN^2, high rim speed, and low C_x/U. It also has fewer blades and vanes relative to current designs and operates in a high temperature environment. These design characteristics result in complex blade and vane geometries and the requirement for advanced single-crystal alloys; both of which are a challenge to the fabrication process. The approach selected to meet this challenge was to cast the blades and vanes in two halves, as shown in Figure 1, using directionally solidified single crystal PWA 1480 material, and then to bond the two halves together.

PARTING LINE
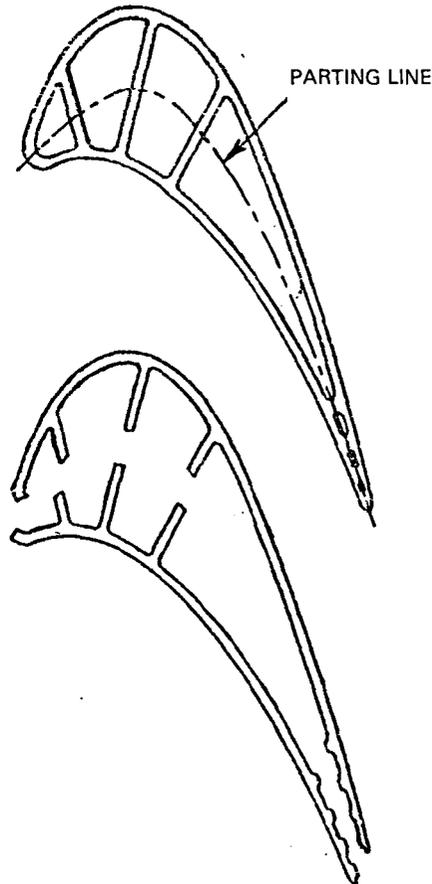
Figure 1   Two-Piece Fabrication Approach for Blades and Vanes

The casting challenges posed by the vane are illustrated in Figure 2. This vane is larger than current designs, having twice the chord and platforms over 50 percent wider. This leads to large cross-sectional area changes which are a challenge to achieving the desired directional solidification. Other challenges are the thin walls, particularly at the trailing edge, the large coolant flow cavities, the large height-to-thickness ratio ribs, the trailing edge with 62.5 percent pedestal blockage, and the small trailing edge angle.

4
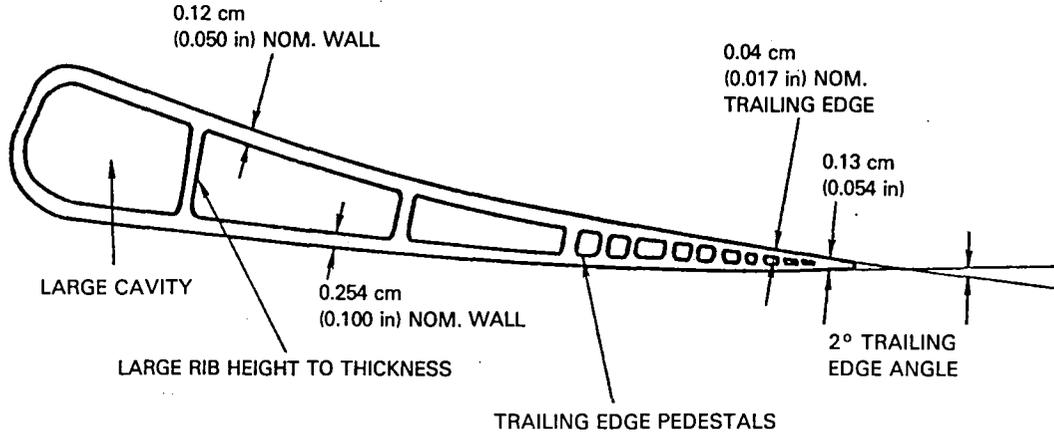
Figure 2   Energy Efficient Engine High-Pressure Turbine Vane Mean Section
Geometry and Attendant Fabrication Challenges

The complexity of the blade design is illustrated in Figure 3. Casting chal-
lenges similar to those for the vane are the thin walls, particularly at the
trailing edge, the large coolant flow cavities, large height-to-thickness
ratio ribs, a trailing edge with 29 percent pedestal blockage, and the small
trailing edge angle. In addition, the blade design is characterized by high
camber, particularly at the root, severe twist from root to tip, high chordal
taper, and a multipass internal cooling air passage with trip strips and turn-
ing vanes. The fabrication challenges here are obvious.

Bonding these complex shapes posed similar challenges. The ideal bond plane
contour is a flat section or simple curve with minimal camber. This was readily
achieved on the Energy Efficient Engine vane by placing the bond plane off the
true leading edge as shown in Figure 4. This simple contour could not be
achieved on the blade because of its severe twist and camber. However, care
was taken to minimize camber in the heavy root section and smooth out the
transition between the airfoil and root. The transition on the leading edge
side was reduced to some degree by locating the bond plane away from the true
leading edge as shown in Figure 5. This was a departure from previous experi-
ence. Another challenge was the complex internal design of the blades and
vanes due to the orientation of the ribs and pedestals and large size and
large length/thickness ratio of the ribs.
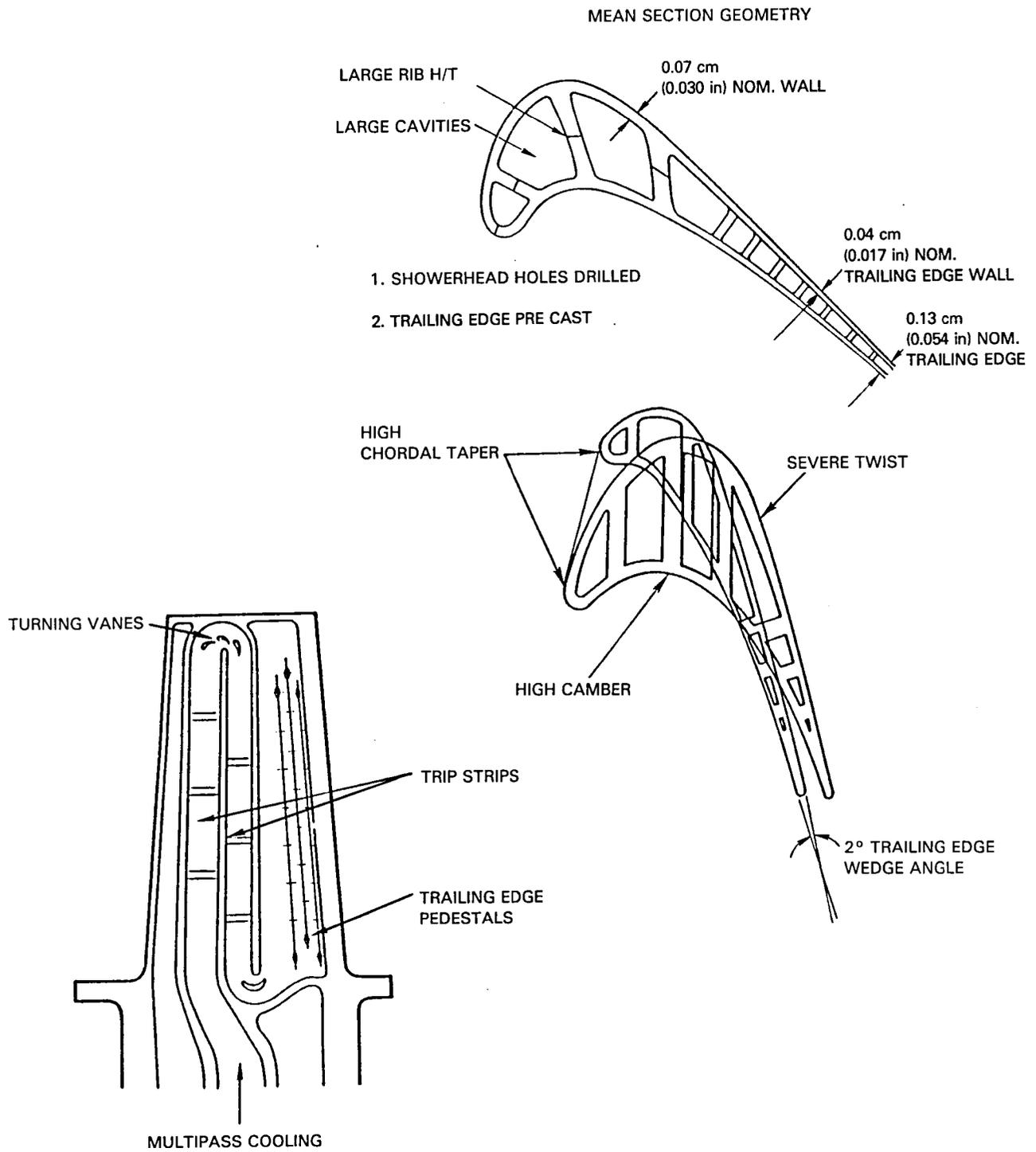
Figure 3   Energy Efficient Engine Turbine Blade Geometry and Attendant Fabrication Challenges

BOND
PLANE
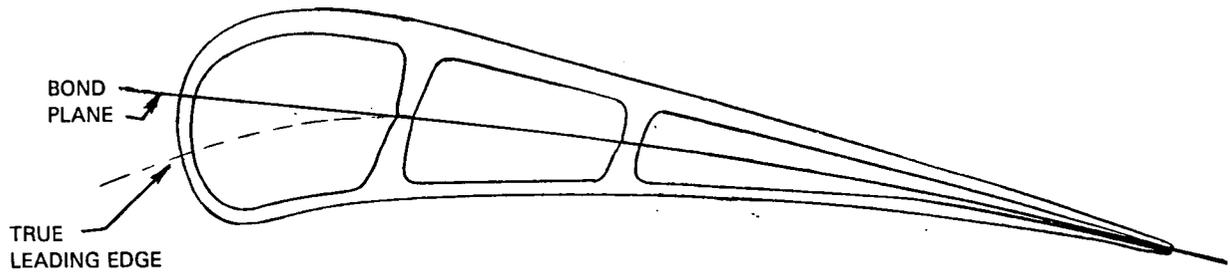
TRUE
LEADING EDGE

Figure 4   Energy Efficient Engine Vane Bond Plane Displaced from True
Leading Edge

TIP   BOND PLANE

THE CROSS-SECTIONS ILLUSTRATE THE HIGH TWIST
AND CAMBER OF THE ENERGY EFFICIENT ENGINE
BLADE. NOTE THE CHANGING POSITION OF THE
BOND PLANE WITH RESPECT TO THE TRUE LEADING
EDGE.

MID   BOND PLANE

ROOT   BOND PLANE
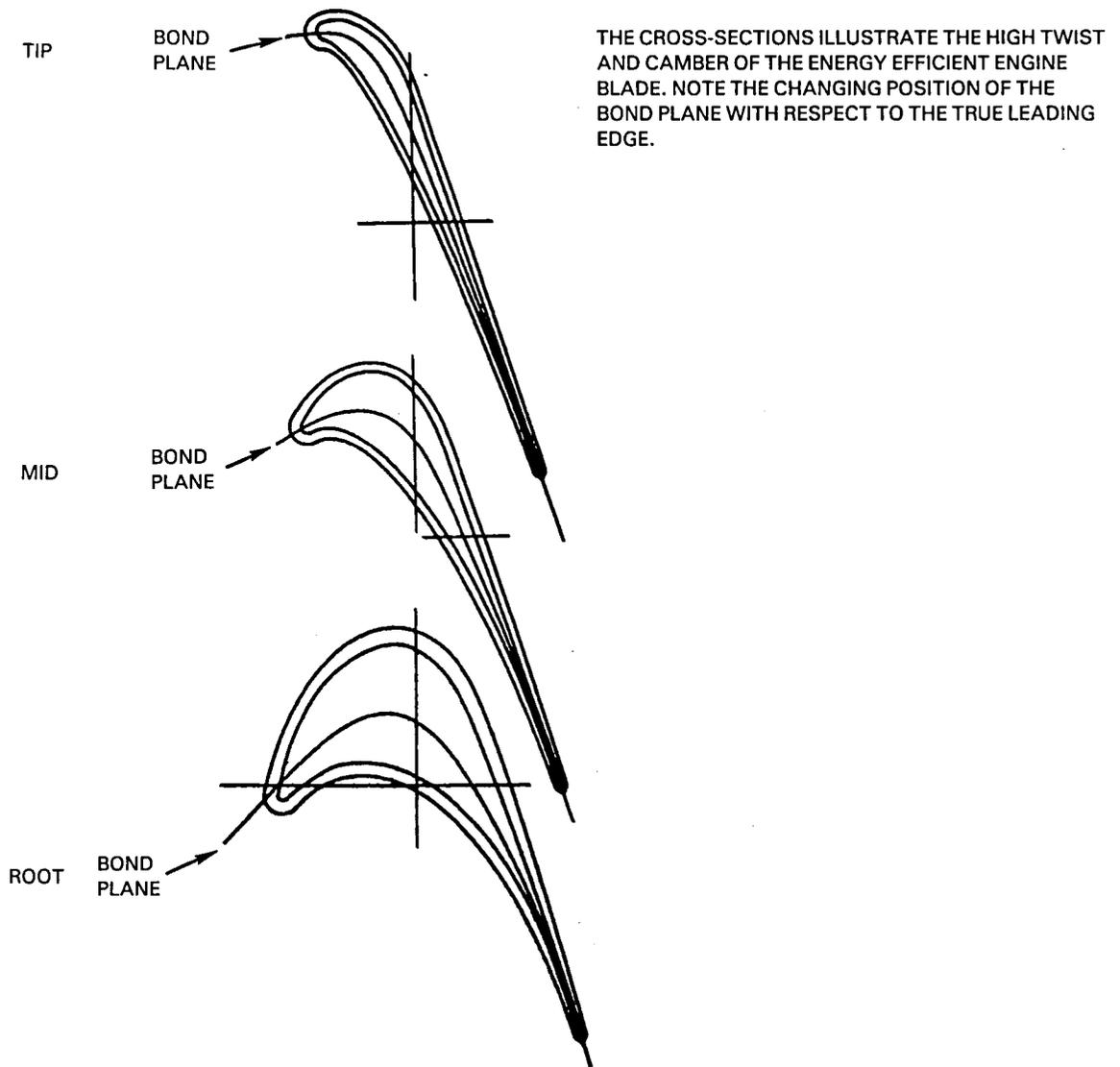
Figure 5   Energy Efficient Engine Blade Airfoil Cross-Sections

External features, outside of the net shape component, were therefore added to the designs to enhance bonding. Due to the large bond area, particularly in the vane shrouds, the bond area was minimized outside of the final part dimensions. This was accomplished by a 0.025 cm (0.010 in.) step in the strongback to separate the two halves. The edge flash on the leading edge was specifically designed (i.e. length, thickness) in both components so that it could be utilized as a load contact point during bonding. This additional loading area appeared necessary to assure bond quality in the critical leading edge bond due to the large size of the Energy Efficient Engine vane and the high camber on the blade.

On both the vane and blade, certain locations in the shroud and root areas were designed to maximize bond tool contact area and to assure tooling stability. In particular, material was added over and above normal machining stock, to both sides of the blade root section with a 4-degree taper on one side to facilitate bonding tool assembly. Vane platform areas were designed sufficiently wide to allow adequate contact area to prevent bond tooling instabilities during assembly.

4.0 CASTING FEASIBILITY

4.1 Overview

The approach used to meet the casting challenges posed by the complex geometries of the high pressure turbine component blades and vanes was to employ an established casting procedure and modify it as necessary to resolve specific problems encountered.

Of the various types of casting processes, investment casting is particularly suited to the fabrication of blades and vanes. Through investment casting, items with intricate shapes and smooth finishes can be produced, moderately high melting point alloys may be used, and close tolerances can be maintained. For this type of casting, also known as the "lost-wax" process, the pattern is made of wax in a metal die by injection molding. A "shell-coat" ceramic mold is build up around the wax pattern by successive dippings into a ceramic slurry. When the ceramic mold has dried, it is fired in a furnace to burn out the wax. After the wax has been removed, the ceramic mold is preheated and the metal poured. When the metal solidifies, the casting is removed by breaking the mold.

The use of coring increases the number of steps in the production of casting and, thus, increases the number of variables affecting a yield. Specifically, cores can shift, break, crack shells, and alter gating requirements.

To provide sound castings, it is essential that the mold pattern cavity be completely filled by the molten metal. To compensate for volumetric and solidification shrinkage, molten metal must be fed to critical areas of the pattern cavity until complete solidification occurs. It is the function of the gating system to provide for this condition and, because gating requirements cannot be accurately calculated, a satisfactory gating configuration is not normally established until after many trials.

Since most materials shrink upon cooling, shrinkage must also be taken into account in the design of pattern tools. Because waxes and castings shrink and ceramic dimensionally change during casting, a combined metal-wax-ceramic shrink factor, based on experience, is applied. This shrink factor normally runs about two percent.

The basic elements of the casting procedure used for this program are shown as a logical sequence of events in Figure 6. Each is discussed in more detail in the following sections of this report. The objective of this portion of the total effort was to evolve a casting procedure that would ensure a high degree of reproducibility of two-piece blades and vanes.

4.2 Wax Pattern Preparation

4.2.1 Process Description

The wax pattern for the parts to be cast is formed in a wax mold assembly. The primary elements of this assembly are the mold, the wax pattern itself, and the core (or strongback). An exploded view of a typical assembly for a two-piece casting is illustrated in Figure 7.
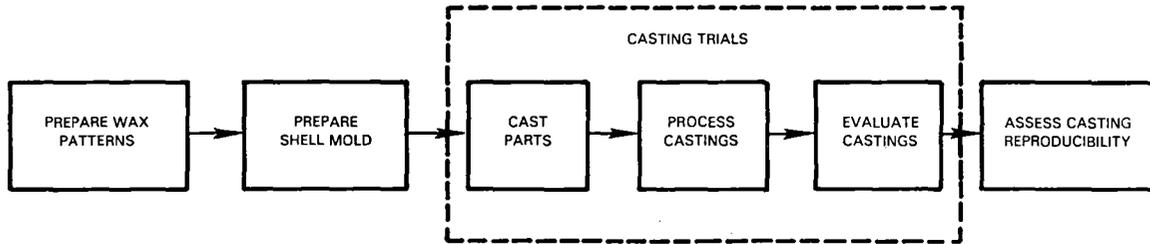
Figure 6   Steps in Achieving Casting Feasibility
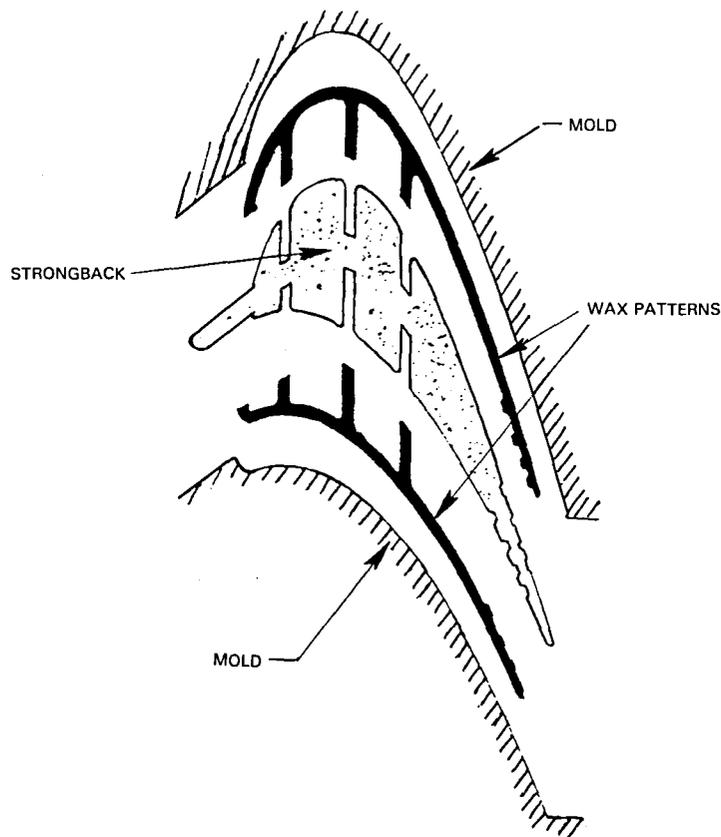
Figure 7   Typical Wax Mold Assembly for a Two-Piece Casting (Exploded View)

The mold defines the external contours of the blade or vane to be cast and therefore defines the external contour of the wax pattern that represents the part. The strongback defines the blade or vane internal geometry and performs the dual role of core for the wax mold and, ultimately, the core for the actual casting.

Strongback and mold designs were dictated by the high pressure turbine blade and vane geometries that evolved from the component preliminary design effort. Before fabrication, these designs were reviewed to insure that the proper draft angles, expansion regions, and blend radii were included to facilitate single crystal growth in the casting process. Strongbacks, typical of those fabricated for the blade and vane, are illustrated in Figures 8 and 9. The strongbacks and wax pattern molds were fabricated by vendors using established techniques. Vane and blade strongbacks were installed in the respective wax pattern molds as shown in Figures 10 and 11. Molten wax was then injected under pressure to form the shaped articles shown in Figures 12 and 13. The wax injection procedure is influenced by numerous process variables which affect the pattern quality. These included wax formulation, die venting, ingate location, wax pads, pinning, wax injection pressures 1,378 - 1,723 kPa (200 - 250 psi), wax temperatures 65 - 76°C (150-170°F)) and flow rates. All were optimized to obtain acceptable wax pattern quality. Visual inspection of each wax pattern was combined with radiographic (X-ray) and measurement inspections to ensure proper wax fill and strongback integrity and proper dimensions on the wax patterns.

The inspected wax patterns were then assembled with wax sprues, gates, helical restrictions' seed cavities, risers and pour cups suitably designed and located so as to address specific casting problems anticipated or encountered during the early casting phase of the program.

4.2.2 Blade Wax Pattern Preparation

Wax injection of the blade configuration presented challenging mold filling and dimensional tolerance problems. The initial injections using a standard investment casting wax formulation showed extensive areas of non-fill on the trailing edge area (Figure 14), as well as numerous strongback cracks. The primary cause of the non-fill problem (and possibly strongback cracking as well) was attributable to strongback misalignment which occurred during wax injection. Adjustments to the wax temperatures, wax flow rate and pressures were unsuccessful in eliminating the problems. However, replacement of the hard metal locating pins with soft wax pads and positive contact trailing edge pinning successfully reduced the number of strongback cracks and substantially eliminated the trailing edge positioning problem. Increasing the air venting at the mold die trailing edge plus use of a less viscous wax mixture also improved the filling in that area.
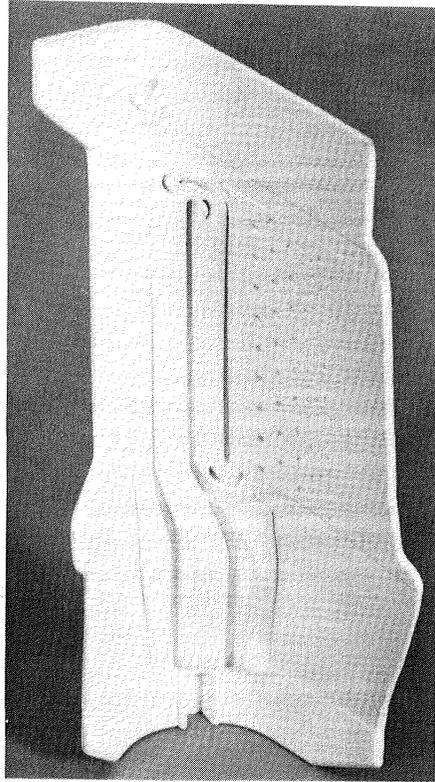
Figure 8   Pressure Side of Energy Efficient Engine First Stage Turbine Blade Strongback
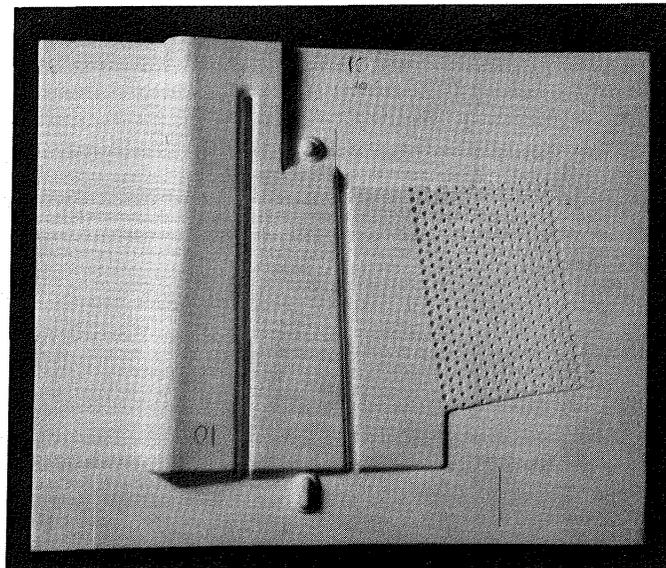
Figure 9   Pressure Side of Energy Efficient Engine First Stage Turbine Vane Strongback
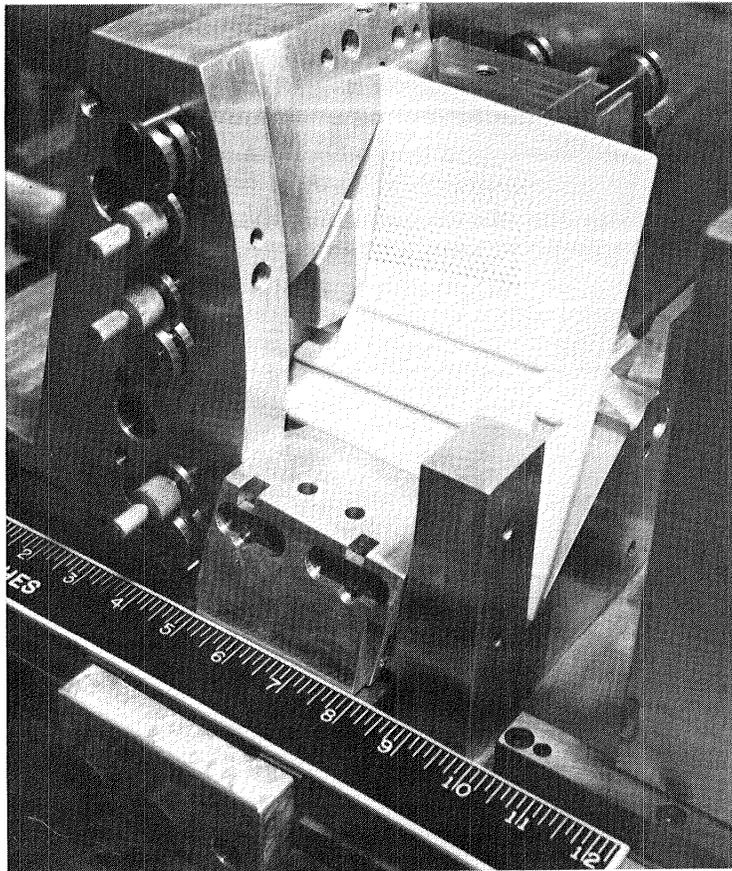
Figure 10   Energy Efficient Engine Turbine Vane Wax Injection Mold
             Showing Installed Strongback
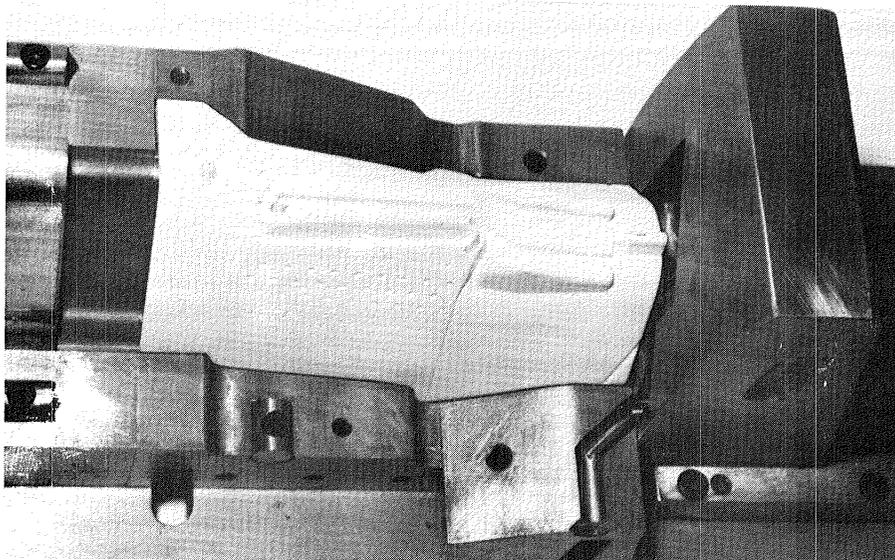
Figure 11   Energy Efficient Engine Turbine Blade Wax Injection Mold
             Showing Installed Strongback

13
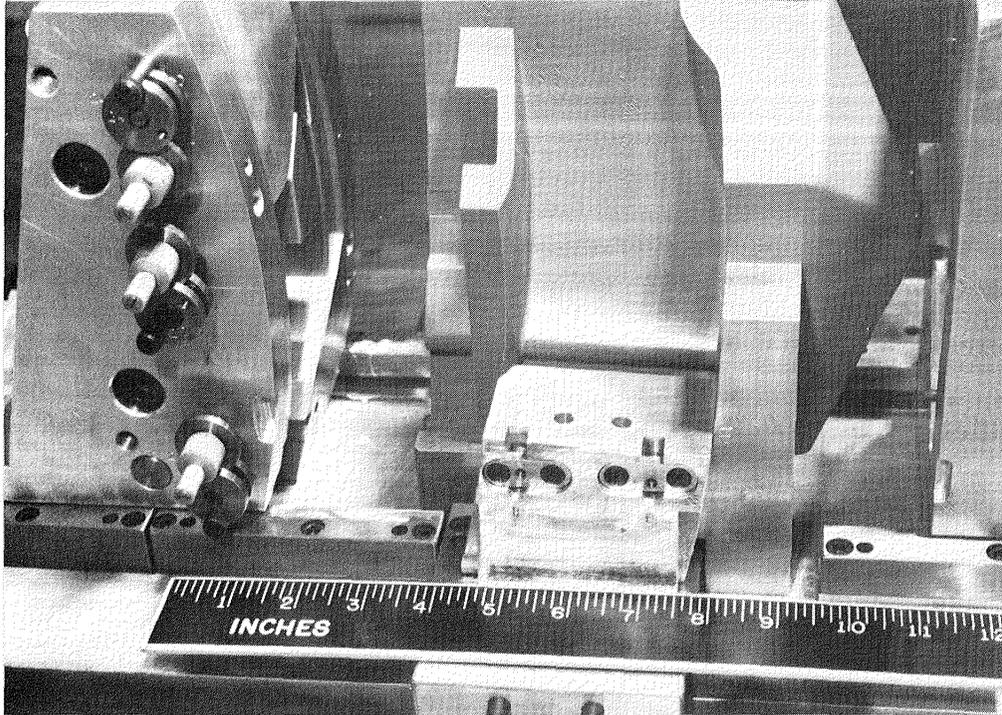
Figure 12 Energy Efficient Engine Turbine Vane Wax Injection Mold Showing
Wax Pattern, Leading Edge Down
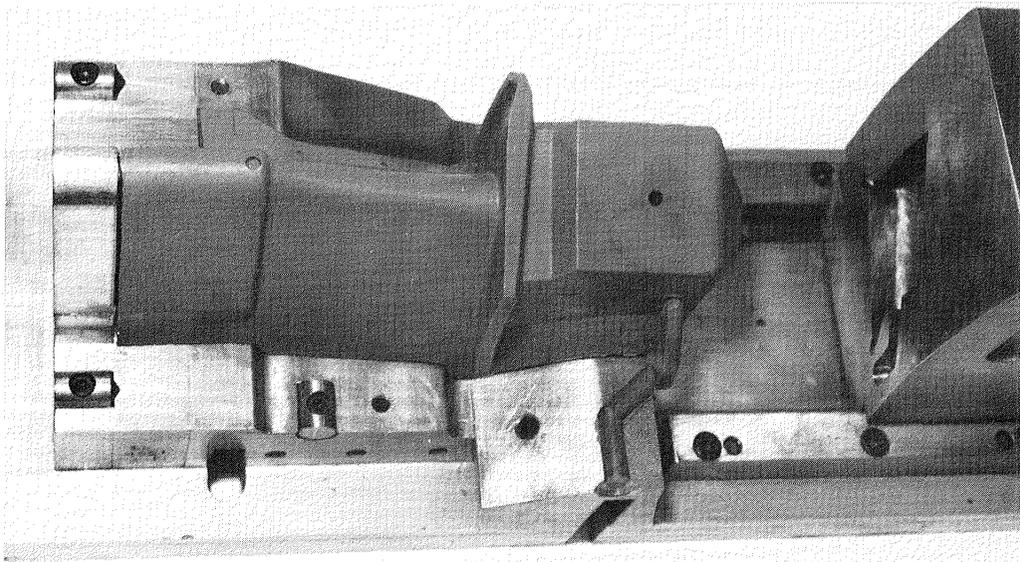
Figure 13 Energy Efficient Engine Turbine Blade Wax Injection Mold Showing
Wax Pattern

14
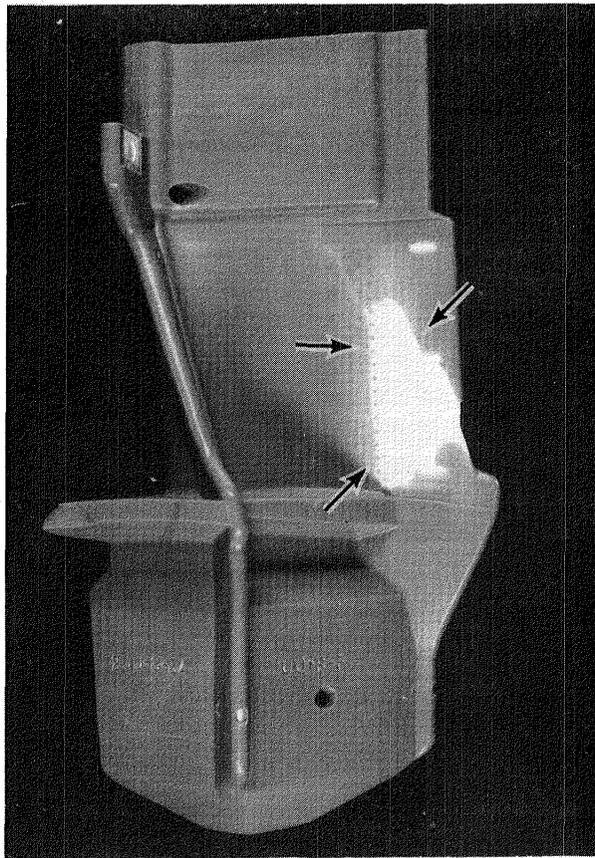
Figure 14   Initial Energy Efficient Engine Blade Wax Injection Illustrating
             Area of Non-fill on the Trailing Edge

Once proper strongback positioning was achieved, measurement of the wax trail-
ing edge thickness revealed that the required 0.04 cm (0.017 in.) thick walls
were actually only 0.03 cm (0.014 in.) thick. To correct this, the mold die
was opened at the trailing edge through the use of 0.01 cm (0.005 in.) shims
and air vents were added. Subsequent injections indicated an unexpected wax-to-
ceramic delamination problem onthe concave strongback surfaces, as shown in
Figure 15. This problem was thought to be due to the extremely high camber of
the blade design and the absence of throughcore wax pins typically used in
single-piece castings. The problem was solved by pre-heating the strongback
prior to wax injection which improved wax-to-strongback adhesion.

These modifications to the wax injection die and wax injection procedures
provided the fully acceptable blade wax patterns shown in Figure 16.

4.2.3. Vane Wax Pattern Preparation

Wax injection of the first vane configuration met with similar non-fill and
strongback cracking problems as the blade. In addition, strongback cracking
occurred during the fabrication process.
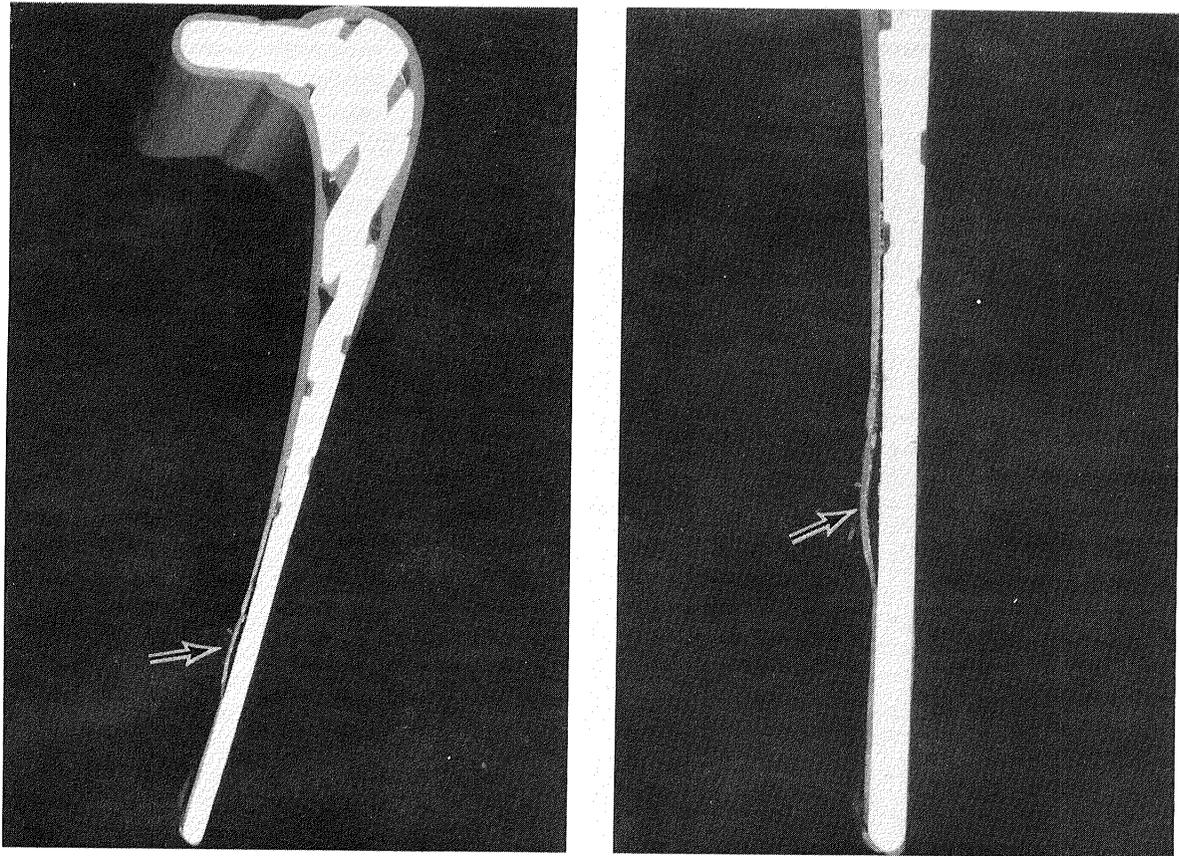
Figure 15   Transverse Section through an Unacceptable Wax Pattern Showing Wax
             Delamination on Concave Strongback Surface

Modifications to the basic strongback design, which included increased rib
fillet radii and elimination of the ribs in the core print area prevented
strongback cracking that occurred during fabrication, but failed to eliminate
cracking of the strongbacks during wax injection.

The implementation of the same corrective action that was successful in elimi-
nating the blade wax injection problems, specifically, wax pad replacing the
metal hard point locators, die vents, and the use of a high fluidity wax mix-
ture, failed to produce the desired results. The strongback continued to show
cracking due to wax injection and some small areas of non-fill persisted on
the vane trailing edge as shown in Figure 17.
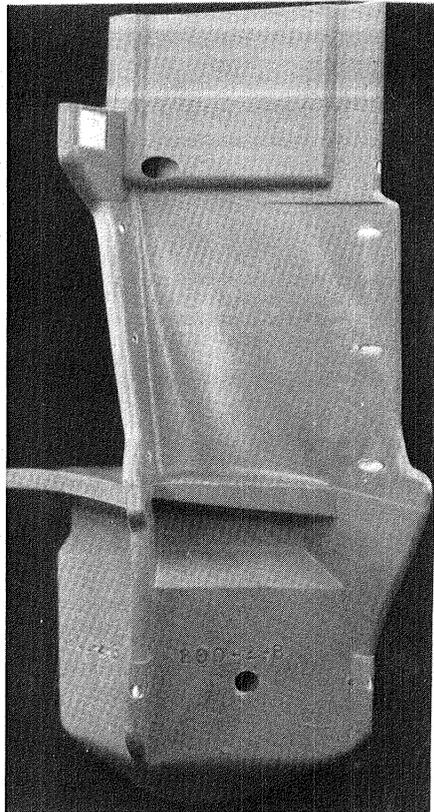
Figure 16   Injected Energy Efficient Engine First Blade Strong back
             Illustrating Acceptable Wax Pattern
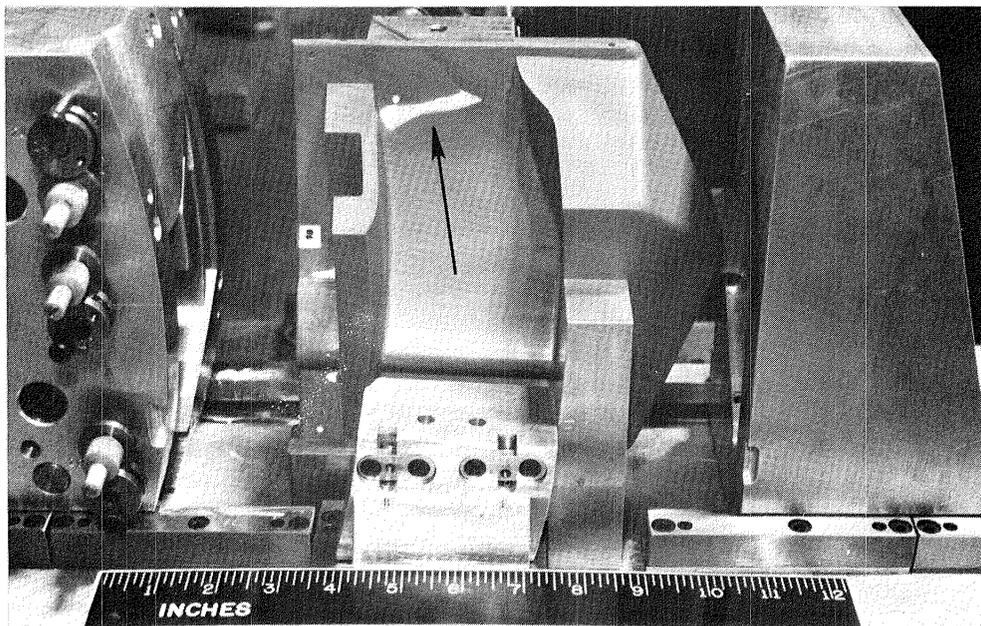
Figure 17   Initial Energy Efficient Engine Vane Wax Injection Illustrating
             Area of Non-fill on the Trailing Edge

Careful observation of the mold filling sequence during wax injection revealed an interesting flow pattern which indentified the reason for the strongback cracking and non-fill. Specifically, the location of the single wax ingate forced complete wax fill on the convex side of the strongback prior to filling on the concave side. The resultant pressure differential across the strongback was believed responsible for the strongback cracking. Furthermore, filling of the thin trailing edge was prevented by improper wax flow patterns and premature wax solidification which "froze-off" the wax at the strongback core print prior to complete fill. Correction of the wax injection problems required a modification to the vane die which provided dual wax in-gates aimed at uniform wax injection on both sides of the strongback; eliminating the pressure differential. In addition, the strongback core print was trimmed to provide better wax flow to the thin trailing edge vicinity. Relocation of the soft wax pads and wax injection pressure adjustments to the modified wax injection die provided the acceptable vane wax patterns, shown in Figure 18.
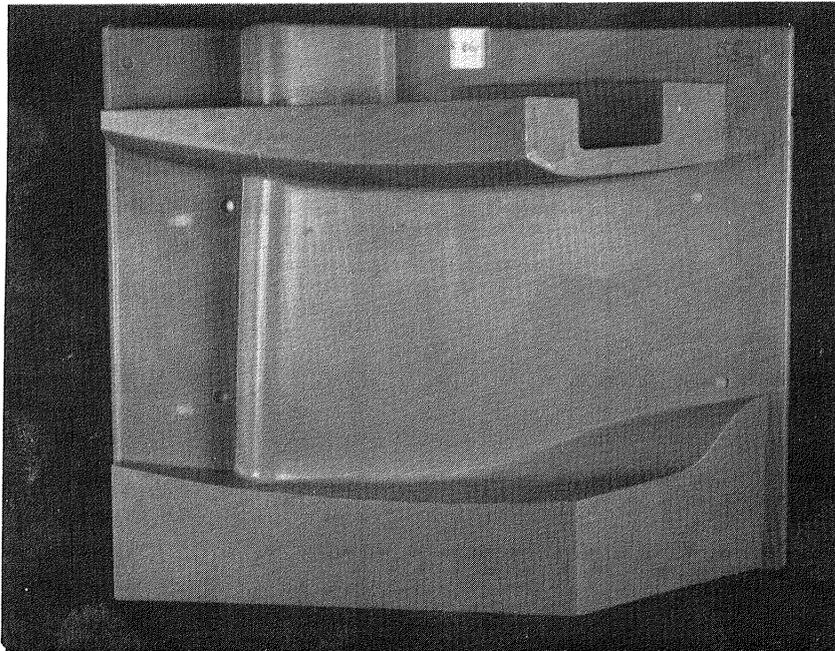
Figure 18   Injected Energy Efficient Engine First Vane Strongback
             Illustrating Acceptable Wax Pattern

4.3 Shell Mold Preparation

4.3.1 Process Description

Once the required wax pattern definition was achieved, the next step was to prepare the mold in which the blade and vane airfoil shapes were to be cast.

The molds for the single crystal casting trails were fabricated by building up a ceramic shell on assemblies of injection molded blade or vane wax patterns and gating components.

An alumina-silica (Al_2O_3/SiO_2) mold shell system was selected for the casting trails because of its high temperature capability. This system represents the current ceramic shell technology for advanced high temperature applications and has been shown to withstand hot zone temperatures in excess of 1648°C (3000° F) in some restrictive casting geometries.

The ceramic shell was built up by successive applications of refractory slurry and franular (stucco) refractory coatings to obtain the desired thickness, mold strength, and thermal characteristics. Each ceramic application was dried in air drying cabinets or drying tunnels. Drying temperature was carefully controlled to preclude melting of the wax in the wax pattern.

After the fully built-up "green" shell mold assemblies were thoroughly dry, the wax was melted out by using either a steam autoclave or a gas-fired furnace.

The wax removal leaves a mold cavity within the shell of the desired configuration as shown in Figure 19. The shell may require additional firing to achieve the desired strength. However, strongback characteristics could be adversely affected by the temperatures associated with the additional firing, so the process required careful monitoring.
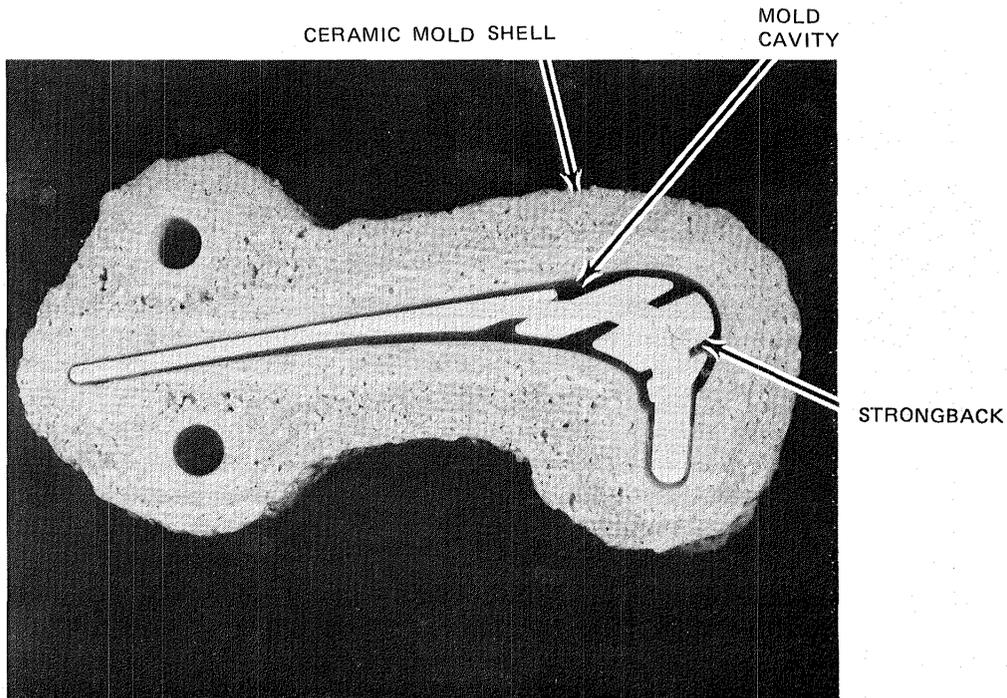
Figure 19   Transverse Section through Blade Mold Assembly Showing Desired Mold Cavity

4.4 Casting

4.4.1 Process Description

The commercial withdrawal (or high rate solidification) process has been used to manufacture unidirectionally solidified superalloy blades and vanes for the past twenty years. This same process and equipment was employed to make single crystal castings. A photograph of the equipment and a schematic showing the principles of operation are presented in Figures 20 and 21.
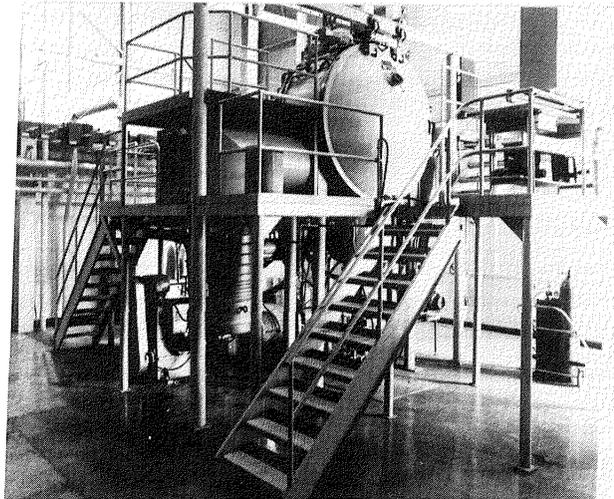
Figure 20   Commercial Withdrawl Casting Furnace

In the commercial withdrawal casting furnace, the processing sequence involves induction (or possibly resistance) preheating of an open-ended shell mold attached to a water cooled copper chill plate held on a movable shaft in a vacuum environment. The single crystal alloy charges are melted by induction or electron beam methods in a separate operation and then poured into the pre-heated shell mold. The filled mold is then withdrawn through a baffle arrangement at a controlled rate schedule, which must be specifically tailored to the mold cavity geometry filled by the molten metal. The completely withdrawn mold is then cooled to room temperature prior to post-cast processing.

After solidification and cooling to room temperature, the molds are processed as follows. The shell material is carefully removed from each casting prior to heat treating to minimize risk of recrystallization. Residual strongback material is removed with the use of a caustic solution. This procedure is followed by alumina blasting with a suitable grit type, size and pressure. The parts are then brighted in a ferric chloride treatment solution and anodically etched to reveal the single crystal grain structure. Visual examination to identify surface defects such as nucleated grain, freckles, non-fill, porosity, cracks or webs is followed by radiographic inspection to detect any significant internal flaws. The back reflection Laue x-ray method was utilized to

20

determine the single crystal primary and secondary grain orientation of the part halves. Dimensional measurements of the blades and vanes are compared to the wax pattern to calculate accurate strongback and metal shrink factors and determine wall thickness deviations during casting, in addition to assessing any material loss due to pre-bond cleaning and etching procedures. These data could be substantially used to calibrate the strongback and wax pattern tooling, if necessary.

RADIATION HEATING

MOLTEN METAL

RADIATION COOLING

BAFFLE

CERAMIC MOLD

SINGLE CRYSTAL SELECTOR (HELICAL RESTRICTION)

WATER COOLED CHILL PLATE

SINGLE CRYSTAL SEED

SINGLE CRYSTAL CASTING PROCESS
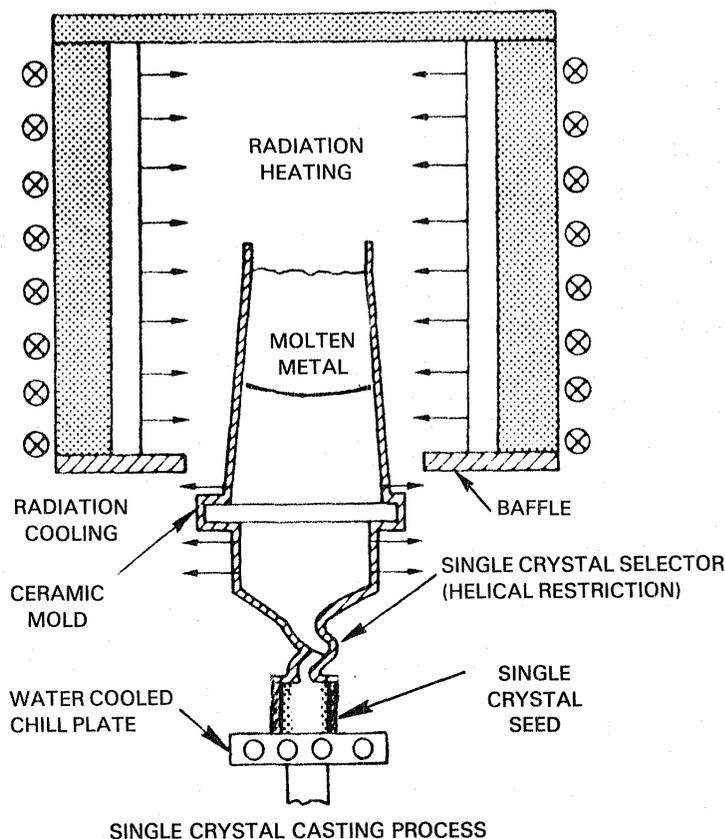
Figure 21   Schematic of the Commercial Withdrawal Process Used to Cast Seeded Single Crystals

Most production equipment is sized to accommodate a number of cast turbine airfoils in a single solidification cycle (a multiple-article clustered mold, for example). The large size of the Energy Efficient Engine blade and vane articles to be cast, coupled with the associated heat management requirements and molten alloy charge size, led to the selection of single article mold designs as shown in Figures 22 and 23. Although this could restrict productivity in a more conventional casting facility, for experimental purposes, it allowed maximum flexibility in the use of radiation baffles and heat extraction techniques. Furthermore, the single unit mold design closely approximated casting configurations and heat transfer conditions suitable to the Pratt & Whitney Aircraft Automated Casting Foundry and, therefore, facilitated the establishment of starting point casting parameters for the high production rate Automated Casting Foundry operation.
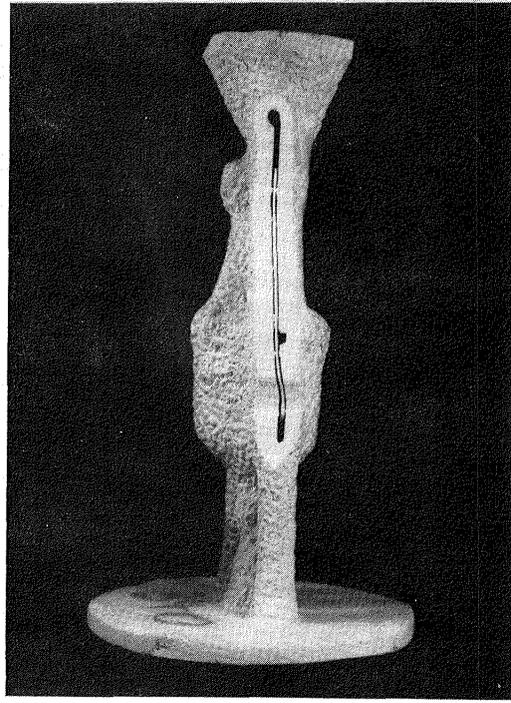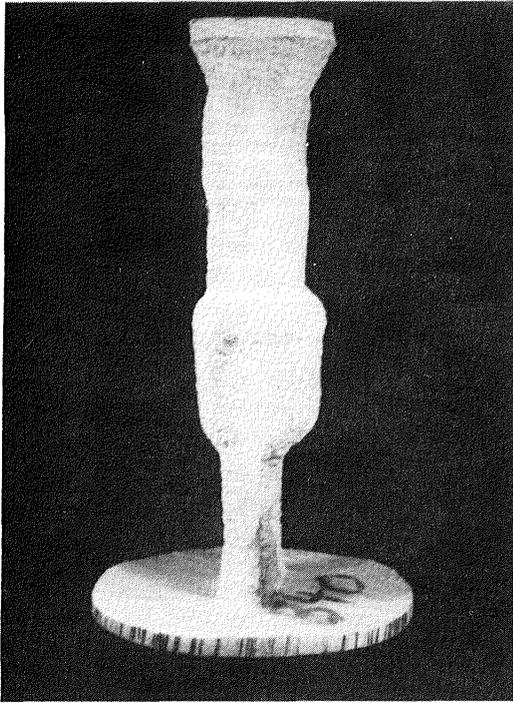
Figure 22   Single Unit Root-down Mold Assembly for Casting Single Crystal
             Energy Efficient Engine First Stage Blades. Sectioned Mold Shows
             Location of Strongback in the Mold.
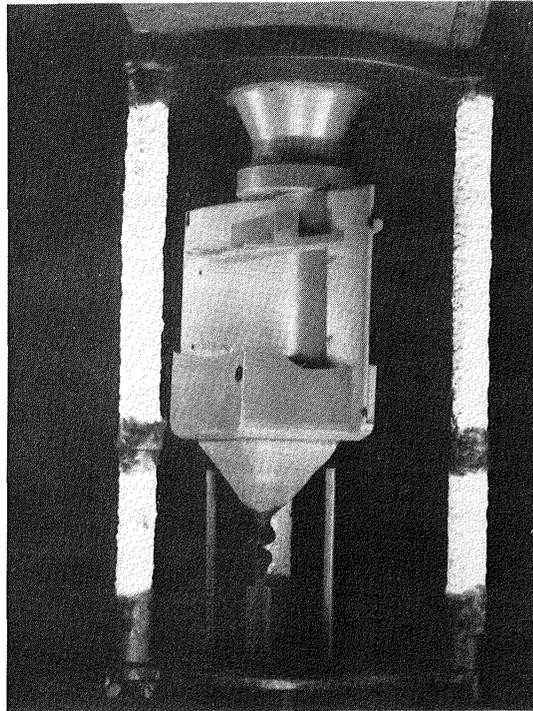
Figure 23   Single Unit Outer Shroud-down Wax Assembly Used for Casting Single
             Crystal Energy Efficient Engine First Stage Vanes

Optimization of the casting parameters (i.e., hot zone temperatures, pour temperatures, withdrawal rate schedule, baffling designs) was dictated by the extensive heat control requirements imposed by the unusually large masses and cross sectional area changes associated with the vane shrouds as well as the large size and twist of the blade design. Unless the proper direction and magnitude of heat flow (heat balance) is maintained throughout the casting cycle, large masses often lead to porosity, freckling and/or grain nucleation as well as poor quality single crystals due to misalignment of the dendrites.

4.4.2 Preparation of Master Melt

The single crystal alloy (PWA 1480) charges for each of the casting trials conducted in this program were sectioned from an experimental commercial master heat which was using commercial grade starting elements (listed in Table I).

TABLE I

PWA 1480 MASTER HEAT CHEMICAL ANALYSIS RESULTS IN WEIGHT PERCENT

FOR MAJOR ELEMENTS

MAJOR ELEMENT	P-9799	PWA 1480 SPECIFICATION (NOMINAL)
Chromium	10.20	(10.0)
Cobalt	4.76	(5.0)
Tungsten	3.94	(4.0)
Titanium	1.37	(1.5)
Tantalum	11.93	(12.0)
Aluminum	5.03	(5.0)
Nickel Plus Trace Elements	Remainder	Remainder

The master melting procedure consisted of vacuum induction melting an elemental charge in a rammed magnesia crucible. Following a brief homogenization period, the melt temperature was reduced and measured amounts of the more highly reactive elements were added. The melt was subsequently reheated, cooled following a short stabilization period and poured to form ingots 8.89 cm (3.5 in.) in diameter by approximately 121.92 cm (48 in.) long; a size compatible with casting furnace capability. A vacuum of less than 10 microns was maintained throughout the melting operation to maintain melt purity.

Chemical analysis of the master heat was conducted to establish composition control. The results listed in Table I represent the certified chemical analysis report for the heat utilized in this program. The results show that all the major elements were within PWA 1480 specifications.

4.4.3 Casting Trials

Casting is as much an art as a science, and casting techniques depend to a great extent upon empirical information and trial-and-error methods. Before a mold can be expected to produce satisfactory yields, trial castings must be produced. Invariably, the first trial runs indicate the need of some modification. While these modifications are often limited to simple changes, a major redesign of a die is sometimes necessary. On the average, a foundry will require about eight weeks to develop techniques before an acceptable yield is achieved depending on the type of inspection required. An extensive casting effort was required during this program to define the optimum casting parameters needed to (1) produce single crystal airfoils and (2) control airfoil dimensions.

4.4.3.1 Blade Casting Trials

Casting the two piece high pressure turbine blade shape for the Energy Efficient Engine represented the first application of basic single crystal casting technology to large size cast and bonded superalloys. The blade design incorporates large root cross section (approximately 7.62 cm^2 (3 in.^{2})) and chord width (approximately 8.63 cm (3.4 in.)) coupled with a high twist, high camber airfoil. The blade design further stretches basic single crystal state-of-the-art casting technology by requiring crystal solidification control of the secondary grain orientation in addition to the primary orientation, as shown in Figure 24. This requirement which was needed to improve the vibration characteristics of the blade trailing edge tip, necessitated seeding for the desired orientation of the single crystal growth. The seeding and subsequent (epitaxial) single crystal growth of a large two piece airfoil such as the blade configuration had not been previously attempted. The single unit root down mold design was selected to minimize the concerns associated with the need for extensive lateral grain growth due to the large cross-sectional area change in the root-to-airfoil transition region of the Energy Efficient Engine blade configuration (see Figure 25). Furthermore, this design provided for more efficient radiation heat baffling in the casting furnace so that the large single crystal blade shape could be grown at relatively low casting temperatures, approximating columnar grain growth conditions.

Referring to Figure 21, numerous adjustments to the start conditions, such as relocation of the chill plate relative to the hot zone and improved heat baffle modifications, were coupled with withdrawal rate adjustments and helical restrictions to successfully seed and grow single crystals of the desired primary and secondary orientations. It was discovered that minor modifications to the mold design could alter the filling characteristics of the mold such that compensating adjustments to the casting parameters were necessary to maintain proper seed meltback and achieve the epitaxial growth illustrated in Figure 26. Extraneous nucleation was avoided by maintaining the proper temperature gradient to withdrawal rate (G/R) relationships throughout the solidification cycle.

24
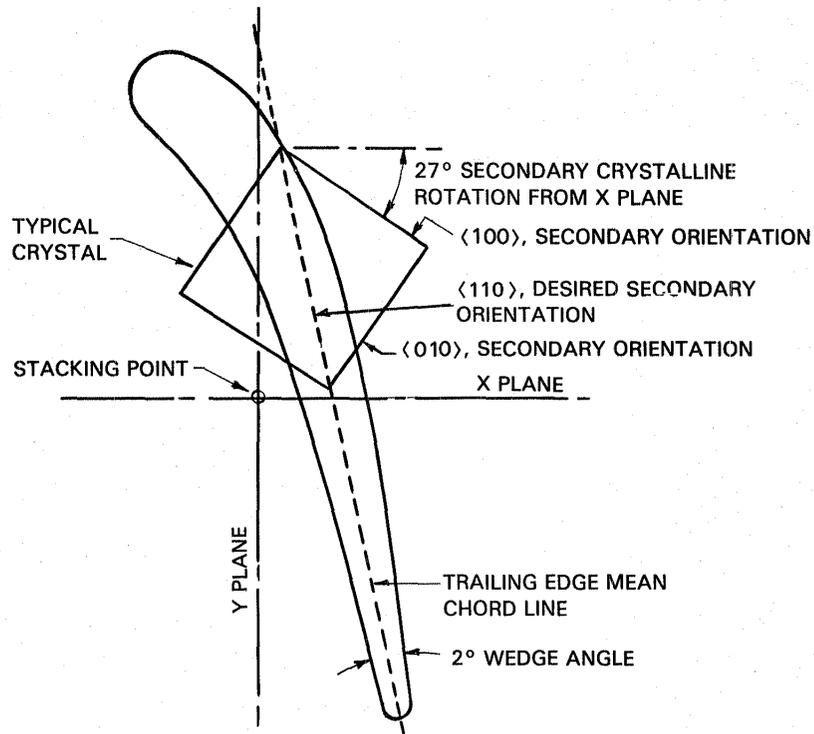
Figure 24   Schematic of Blade Airfoil Tip Section Showing Desired Secondary
             Crystal Orientation Rotated 27° from X Plane. Primary orienta-
             tion, <001> , is Radial and Coincident with Stacking Point.
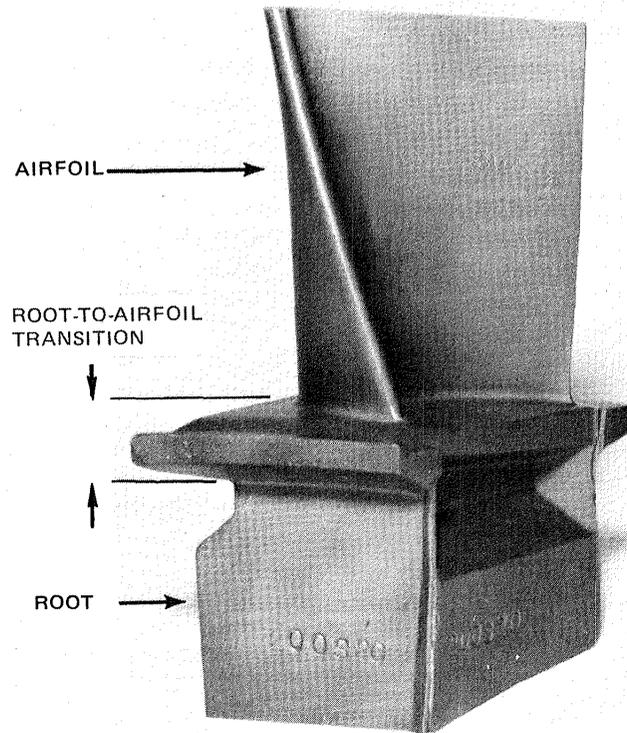
Figure 25   Energy Efficient Engine Turbine Blade Configuration Showing Large
             Cross-Section Area Change in Root-to-Airfoil Transition Region

SOLIDIFIED ALLOY
SHOWING COLUMNAR
GRAIN STRUCTURE

LIQUIDUS MELTBACK
AT SEE-MOLTEN ALLOY
INTERFACE

SEED-MOLTON
ALLOY
INTERFACE

ORIGINAL SINGLE
CRYSTAL SEED
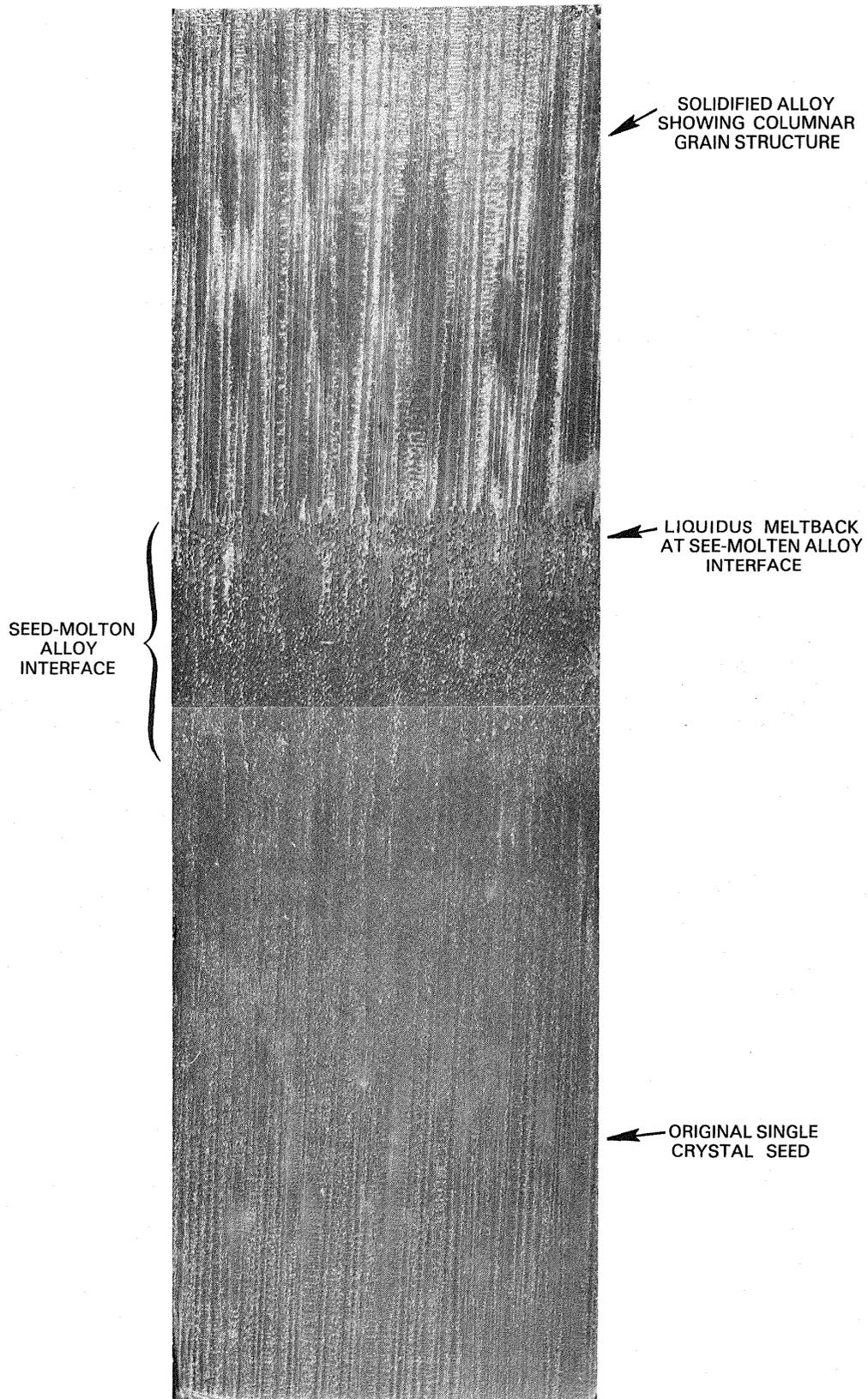
Figure 26   Photomicrograph of a Longitudinal Section Through a Typical Seed
Showing Epitaxial Growth

At the initiation of blade casting trials, a problem developed wherein the PWA 1480 material reacted with the aluminum nitrate coated SR200-2 strongback formulation to form the localized river patterns and melt penetration shown in Figure 27 as well as the general surface roughness shown in Figure 28. An internally funded program was subsequently conducted at Pratt & Whitney Aircraft aimed at evaluating the interaction of a large number of available strongback formulations against PWA 1480 at approximately 1551°C (2825°F), near typical single crystal casting temperatures. One low pressure strongback formulation, identified as SR200-S, was found to be acceptable. Unlike the SR200-2 formulation, the SR200-S strongback did not require any protective surface coating. This strongback formulation, coupled with reduced hot zone temperatures (1496°C (2725°F) versus 1537°C (2800°F)) and pour temperatures (1523°C (2775°F) versus 1565°C (2850°F)), successfully eliminated the reactivity problem.

Initial casting trials also clearly showed a trailing edge metal non-fill problem similar to the non-fill encountered during wax injection. Varying degrees of non-fill were evident and manifested themselves in the form of pedestal non-fill and/or rounding, cold shuts and even voids as shown in Figures 29 and 30. The latter manifestations of the problem were most serious since they frequently resulted in extraneous nucleation and growth.
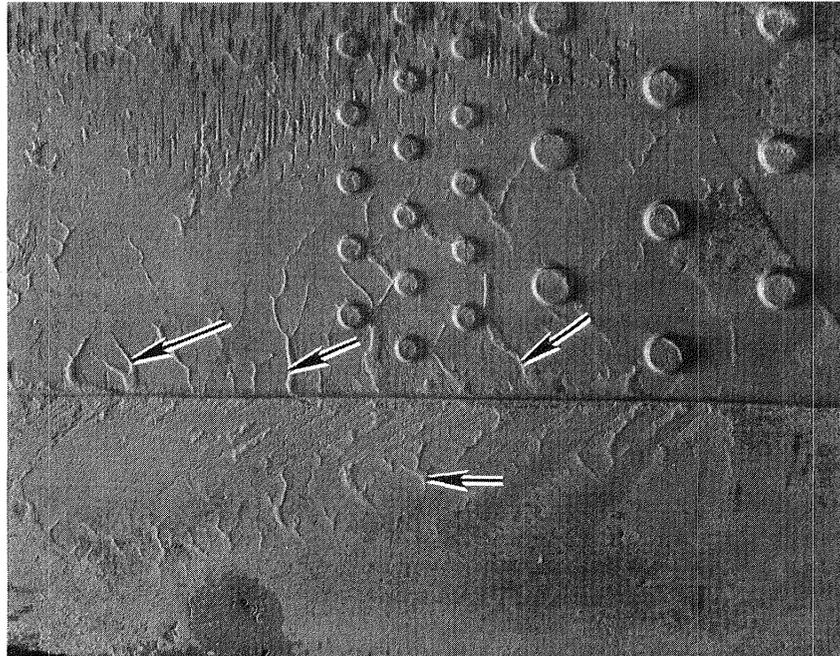
Figure 27   PWA 1480 Surface Cast Against an Aluminum Nitrate Coated SR200-2 Strongback Showing Localized River Pattern
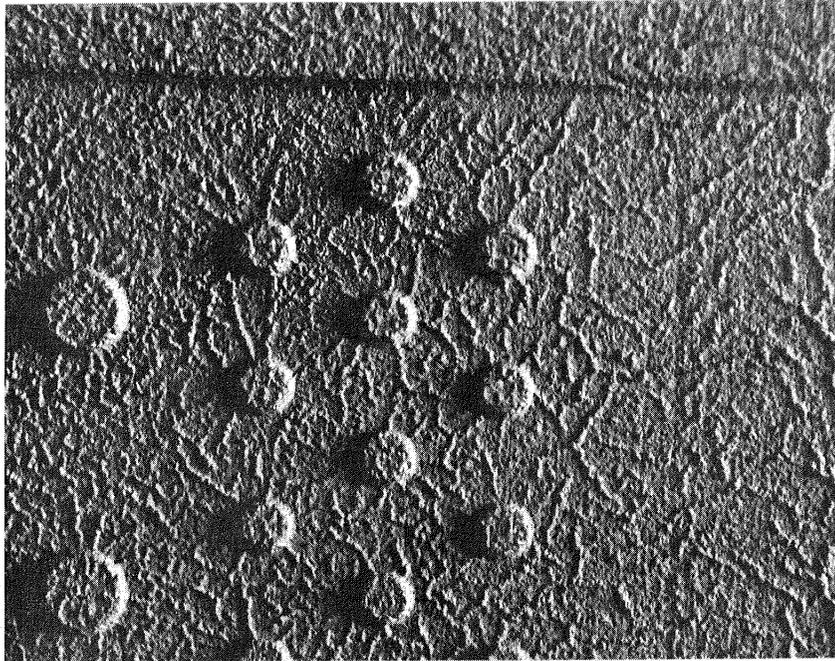
Figure 28   PWA 1480 Surface Cast Against an Aluminum Nitrate Coated SR200-2
              Strongback Showing General Surface Roughness
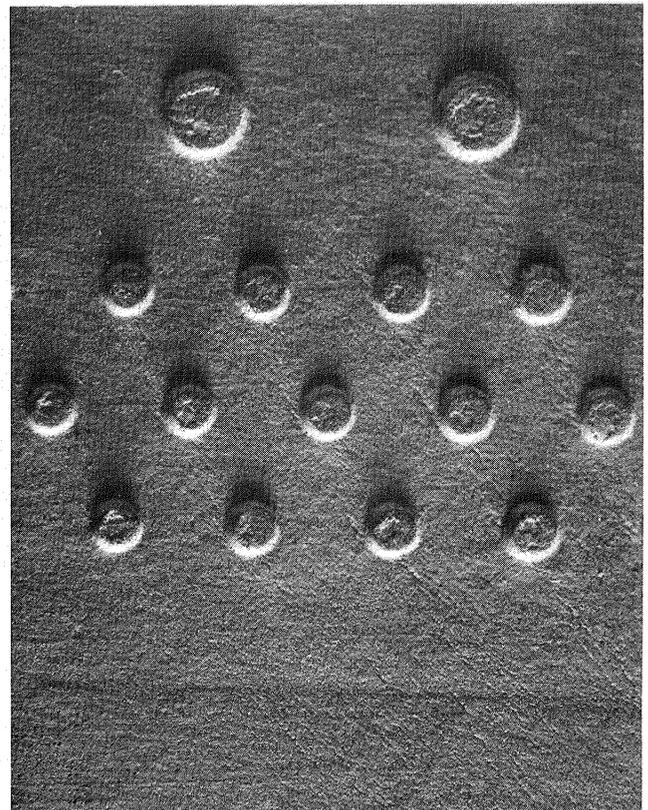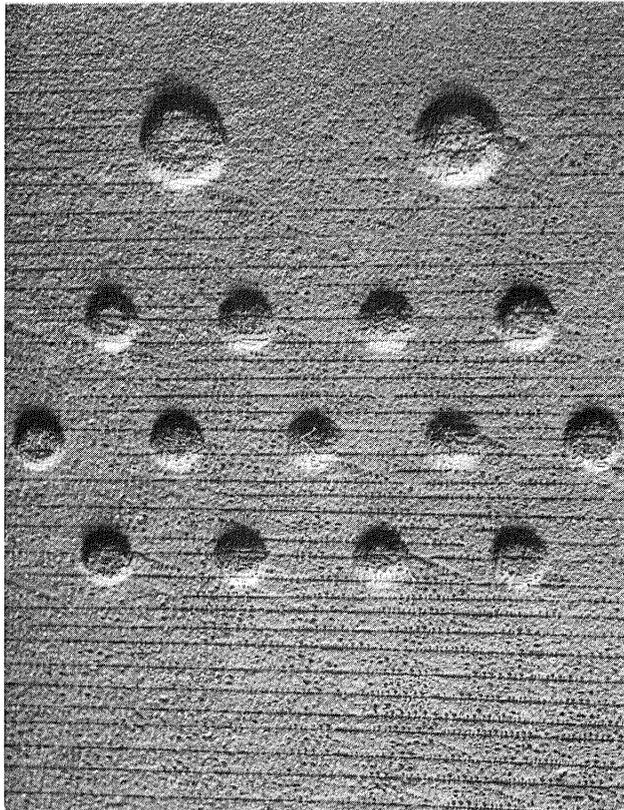
Figure 29   PWA 1480 Cast Surface Illustrating Pedestal Rounding (Left) as
              Compared to Properly Filled Pedestals (Right)

28

Part of the problem was discovered to be due to shifting and bowing of the strongback near the tip section during the pour cycle. This resulted in undesirable casting thickness distributions and thin trailing edge walls, as illustrated in Figures 31(a) and (b). This strongback problem was resolved by modifying the blade wax pattern so that positive contact strongback positioning pins could be built into the shell mold at the strongback tip section and "slip-joint" strongback positioning pins could be built into the shell mold at suitable trailing edge positions. This modified wax pattern is shown in Figure 32. These corrective measures effectively solved the strongback bowing and shifting problems as illustrated in Figures 33(a) and (b). The remainder of the non-fill problems were solved by the synergistic effects of a more rapid metal pour, increased metallostatic head, and a longer mold "soak" in the furnace temperature environment before pouring.

GROWTH DIRECTION ↑
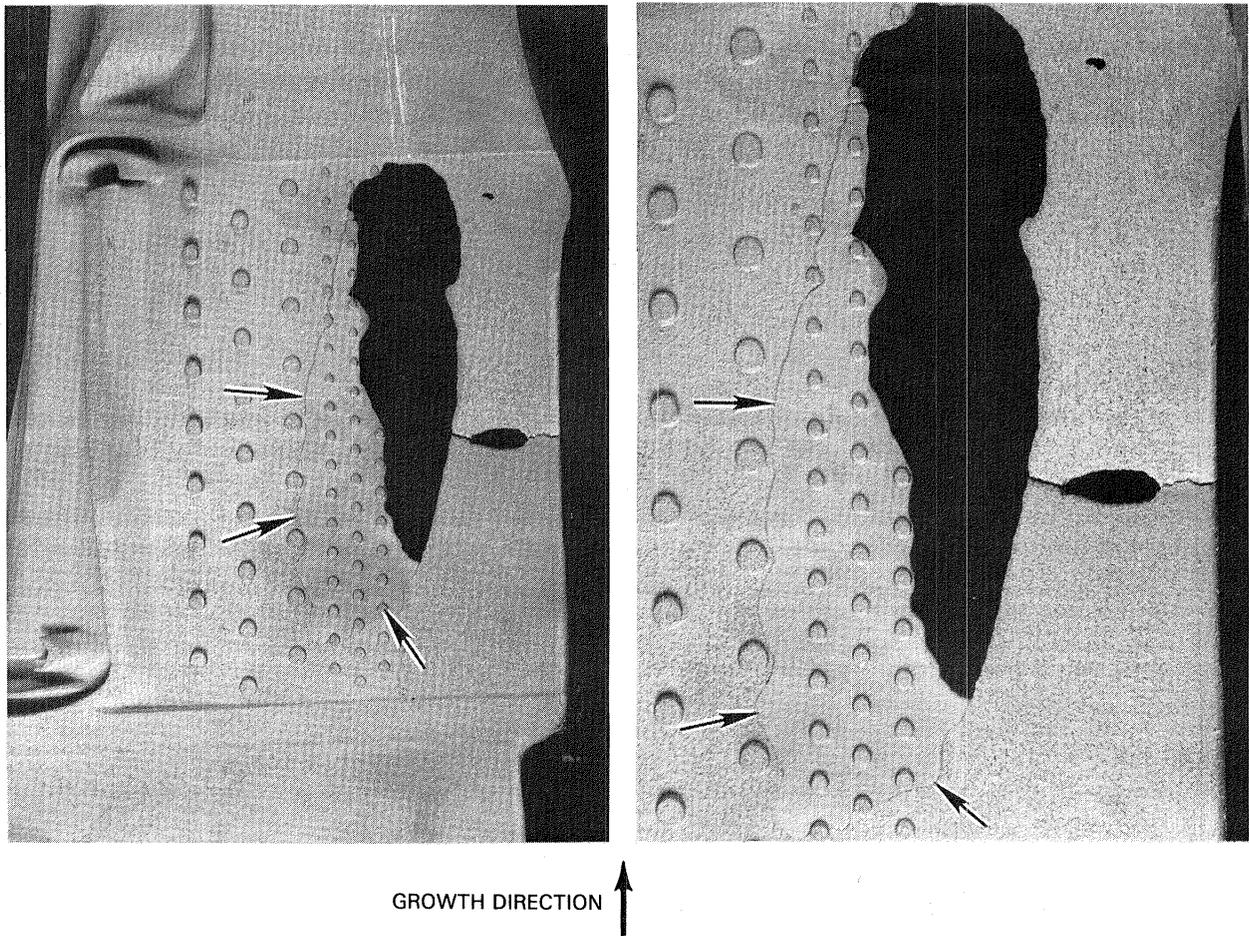
Figure 30   Concave Energy Efficient Engine Blade Half Showing a Cold Shut
             Adjacent to an Area of Non-fill

Another unexpected problem (at least in degree) became apparent during the early casting trials. The problem was one of extensive mold distortion at the elevated temperatures in the casting furnace which resulted in dimensionally oversized airfoils, up to 0.076 cm (0.030 in.) oversize at the trailing edge midspan location. (Dimensional control is discussed in Section 4.5.4.) Since it was known that the alumina-silica shell was inherently dimensionally unstable in large flat slabs (particularly at elevated temperatures), an initial

series of casting trials was conducted to determine the effects of reduced hot zone temperatures. It was discovered that the large single crystal airfoils could be grown in single unit mold designs at surprisingly low hot zone temperatures (as low as 1482°C (2700°F)). However, due to the size of the single crystal blade, mold distortion, although reduced in magnitude, still persisted and produced unacceptable airfoil dimensions.
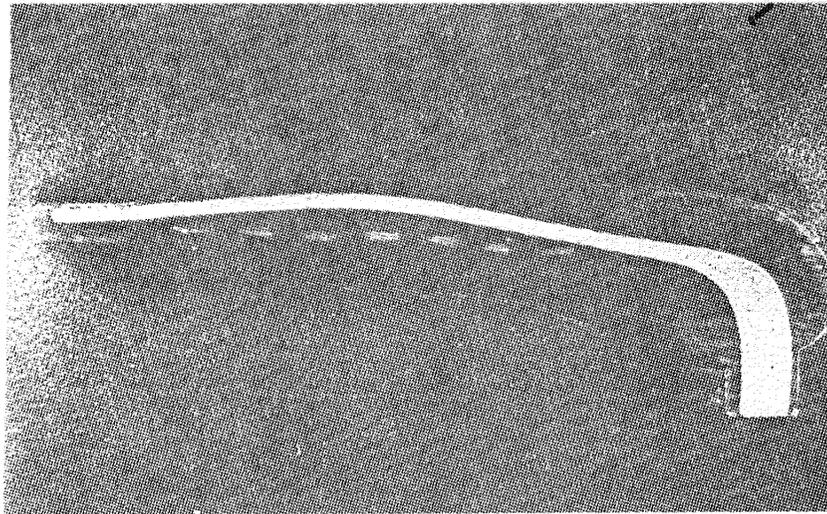
(A)
BOWED STRONGBACK
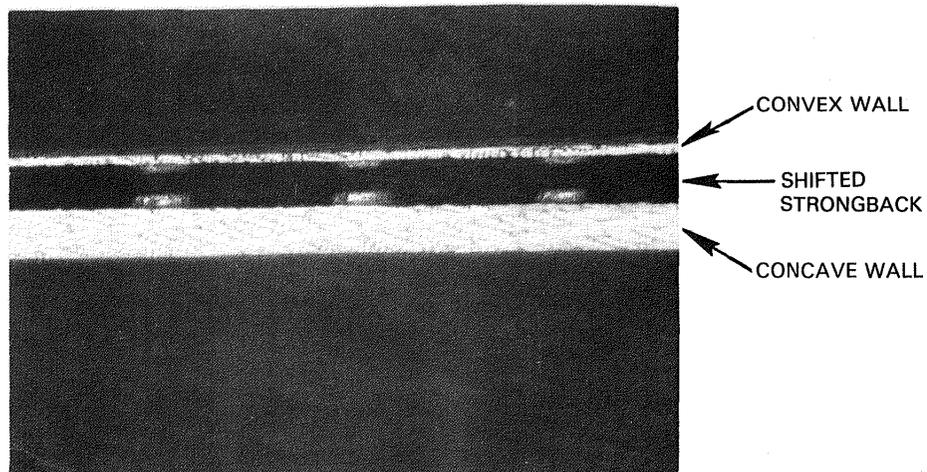
(B)
TRAILING EDGE WALL THICKNESS NON-UNIFORMITY
DUE TO STRONGBACK SHIFTING

Figure 31   Illustration of Strongback Bowing and Shifting Problems
Encountered During Blade Casting Trials

Therefore, a second series of casting trials was conducted to evaluate numerous shell reinforcement schemes, including localized shell build-up, ceramic and metal reinforcement techniques and withdrawal rate adjustments. The results of these casting trials demonstrated that the most effective method of producing acceptable airfoil dimensions was to increase the thickness (0.50 cm (0.20 in.) to 1.27 cm (0.50 in.) or greater) of the shell. Since it was advantageous to maintain the lowest possible hot zone temperatures, additional radiation baffling was added and casting parameters adjusted to compensate for gradient losses sustained due to the increased shell thickness. Final blade casting dimensions were maintained oversize such that normal blade post-cast processing (alumina blast, grain etch and prebond cleaning) yielded parts that were within the design dimensional tolerance band.

POSITIVE CONTACT
PINNING LOCATION
AT STRONG BACK TIP

SLIP-JOINT
PIN LOCATIONS
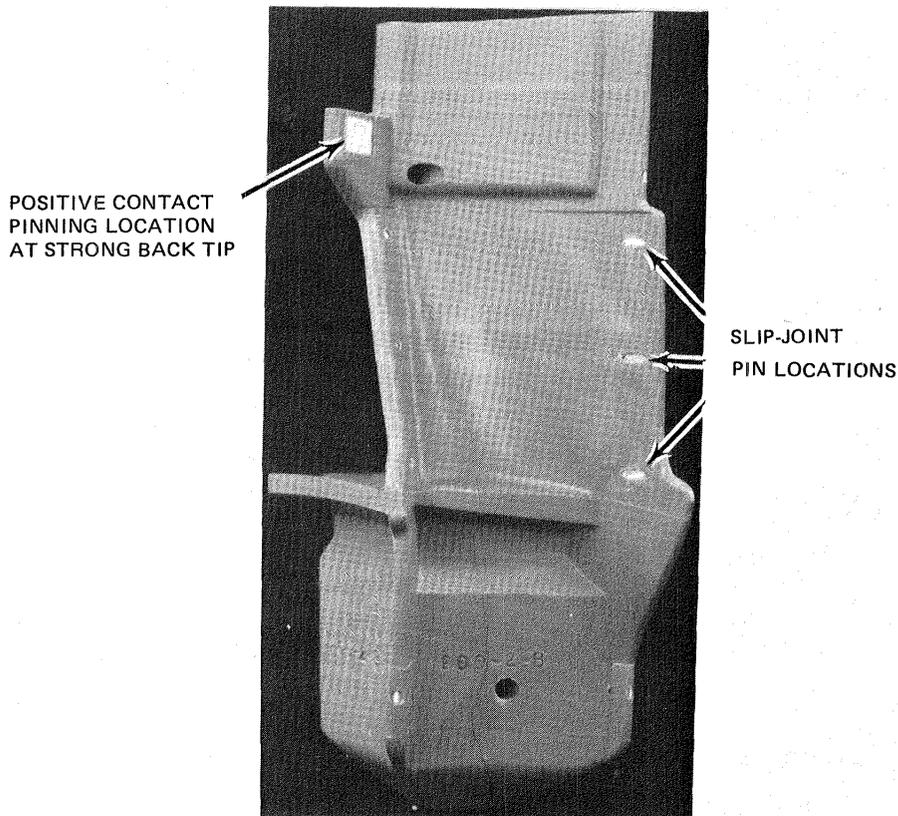
Figure 32   Modified Blade Wax Pattern Showing Provisions for Building
             Strongback Holding Pins into the Shell Mold
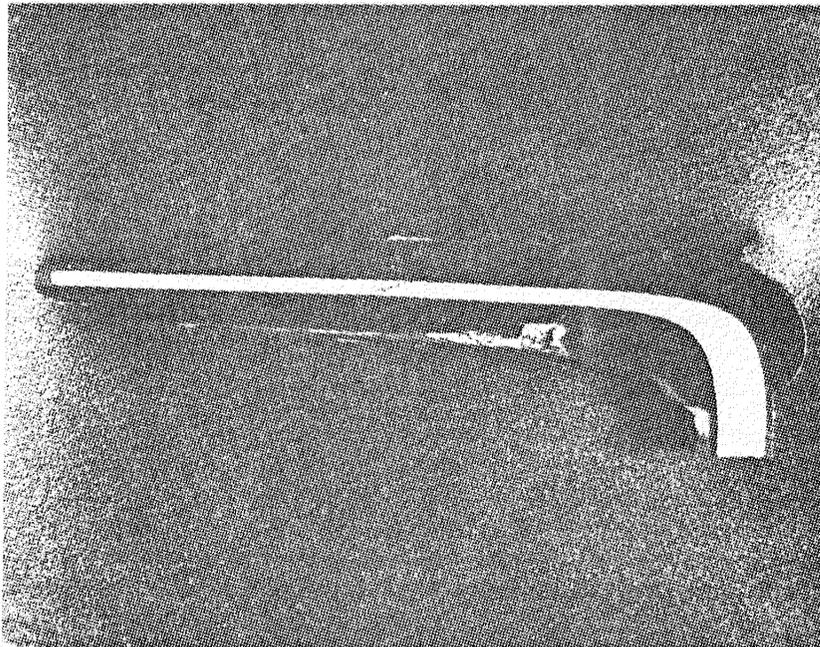
(A)
STRONGBACK BOWING ELIMINATED
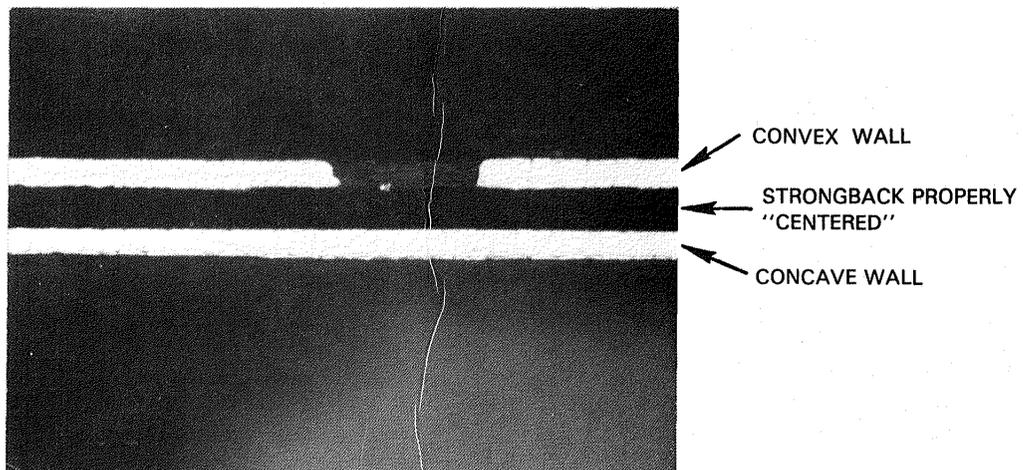
(B)

DESIRED TRAILING EDGE WALL THICKNESS UNIFORMITY ACHIEVED

Figure 33   Effects of Positive Contact Pinning of the Strongback at the Blade Tip and Slip-Joint Pinning of the Strongback at the Blade Trailing Edge

Metallographic examination of the PWA 1480 surfaces which had been in contact with ceramic (strongback or alumina-silica shell) revealed various amounts of a platelet phase as shown in Figure 34. The phase was characterized to be high in titanium and tantalum by microprobe analysis, identifying the platelets as Laves phase. Post-cast processing (alumina blast, grain etch plus prebond cleaning) was found to eliminate the platelet phase prior to the bonding operation.
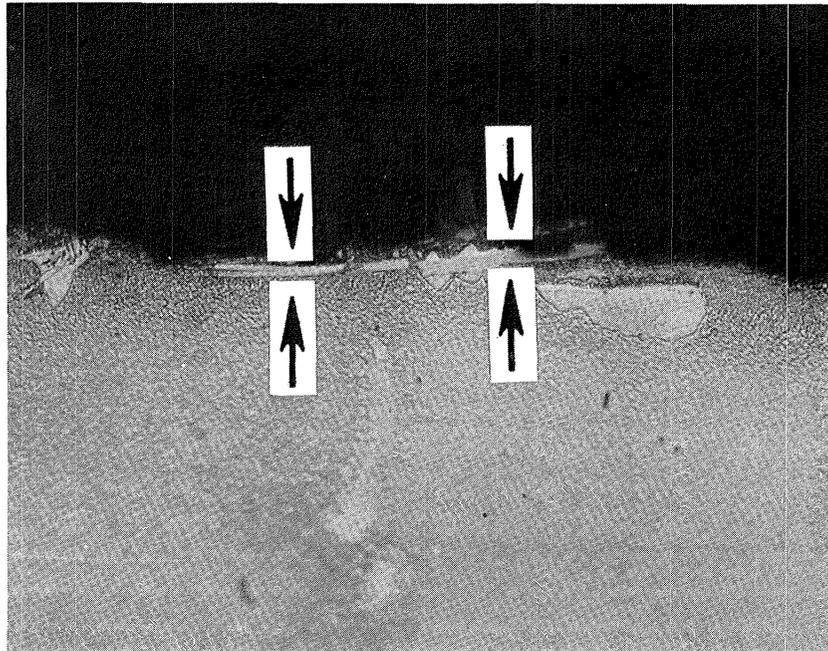
Figure 34   Microstructure of As-cast PWA 1480 Platelet Phase on the Cast Surface

Fluorescent penetrant and radiographic inspections of the blade castings revealed numerous inclusions in the thin trailing edge airfoil regions near the blade tips. Metallographic examination showed the inclusions to be due to slag (dross) type inclusions (Figure 35) traceable to the experimental master melt. Slag-type inclusions were subsequently minimized by employing less reactive melt crucibles, ceramic ball filters in the mold pour cup to filter out impurities, and pouring the molten alloy with the induction power still on.

Visual and zyglo inspections of blade castings from the root-down mold design revealed unacceptable shrinkage porosity on the blade root platforms. The careful placement of blind risers coupled with precise withdrawal rate changes eliminated this problem, as shown in Figure 36.

MAG: 100X

MAG: 100X

Figure 35   Metallographic Sections Showing Dross-Type Inclusions
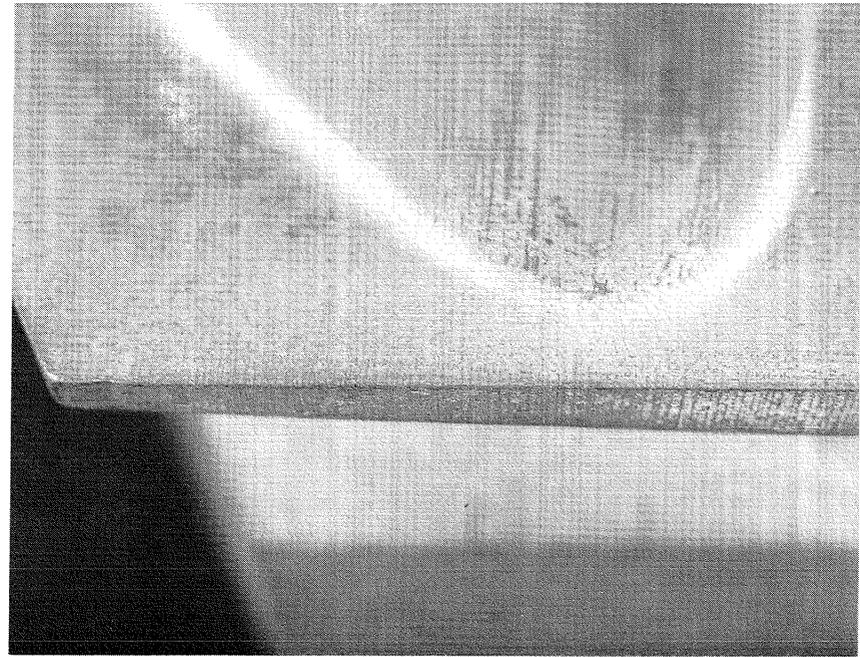
Figure 36   Two Energy Efficient Engine Blade Halves Showing Extent of
Shrinkage Porosity on Root Platform Before (Left) and After
(Right) Addition of Blind Risers and Withdrawal Rate Changes

4.4.3.2 Vane Casting Trials

In many cases, the problems encountered in casting the vane were very similar to those encountered in the blade. The similarities, however, were expected due to the similarities in design, specifically two piece airfoils, thin trailing edge walls, small wedge angle and the use of PWA 1480 against low pressure strongback formulations. Although the vane design did not require secondary crystal orientation control, the ability to control primary and secondary orientation to +3 degrees would permit interchangeability of vane halves (bonding the convex vane half from one mold to the concave vane half from a second mold without producing grain boundaries at the bond joint). Since interchangeability of vane halves is particularly attractive from a yield standpoint, it was decided to seed the vane castings to achieve the desired crystal orientation. Due to the basic size difference between the vane and the blade, the problems although similar, were multi-parametric and in many cases required different corrective action. A typical two-piece vane casting is shown in Figure 37.

INNER SHROUD

TRAILING EDGE

LEADING EDGE

OUTER SHROUD
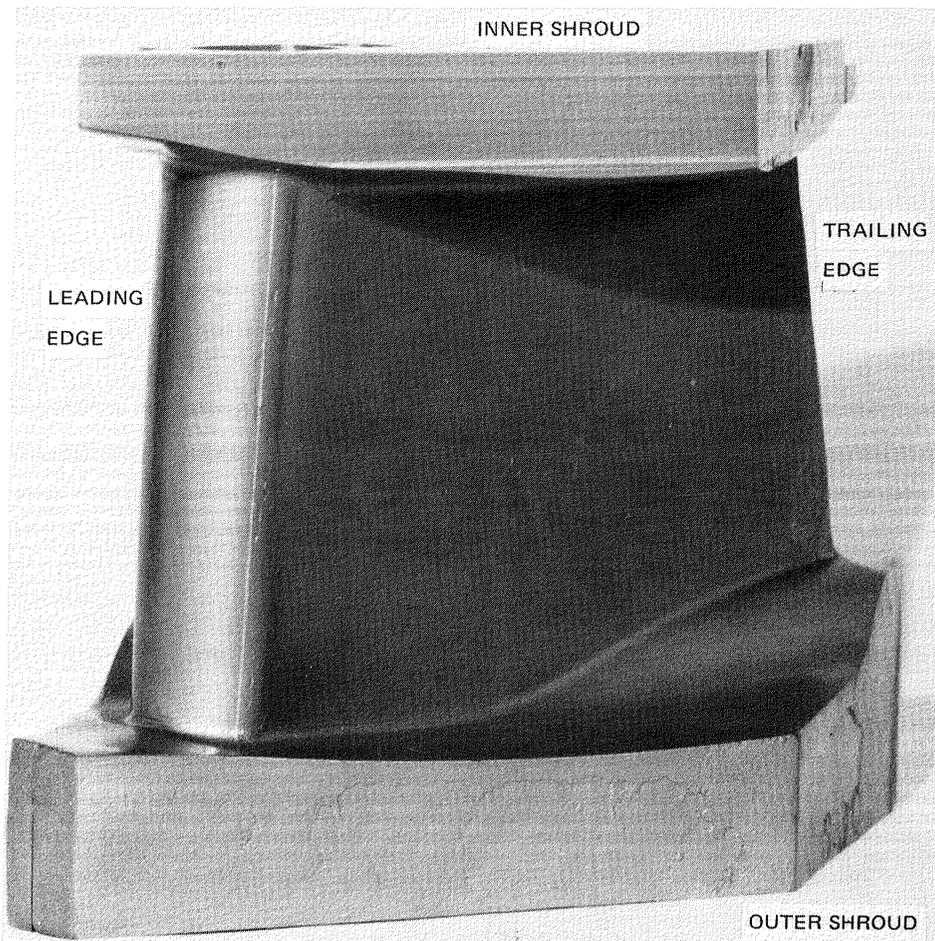
Figure 37   Bonded Energy Efficient Engine First Stage Turbine Vane
             Configuration

The establishment of epitaxial growth was successfully achieved by using the single article mold design and starting conditions established during blade casting trials. However the growth of acceptable single crystal through the relatively large shrouds (vane platform areas) met with considerable difficulty. The initial trial vanes were cast outer shroud-down and exhibited numerous freckle chains in the large expansion section below the outer shroud as shown in Figure 38. Extensive grain nucleation was evident on the inner shroud particularly at the extremities of the shroud and the thin weight pocket areas as shown in Figure 39. A reduced expansion section and increased ramp angle, coupled with a faster withdrawal rate eliminated the freckling problem. However, filled weight pockets, feeding modifications and extensive hot zone temperature to withdrawal rate (G/R) ratio adjustments failed to eliminate the inner shroud nucleation problems. The lateral growth needed to produce a single crystal inner shroud in the vane design could not be achieved using the outer shroud down mold design. Therefore, the orientation of the vane in the mold was changed as follows.

GROWTH DIRECTION
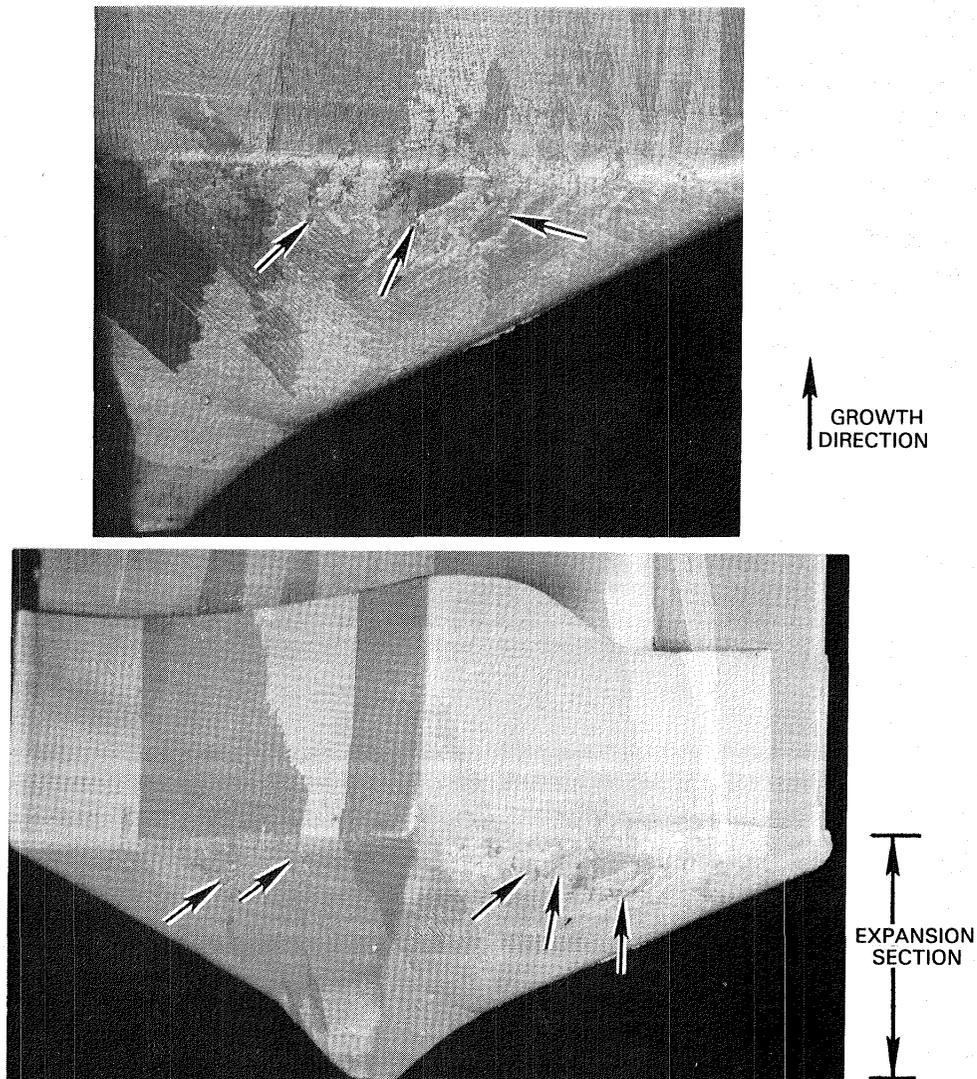
EXPANSION SECTION

Figure 38   Macroetched Energy Efficient Engine Vane Cast Outer Shroud-Down Showing Numerous Freckle Chains in the Large Expansion Section
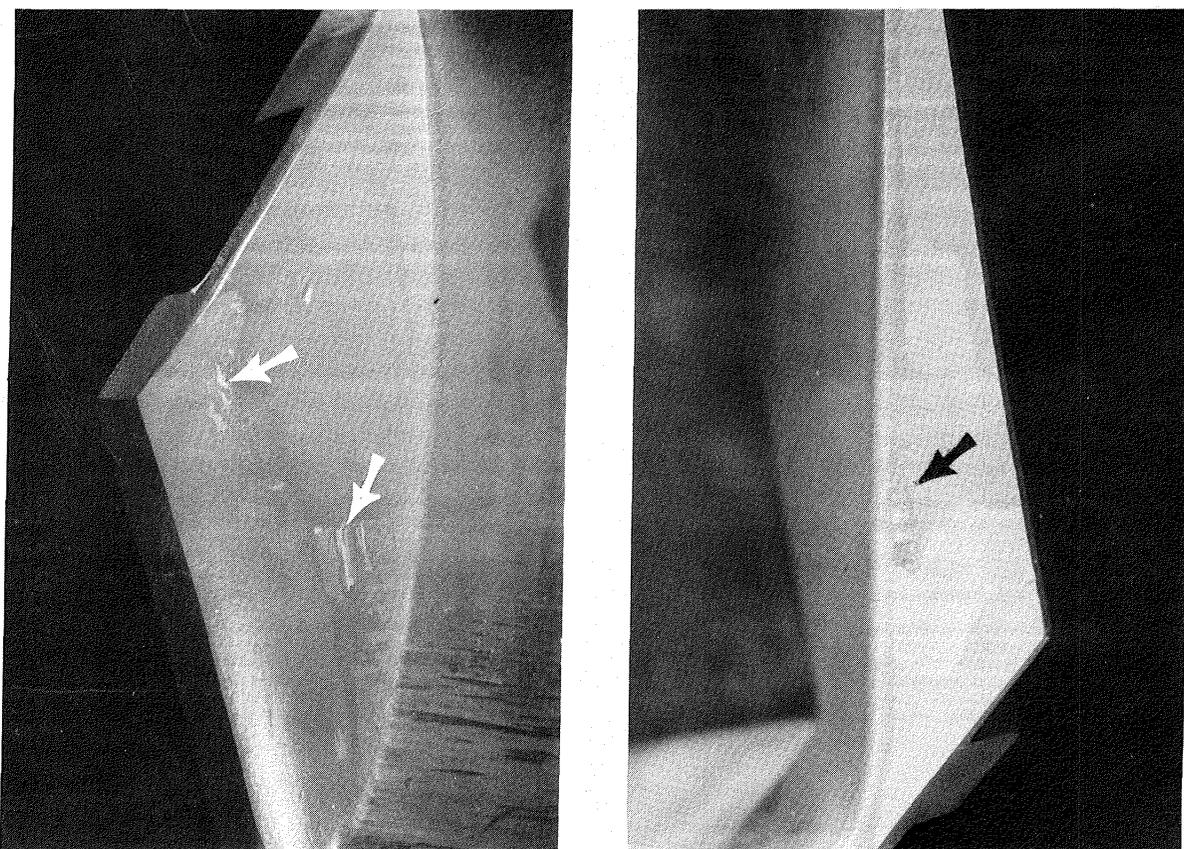
Figure 39   Macroetched Energy Efficient Engine First Stage Vane Showing Grain
Nucleation on Concave and Convex Inner Shroud Platforms

The vane leading edge or trailing edge was oriented down, thereby unidirec-
tionally solidifying the vane along an axis parallel to its chord width as
shown in Figure 40. This unique part orientation required a minor relocation
of the seed in relation to the new growth axis in order to position a <001>
secondary orientation parallel to the vane stacking line (note that seeding
now becomes mandatory since seeding the vane halves was not only desirable for
interchangeability of blade halves, but necessary to cast the vane in single
crystal form). Since the <001> orientations in the cubic system exhibit four
fold symmetry the particular <001> secondary direction which was oriented
parallel to the stacking line is irrelevant. The leading and trailing edge
down orientations eliminated the lateral single crystal growth problems and
provided for excellent airfoil and shroud single crystallinity as well as good
filling of the trailing edge region for the trailing edge down method. Extra-
neous nucleation was avoided by maintaining the proper (G/R) relationship
throughout the solidification cycle.
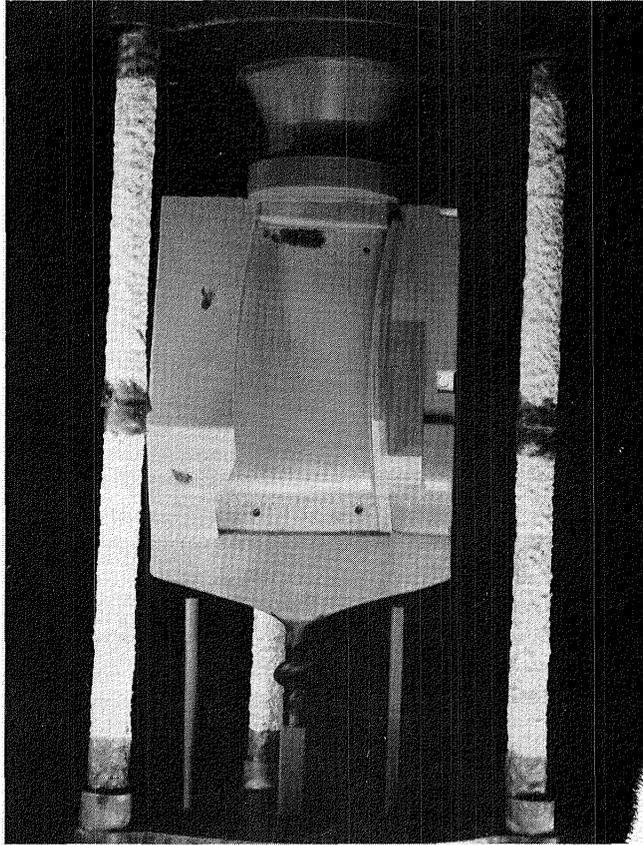
Figure 40   Single Unit Leading Edge Down Wax Assembly Used for Casting Single
             Crystal Energy Efficient Engine First Vanes

The problem of PWA 1480 reactivity with strongback formulations was en-
countered in the vane casting trials as well and was attacked in a manner
similar to that used in the blade casting trials. Again, the Sherwood SR200-S
formulation, which provided sufficient casting strength to enable the use of
"positive" contact strongback pinning, was coupled with relatively low hot
zone and metal pour temperatures to properly locate the strongback. The
leading-edge down and trailing-edge down mold configurations required
"positive" contact pinning at the trailing or leading edges, respectively,
whichever was at the top of the mold. The platelet phase (Laves) was again
successfully removed by post-cast processing operations prior to bonding.

Early outer-shroud down casting trials had exhibited trailing edge non-fill
problems which varied from voids to pedestal non-fill and/or pedestal rounding.
These non-fill problems were eliminated by using the trailing edge down mold
design which provided a substantial increase in metallostatic head pressure
and improved metal flow patterns in the thin trailing edge vicinity. Consistent
with the blade casting results, dimensional measurements of the large slab-
like vane airfoil geometry revealed extensive mold distortion at elevated
temperatures. In some cases, the airfoil wall thickness was found to be up to

100 percent oversize relative to the original wax. An extensive casting program was subsequently conducted, similar to the blade casting effort, to determine the optimum casting parameters needed to produce dimensionally acceptable single crystal vane airfoils. The initial casting trials incorporated lower hot zone (1496°C (2725°F)) and pour temperatures (1523°C (2775°F)), comparable to those developed for the blade, which included a 100 percent increase to approximately 1.2 cm (0.5 in.) in the shell mold thickness. These corrective measures substantially reduced the magnitude of the mold distortion but parts were still oversize. Therefore, another series of casting trials (similar to those for the blade) was conducted aimed at evaluating numerous shell reinforcement schemes. These included localized shell build-up, ceramic and metal reinforcement techniques and withdrawal rate adjustments. It was empirically determined that a series of three PWA 1480 metal plates enclosing the airfoil portion of the vane (Figure 41), coupled with the trailing edge down mold design, lower casting temperatures and increased shell thickness, produced single crystal vanes which were dimensionally acceptable after the post-cast processing operations required for pre-bond cleaning and inspection had been completed.
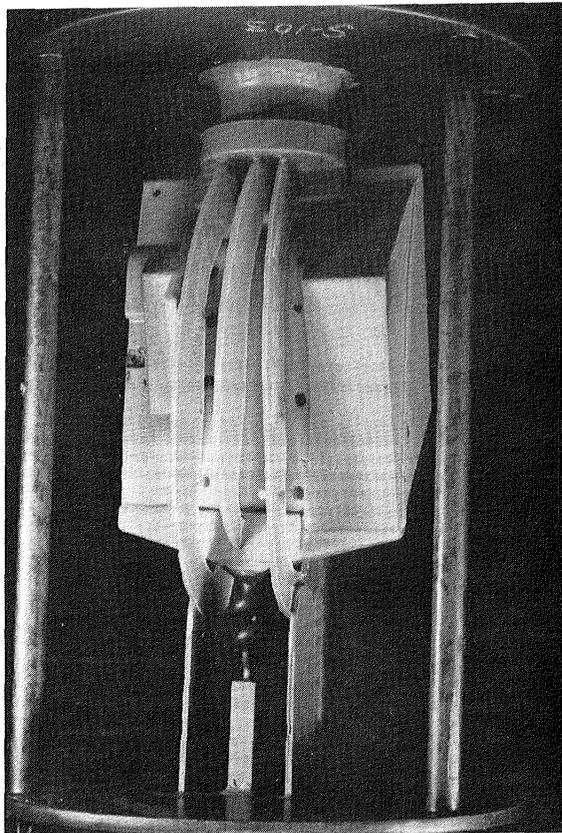
Figure 41   Energy Efficient Engine First Stage Vane Wax Assembly Illustrating Three Metal Plate Reinforcement Technique on a Trailing Edge Down Mold Design

An unexpected problem was encountered during post-cast processing of the vane. Extensive metal penetration into the shell was observed in the "S" wall vicinity of the outer-shroud down castings. Review of the shell dipping operations revealed that the location of the "S" wall to the airfoil fillet radius would not allow prime dips to drain properly prior to subsequent dipping operations. Steps to prevent this problem included slower drying cycles or using the trailing edge-down mold design, which improved the draining of the "S" wall and eliminated the metal intrusion problem, as shown in Figure 42.
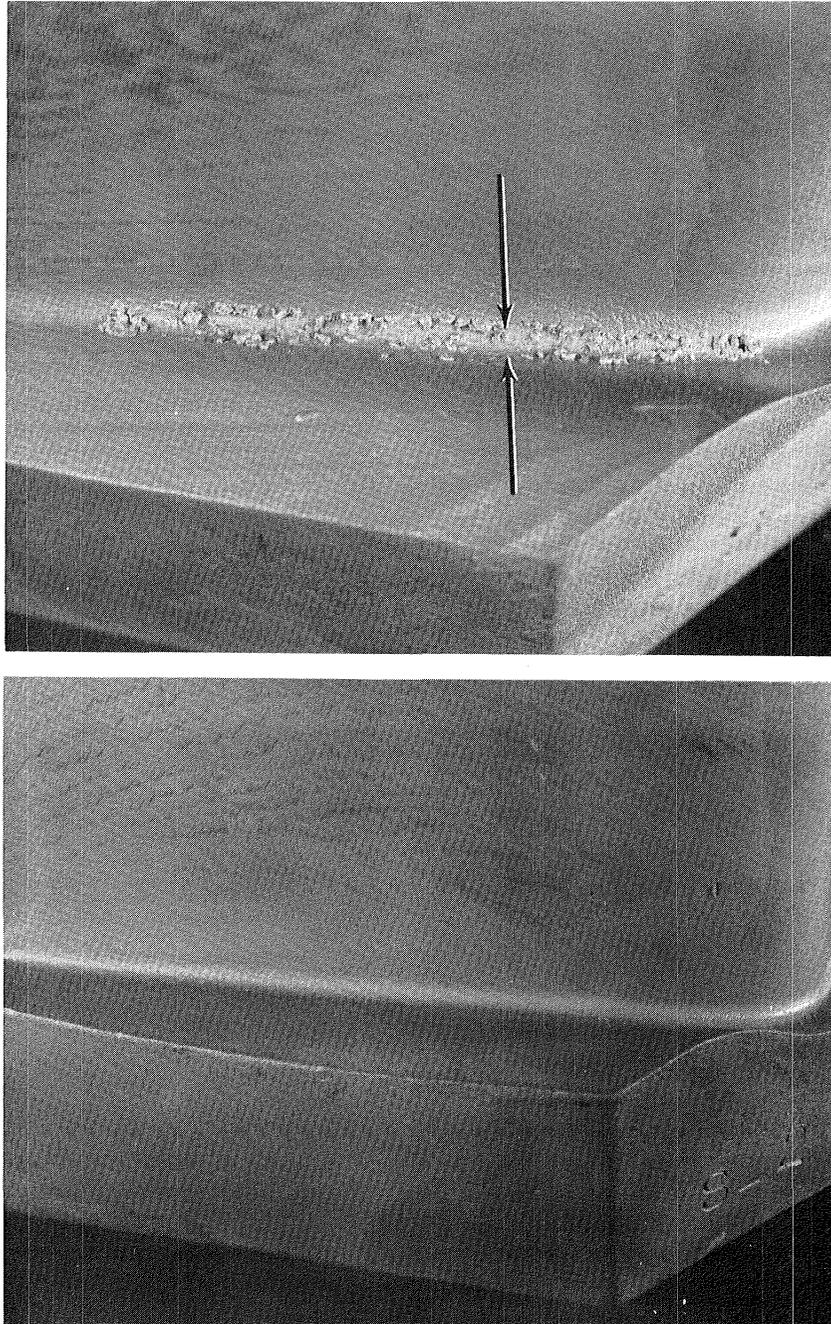
Figure 42   Energy Efficient Engine First Vane Outer Shroud Illustrating Metal Penetration into the Shell in the "S" Wall. Note: Lack of Metal Penetration when Vane was Cast Trailing Edge Down (Bottom Photo).

Similar steps to those used in the blade casting effort were successfully taken to minimize slag type inclusions caused by dross in the master melt. These steps included the use of ball filters and pouring the melt with the induction power-on.

Shrinkage porosity, which was observed on the top of the vane outer shroud (for the outer shroud down mold design), was eliminated by the careful placement of blind risers and use of decreased withdrawal rates at the critical point in the solidification cycle. The shrinkage porosity problem in the shrouds was absent in the trailing edge down mold design. In fact, this became an added advantage to the trailing edge down mold design since sensitive and often complex withdrawal rate changes were not required to prevent shrinkage porosity or facilitate single crystal growth.

4.5. Casting Reproducibility Assessment

The casting trials conducted in this program were aimed at establishing casting feasibility of large two piece single crystal turbine blades and vanes. In addition to evaluating the adaptability of the high rate solidification process to the relatively large single crystal configurations, the procedures and optimized casting parameters developed during these trials were next utilized to examine reproducibility. Four blades and four vanes were cast using the optimized casting parameters (1496°C (2725°F)) hot zone temperature and 1523°C (2775°F) metal pour temperature). The castings were then subjected to a complete evaluation.

Two basic types of castings were produced during the course of the program: solid blade and vane airfoils for mechanical property and microstructural substantiation and blade and vane halves for bonding and bench testing. The solid airfoil castings were necessary in order to provide machined-from-vane (MFV) and machined from blade (MFB) specimens large enough to be suitable for mechanical properties testing. Sufficient material thickness was not available in the vane and blade halves to do this. These solid castings were processed in a manner similar to the blade and vane halves in order to obtain accurately simulated material properties. For example, the solid hardware was solution heat treated in order to achieve optimum metal properties. Metallographic evaluation was conducted to verify the critical solution heat treat variables. The solid blades and vanes were then subjected to a simulated diffusion coating cycle and precipitation strengthening (aging) heat treatment. Standard Pratt & Whitney Aircraft practice was used to remove the machined-from-vane (MFV) and machined-from-blade (MFB) test specimens from the solid castings for subsequent tensile and creep-rupture testing (ref. Section 5.0, this report).

In order to evaluate reproducibility, certain PWA 1480 material specification requirements such as chemistry control, microstructure and orientation control were examined. These are discussed in the following sections.

4.5.1 Chemistry Control

Chemical analyses were performed for both the bottom and top sections of a PWA 1480 blade casting. The results indicated that all the major elements were within PWA 1480 specifications and that no significant elemental losses of the major elements occurred during casting (Table II).

TABLE II

ELEMENTAL LOSSES OF MAJOR ELEMENTS DURING CASTING

Major Element	Master Heat	Energy Efficient Engine Blade Chemical Analysis (Wt%)		PWA 1480 Specifications (Nominal)
		Root*	Tip*	
Chromium	10.2	10.6	10.3	(10.0)
Cobalt	4.8	5.0	5.0	(4.0)
Aluminum	5.0	5.2	5.0	(5.0)
Titanium	1.4	1.50	1.51	(1.5)
Tantalum	11.9	11.8	12.0	(12.0)
Tungsten	3.9	3.8	3.7	(4.0)

* Differences from master heat result because the mixture of elements is not entirely homogeneous and concentrations may vary within the castings.

4.5.2 Microstructure Control

Metallographic examination of sections through solid blades and vanes were conducted after solution heat treatment at 1287°C (2350°F) for 4 hours. The results clearly demonstrated that fully acceptable microstructures were achieved in both the blade and the vane. Close examination revealed a section size affect which was due to macrosegregation in the large blade root and vane shroud sections. The large vane shrouds indicated acceptable levels of gamma prime, γ', solutioning and the thinner airfoil sections indicated complete gamma prime solutioning as shown in Figure 43. These heat treatment variations were not totally unexpected and previous mechanical testing has shown both structures yield acceptable mechanical test properties (Reference 1).
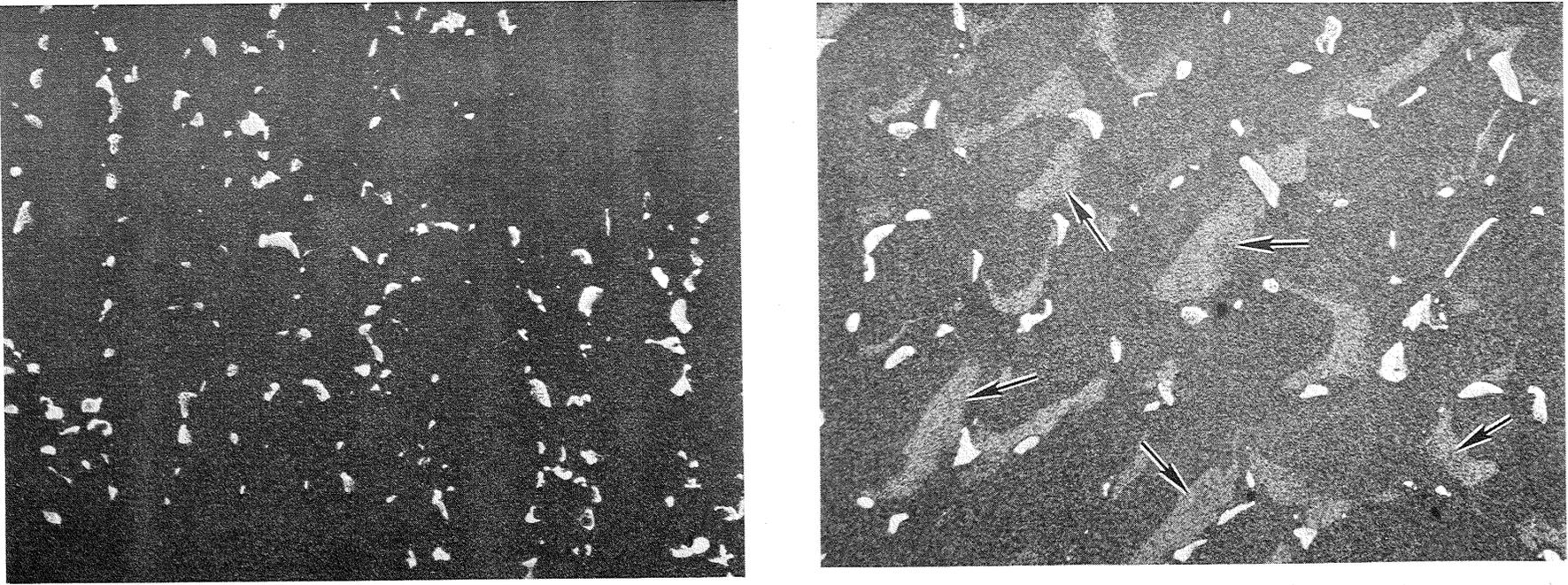
Figure 43   Photomicrographs of Sections through Solution Heat Treated PWA
1480 Energy Efficient Engine Blade and Vane Showing Complete
(Left) and Partial Solutioning (Arrows-Right) of the Gamma Prime

4.5.3 Crystallographic Orientations Control

Back reflection Laue x-ray analysis of seeded blades and vanes was conducted to confirm visual observations of crystallographic orientation control. This method utilizes a beam of white radiation which is allowed to impact on the single crystal. The Bragg angle (which is the angle at which diffraction occurs) is, therefore, fixed for every set of atomic planes in the crystal. Each diffracted beam has a different and distinct wavelength which collectively, form an array of spots on a photographic film. This array is commonly termed a Laue pattern and the positions of the spots on the film depend on the orientation of the crystal relative to the incident beam (Reference 2). Since the orientation of the blades and vanes was determined from the location of the Laue spots on the film, it was necessary to construct fixturing to orient the incident beam parallel to the stacking line of the part as shown in Figure 44. Prominent features of the <001> Laue pattern which allow for the determination of primary and transverse (secondary) cube directions are shown in Figure 45. A typical Laue (x-ray diffraction) pattern showing control of the crystal orientation in the blade is shown in Figure 46.
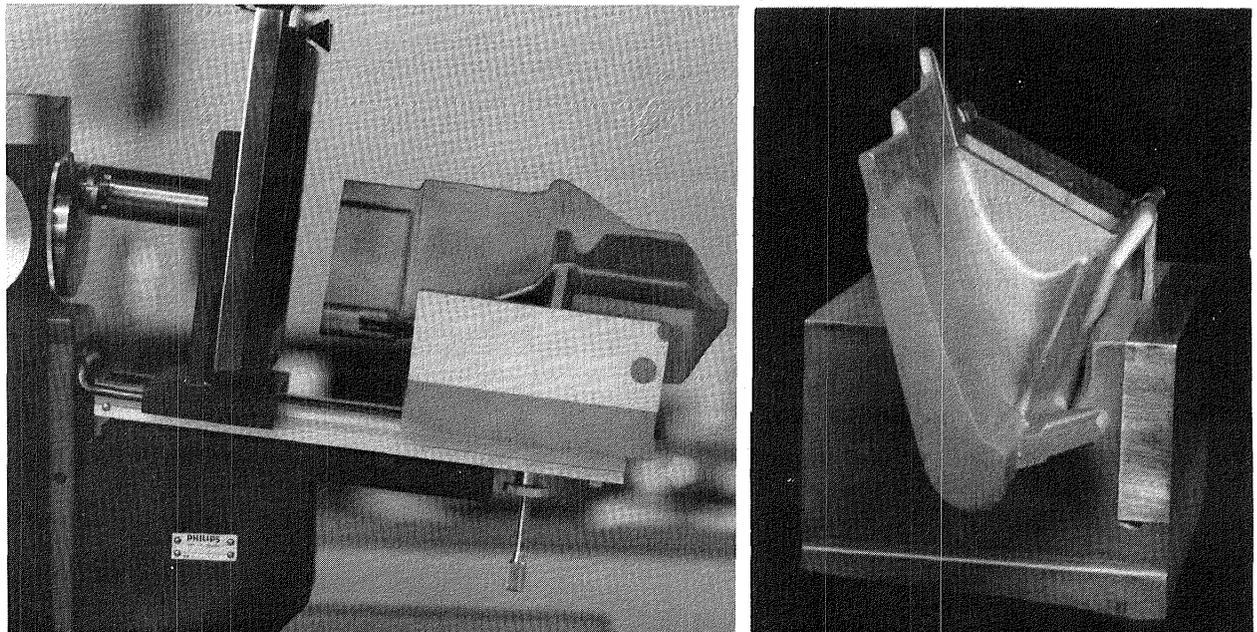
Figure 44   Laue Fixture Utilized to Orient the Incident Beam Parallel to the Stacking Line of the Energy Efficient Engine First Blade

TO [010]

TO [110]

TO [100]

[001]

⟨319⟩
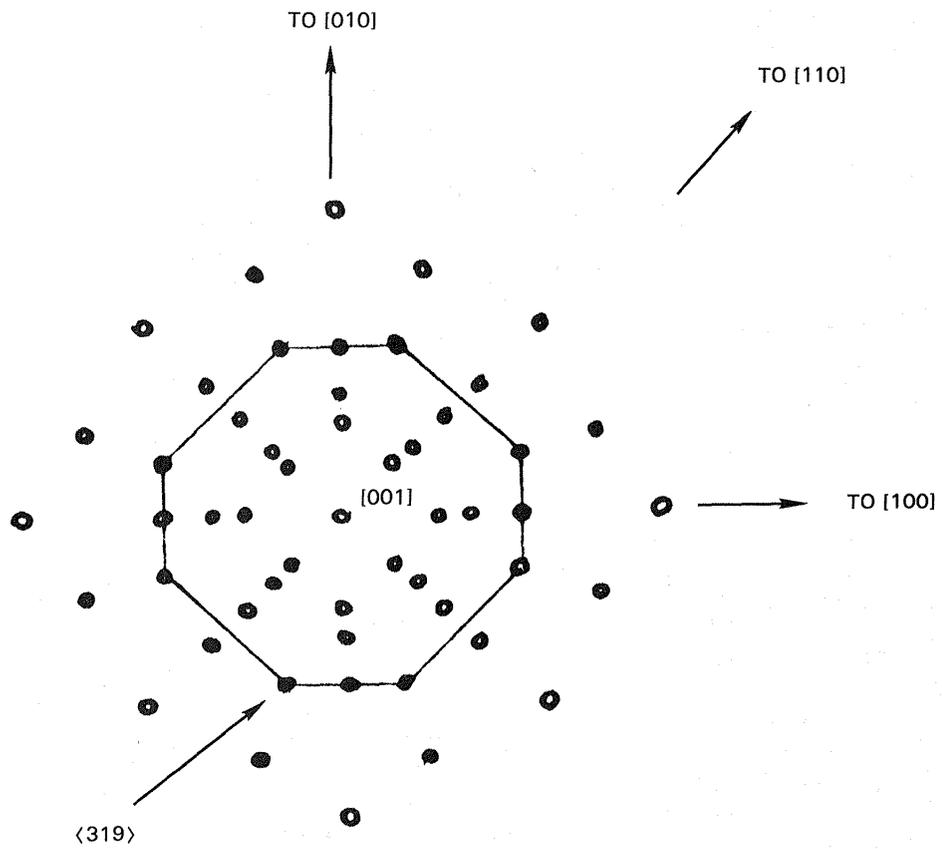
Figure 45   Schematic of a Typical <001> Laue Pattern Showing Prominent
Features
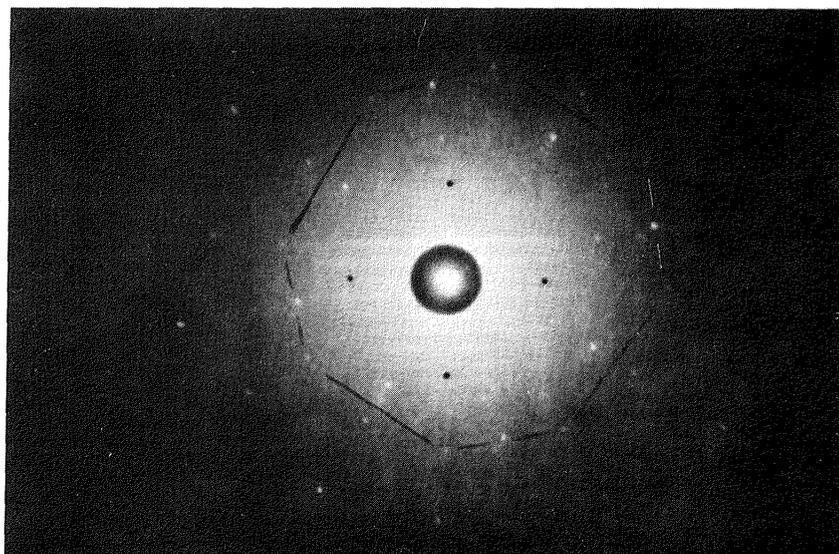
Figure 46   X-Ray Diffraction (Laue) Polaroid Showing Control of Crystal
Orientation in Typical Energy Efficient Engine First Stage Blade

The results of seeding both the blade and vane configurations are shown in Table III. These data demonstrate the ability to achieve epitaxy and controlled single crystal growth in both the blade and vane configurations. Certainly, the blade goal that the secondary crystalline axes <100> and <010> be rotated $27° \pm 5°$ from the blade x-y coordinates was controlled in that $-26.25° \pm 2.\overline{25}°$ was achieved for one blade and $-27 \pm 1°$ for a second blade. The vane results of $2° \pm 2°$ and $5° \pm 2°$ from <001> were well within the $10° \pm 3°$ goal.

TABLE III

BACK REFLECTION LAUE DATA FOR SEEDED
ENERGY EFFICIENT ENGINE BLADES AND VANES

Part	Location	$\underline{x}^1$	$\underline{y}^2$	$\underline{001}$	$\underline{B}^3$
First Vane	Inner & Outer Shrouds	1.5 ± 1.5	1.5 ± 1.5	2 ± 2	4 ± 2
First Vane	Leading Edge & Trailing Edge	$-1 \pm \frac{4}{3}$	$4.5 \pm \frac{1.5}{3}$	5 ± 2	-1.5 ± 1.5
First Vane (Absolute)	Max Allowance Goal			10 ± 3	5 ± 3
First Blade	Airfoil Tip	-4.25 ± 2.25	5.5 ± 3.5	6.25 ± 3.25	-26.25 ± 2.25
First Blade	Airfoil Tip	2 ± 6	4 ± 4	6.75 ± 4.75	-27 ± 1
First Blade (Absolute)	Max Allowance Goal			10 ± 3	27 ± 5

1. X-axis coordinates of the primary single crystal growth direction measured from the stacking line in a direction parallel with a reference surface on the part.

2. Y-axis coordinates of the primary single crystal growth direction measured from the stacking line in a direction perpendicular to a reference surface on the part.

3. B is the angular deviation of the secondary single crystal growth direction measured in a plane perpendicular to the stacking line and referenced to a surface parallel to the blade or vane stacking line.

4.5.4 Dimensional Control (Blades and Vanes)

Excessive mold distortion at the elevated temperatures involved in the initial vane and blade casting trials resulted in oversize airfoils. The amount of oversize varied but was typically in the order of 0.076 cm (0.030 in.) for the vane and 0.063 cm (0.025 in.) for the blade (dimensions are per side).

As discussed in the Casting Trials section, a number of modifications to the process were incorporated to reduce the distortion. These included reduced mold temperature, a thicker reinforced shell structure with additional radiation baffling, adjusted casting parameters, and various bracing schemes. The modifications were effective in reducing the oversize airfoil thickness to 0.033 - 0.015 cm (0.006 - 0.013 in.) for the vane and 0.010 - 0.027 cm (0.004 - 0.011 in.) for the blade, as measured at the trailing edge (see Figure 47).

1537°C - 1551°C (2800°F - 2825°F) MOLD
1565° (2850°F) MELT
0.5 cm (0.2 in) THICK SHELL
NO BRACING

1482°C (2700°F) MOLD
1496 °C - 1510°C (2725°F - (2750°F) MELT
1.01 cm (0.4 in) to 0.12 cm (0.05 in) THICK WALL
VARIOUS BRACING SCHEMES
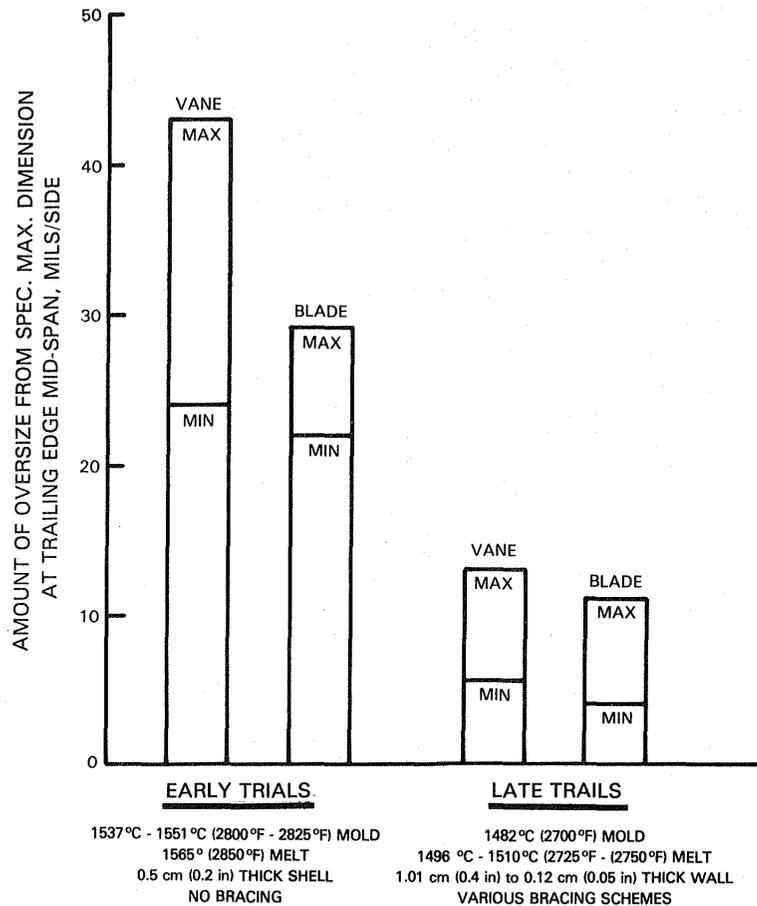
NOTE: REPRESENTS TWO TYPICAL BLADE & VANE CASTINGS

Figure 47   Blade and Vane Thickness Deviations

Shadowgraph comparisons of vane sections to blueprint requirements were not taken since thickness measurements were easily measurable with calipers on casting halves. Inspections of vane and blade strongbacks were completed, however, with results showing dimensions acceptable to blueprint except for the blade rib misalignment discovered during bonding (see section 5.4.2.3 and Figure 74).

Final airfoil thickness dimensions were approximately 0.007 cm (0.003 in.) less than casting dimensions due to post-cast processing which included alumina blast, grain etch, and prebond cleaning.

4.6 Casting Results and Conclusions

During the casting phase of this effort, casting feasibility was demonstrated and several blade and vane halves were made for the bonding trials. In addition, solid blades and vanes were successfully cast and heat treated for use in the materials evaluation tests. All cast specimens exhibited the required microstructure and chemical composition. Single unit mold technology was found to enhance thermal gradient control and crystal growth while permitting lower mold temperatures, which alleviated internal ceramic breakdown of the mold materials. Seeding of the PWA 1480 single crystal material was determined to be necessary in order to assure epitaxial growth and to provide the required primary and secondary crystalline orientation. Several significant problems were addressed and corrected during the course of the casting effort. These are summarized in Tables IV and V. The significant problems are segregated to show those associated with the blade casting effort and those associated with the vane casting effort.

TABLE IV

VANE CASTING EFFORT

Problem Areas	Corrective Action
o Vane Strongback Tolerances	o Improved vendor fabrication technique, fabricated inspection gages.
o Strongback Cracking	o Strengthened strongback outside of airfoil by eliminating extended rib and reducing remaining ribs' sharp corners
o Wax Injection (1) Non-fill (2) Strongback Cracking	o Mixture of high fluidity waxes; die venting; ingate relocation; wax pads; modified pinning; wax temperature, flow and pressure adjustments; trimmed strongback; die temperature
o Seeding Epitaxy (1) Melt-back	o Improved baffling; relocation of chill plate relative to hot zone
o Single Crystal Growth (1) Freckles (2) Lateral Growth (3) Shroud Nucleation	o Incresed withdrawl rate; filled weight pockets, leading edge or trailing edge down; reduced expansion section; increased ramp angle

TABLE IV (Continued)

VANE CASTING EFFORT

Problem Areas	Corrective Action

o Strongback Reactivity
  (1) Welts
  (2) Surface Roughness
  (3) Platelet Phase
	o Lower hot zone and pour temperatures; less reactive ceramic (SR200-S); trailing edge down

o TE and LE Non-fill
  (1) Pedestal Rounding
  (2) Cold Shut
  (3) Voids
	o Trailing edge down; rapid pour; long mold soak; metallostatic head

o Strongback Distortion (1) Bowing	o Lower hot zone temperatures; refined pinning techniques
o Shell Distortion (1) Metal Penetration	o Trailing edge or leading edge down; eliminate binder dip after first prime; close surveillance during dipping
(2) Dimensions (Oversize)	o Increased shell thickness; CaO deletion; lower hot zone and pour temperatures; localized shell build-up; numerous ceramic and metal reinforcement techniques; part orientation; withdrawal rate increase
o Shrinkage Porosity (1) Top Surface of Shroud	o Leading or trailing edge down; blind risers; withdrawal rate

TABLE V

BLADE CASTING EFFORT

Problem Areas	Corrective Action

o Wax Injection
  (1) Non-fill
  (2) Strongback Cracks
	o Mixture of high fluidity waxes; die venting; wax pads; modified pinning; wax temperature and pressure adjustments; wax flow rate; heated strongback

o Seeding (Epitaxy)	o Improved start conditions; relocate chill plate relative to hot zone; helical restrictions

50

TABLE V (Continued)

BLADE CASTING EFFORT

Problem Areas	Corrective Action

o Single Crystal Growth
   (1) Extraneous Nucleation
   (2) Lateral Growth
	o Withdrawal rate adjustments; baffling modifications

o Strongback Reactivity
   (1) Welts
   (2) Surface Roughness
   (3) Platelet Phase
	o Lower hot zone and pour temperatures; less reactive ceramic (SR200-S)

o TE Non-fill
   (1) Pedestal Rounding
   (2) Cold Shut
   (3) Voids
	o Rapid pour; long mold soak; metallostatic head

o Strongback Distortion (1) Tip Bowing	o Lower hot zone temperatures; increased pinning locations
o Shell Distortion	o Localized shell build-up o Increased shell thickness; CaO deletion; lower hot zone and pour temperatures; localized shell build-up; numerous ceramic and metal reinforcement techniques
o Shrinkage Porosity (1) Platform	o Blind risers; withdrawl rate adjustments

5.0 BONDING FEASIBILITY

5.1 Overview

The approach used to meet the bonding challenges posed by the complex geometries of the two-piece high-pressure turbine blades and vanes was similar to that used in establishing casting feasibility, i.e., employ an established bonding procedure and modify it as necessary to resolve specific problems encountered. For this program, existing PWA 1480 Transient Liquid Phase (TLP®) bonding technology and two-piece blade bonding experience provided the reference procedure.

The transient liquid phase bonding process was developed primarily for joining difficult-to-weld high strength superalloys. This combines features of both diffusion bonding and high temperature brazing to produce high strength bonds without the high capital cost and stringent processing requirements usually associated with diffusion bonding. Highlights of this process are illustrated in Figure 48. The transient liquid phase bonding process utilizes an interlayer material (A), similar in composition to the base metal being bonded. Boron is added to the interlayer material as a melting point depressant, so that substantial melting of the interlayer occurs below the incipient melting temperature of the alloy being joined.
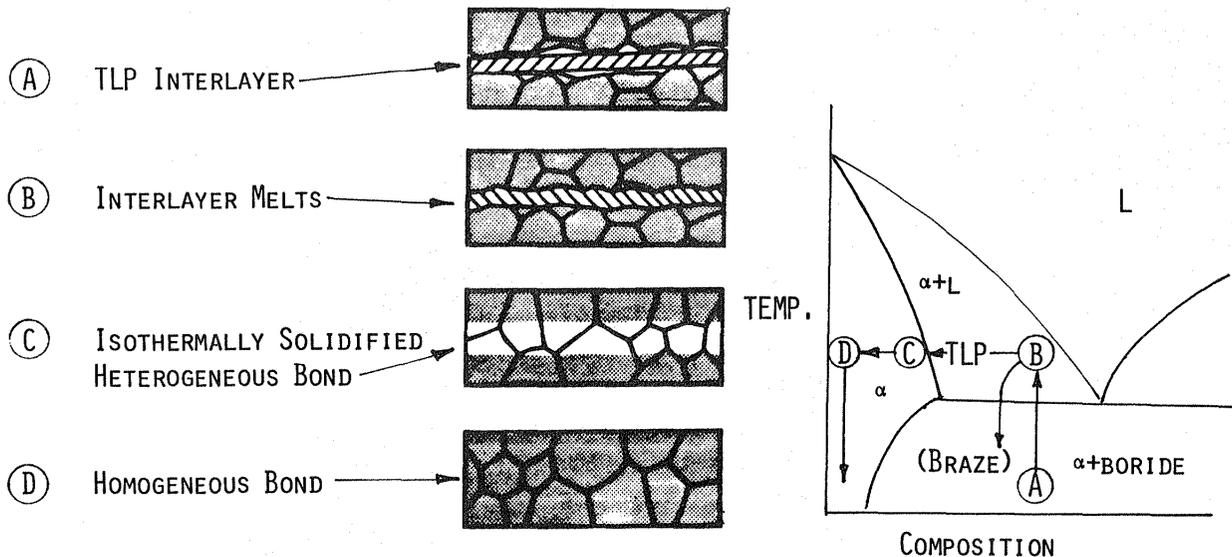
Figure 48   Transient Liquid Phase Bonding Process

A positive load is applied normal to the bond plane and the assembly is heated to the bonding temperature (B), where the transient liquid phase interlayer melts and forms a joint similar to a braze joint. Unlike a braze, however, the

bond is held at the bonding temperature allowing the melting point depressant, boron, to diffuse into the base metal raising the melting-temperature of the joint. A transient liquid phase bond is held at the bonding temperature for a sufficient duration that complete isothermal solidification occurs (C) due to the reduced boron level. The bond cycle can then be continued further (D) to eliminate any chemical or microstructural heterogeneity in the joint area. Homogeneous bonds can be achieved with properties equivalent to or approaching those of the base metal being bonded.

The key features of the process are the thermal cycle and the Transient Liquid Phase interlayer (preform) composition. Bonding thermal cycles are generally developed for each specific material and component property requirements. The cycle must produce the desired bond properties and be compatible with the base metal heat treatment without degrading base metal properties. A suitable transient liquid phase bonding thermal cycle has been identified for bonding PWA 1480 single crystal alloy. The established bonding thermal process for PWA 1480 includes a bonding cycle of 1232°C (2250°F) for 24 hours followed by the full PWA 1480 heat treatment (i.e., solution heat treatment, coating diffusion treatment, and aging treatment).

As part of the company sponsored programs, a transient liquid phase interlayer composition has been established for bonding PWA 1480 single crystal alloy. This transient liquid phase composition is designated TLP® -613 (PWA 1184).

Utilizing the established thermal cycle, the transient liquid phase interlayer produces transient liquid phase bonds with mechanical properties essentially equivalent to the PWA 1480 base alloy. A typical microstructure of a laboratory prepared PWA 1480 transient liquid phase bond is shown in Figure 49. Transient liquid phase bonds with microstructures similar to that shown in the figure have produced 982°C (1800°F) stress rupture lives and isothermal low cycle fatigue properties comparable to the base metal (Figures 50 and 51).
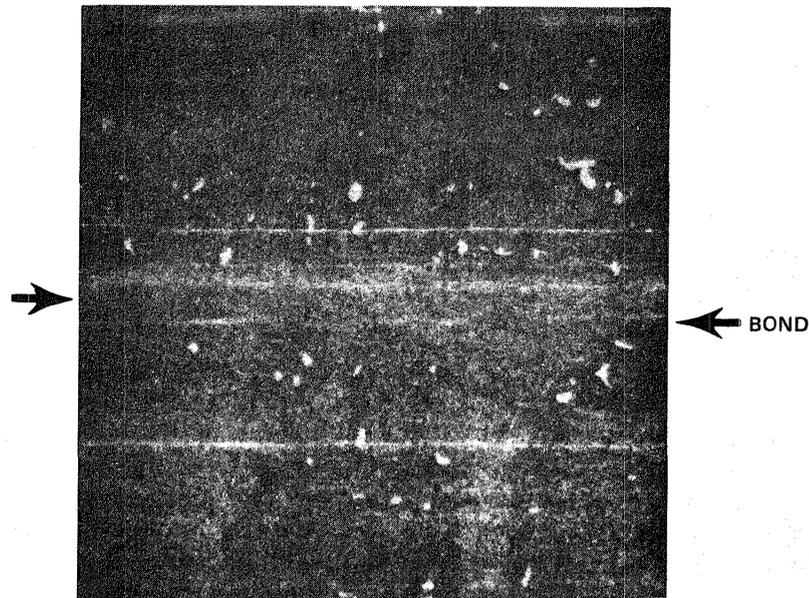
Figure 49   Typical PWA 1480 Transient Liquid Phase Bond Microstructure (Crystallographically Oriented)
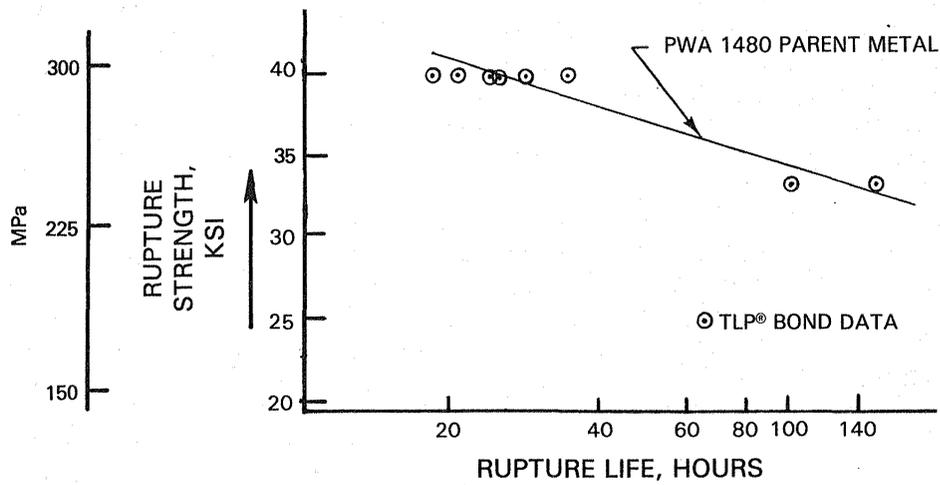
Figure 50   982°C (1800°F) Stress-Rupture Properties of PWA 1480 Single Crystal
Transient Liquid Phase Bond
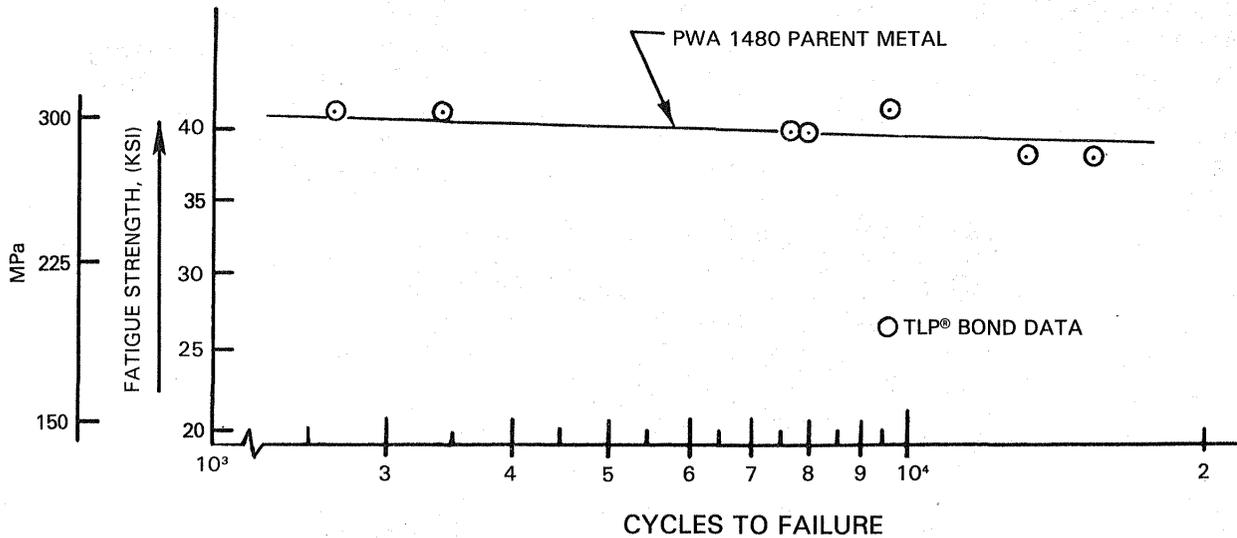
Figure 51   982°C (1800°F) Isothermal Low Cycle Fatigue Properties of PWA 1480
Transient Liquid Phase Bonds

54

Important to the bonding of single crystal alloys is maintaining crystallo-
graphic orientation across the bond plane. Due to the epitaxial growth of the
isothermal solidification front from each mating surface, no undesirable bond
grain boundaries are formed if crystallographic orientation is maintained in
both mating halves. Crystallographic misorientation between the mating halves
will create a grain boundary in the bond causing reduced bond mechanical pro-
perties. Experience has shown, however, that bond stress-rupture properties
are maintained with as much as 5 degrees of misorientation across the bond.

The basic elements of the bonding procedure used for this program are shown as
a logical sequence of events in Figure 52. Each is discussed in more detail in
the following sections of the report. The objective of this portion of the
total effort was to evolve a bonding procedure that would ensure a high degree
of reproducibility of two-piece blades and vanes. Two of the major areas of
concern addressed were (1) achieving good bond plane fit-up between the mating
casting halves and (2) bond tooling that would provide the desired loading
distribution to the cast halves.
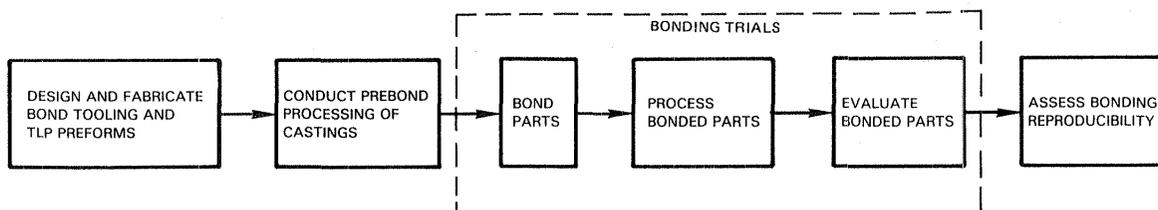
Figure 52   Steps in Achieving Bonding Feasibility

5.2   Bond Tooling and Transient Liquid Phase Preform Design and Fabrication

Bonding of the cast parts is accomplished with the use of a bonding tool
assembly whose primary elements are the bonding tools, the castings to be
bonded, and the TLP$^{\circledR}$ preform. An exploded view of a typical assembly is
illustrated in Figure 53.

The bonding tool is shaped to conform to the external contours of the castings
so that uniform pressure is applied over the surface of the castings. Tool
designs were dictated by the high-pressure turbine blade and vane design de-
tails that defined the blade and vane casting geometries. Bond tooling design
philosophy included provisions for separate fixtures for those areas in the
blade and vane castings where bond line fit-up was anticipated to be a problem.
This "segmented" tooling approach provided a means for "fine tuning" the load-
ing parameters in those critical areas in order to achieve good bonds.
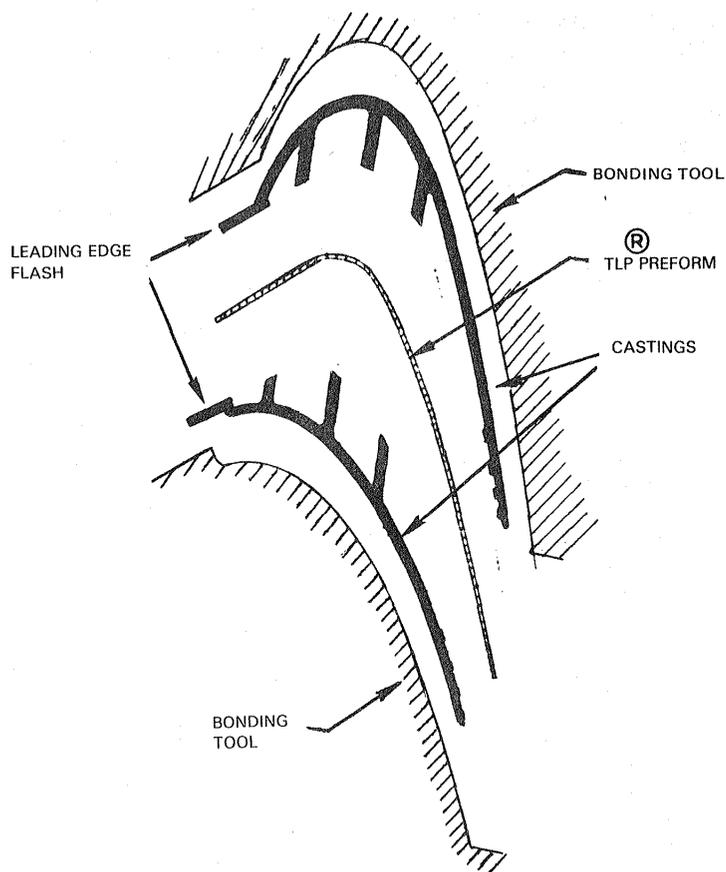
Figure 53   Typical Bonding Assembly for a Two-Piece Casting (Exploded View)

For the vane, this capability was not required because the vane bonding plane was essentially planar. However, the severe twist and camber in the blade air-foil and root sections resulted in a complex bond plane that required separate fixtures for these sections and subsequent modifications to these fixtures in order to achieve satisfactory bonds.

5.2.1   Bond Tooling Design and Fabrication

Although fit-up between the mating surfaces of a transient liquid phase bond is not as critical as for a diffusion bond due to the presence of a liquid phase, joint fit-up is important to attain maximum properties and minimize the bond thermal cycle time. With simple, flat bond surfaces, only small loads 69 kPa (10 psi) are required to achieve adequate fit-up; these loads can be gene-rated by dead weight loading.

In order to achieve adequate fit-up for two-piece blades with curved bond planes, a new loading system was developed at Pratt & Whitney Aircraft which generates higher loads without adding bulk to the furnace load in the form of added dead weight. This system utilizes differential thermal expansion ($\Delta \alpha$) between the blade/die assembly and a low expansion yoke as shown in Figure 54. Minimal preloads are established during assembly to hold the halves together. As the assembly is heated to the bonding temperature, the yoke squeezes the die due to the differences in thermal expansion between the yoke and die. This imposes an increasing load on the halves being bonded together. A typical load characteristic is shown in Figure 55. The specific load/temperature profile of a die system is controlled by deformable spacers with controlled properties and configuration. These spacers are designed to yield during heat-up, reducing the bonding load and preventing over-loading and deformation of the component.

CHARACTERISTICS OF
DEFORMABLE SPACERS
PROVIDE TAILORED
BONDING LOAD

HI α
DIE

COMPONENT

HI α
DIE

LOW α YOKE
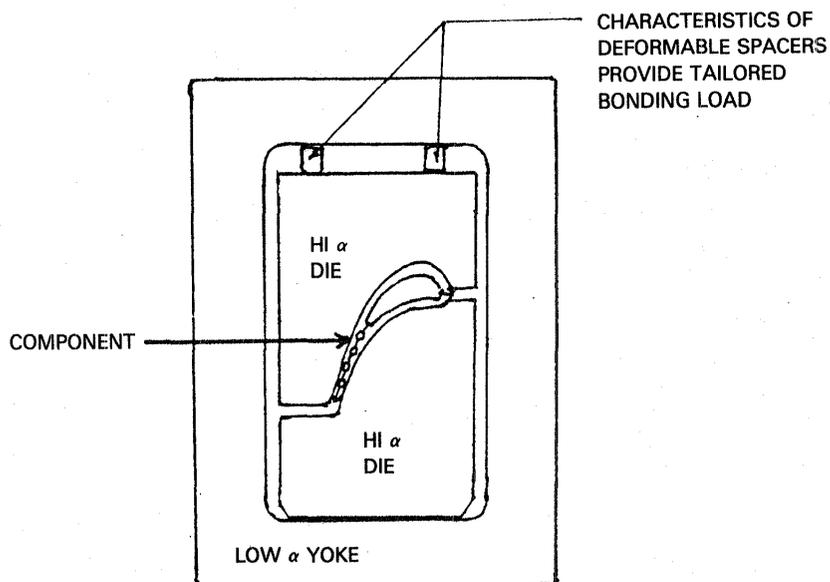
Figure 54   Differential Thermal Expansion Transient Liquid Phase Bond
Tooling Approach

Bond tooling layouts and detail designs were completed for both the Energy Efficient Engine vane and blade configurations. The detail features of the tooling were designed for easy assembly and adaptability during the bonding trial phase of the program. All of the airfoil bonding dies and flat spacers were fabricated from DA-25 material. DA-25 is a conventionally cast alloy similar in composition to the PWA 1480 blade alloy, modified to slightly reduce its compressive strength. The airfoil die halves were investment cast to the actual airfoil contour, requiring minimal grinding on the opposite flat face of the dies. All flat spacers were investment cast to near net shape with grinding required only on the bearing surfaces. All of the low expansion yokes

and tapered spacers were machined from TZM molybdenum alloy. The original deformable spacers were machined from Type 330 stainless steel plate. As the bonding trials progressed, it became necessary to utilize DA-25 deformable spacers. These spacers were investment cast with the required 4-degree taper to allow proper assembly fit during bonding.
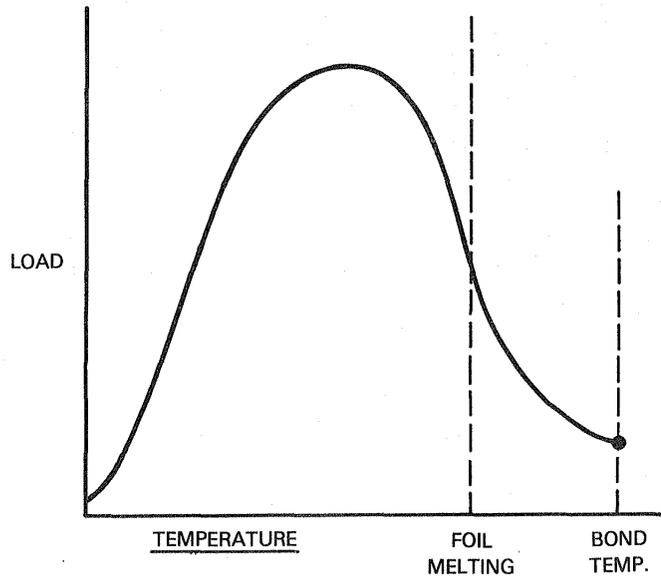
Figure 55   Typical Load/Temperature Characteristics of Differential
             Expansion Transient Liquid Phase Bond Tooling

5.2.2   Transient Liquid Phase Preform Design and Fabrication

The design of the TLP® preform is defined by the contact surface geometry of the mating blade or vane halves at the bond plane. Detail designs of the transient liquid phase foil preforms were generated from digitized layouts of the bonding planes flattened out by computer to form a two-dimensional representation of the bond plane. This procedure was satisfactory for the vane preforms. However, the blade preform designs required additional hand fitting to the actual blade bond plane due to the compound curvature in the blade, which could not be easily simulated by computer techniques. The vane preform was made in two pieces; the leading edge and first rib sections were made in one piece with 0.02 cm (0.010 in.) wide connectors, the trailing edge and interconnected second rib were made as one unit. Connectors which were 0.02 cm (0.010 in.) wide were added to support pedestal bond areas and reinforce the rib section for handling purposes. A typical vane preform is illustrated in Figure 56. The blade preform was made in three distinct sections. The first section included the leading edge, tip, tip turning vanes and third rib. The second piece was comprised of the trailing edge root section, root end turning vane and second rib. The third preform covered the pedestal array. An example of the blade preform is shown in Figure 57.
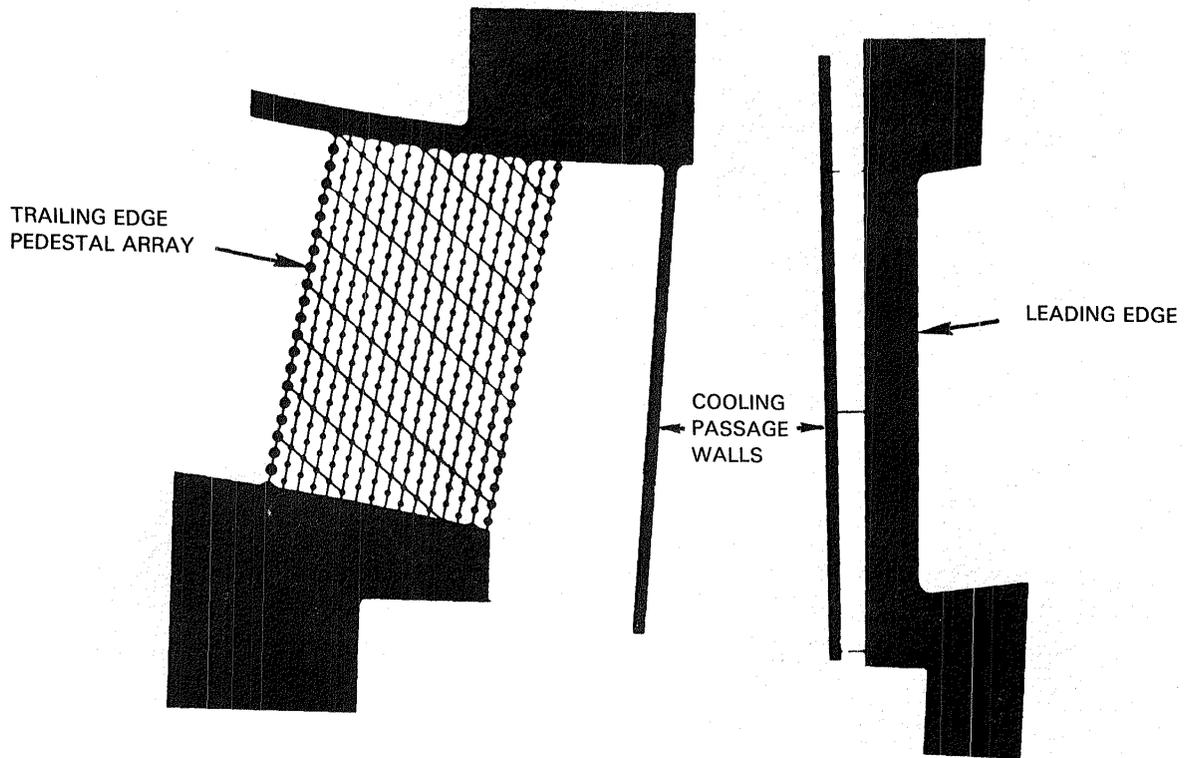
Figure 56   Two-Piece Vane Transient Liquid Phase Foil Preforms
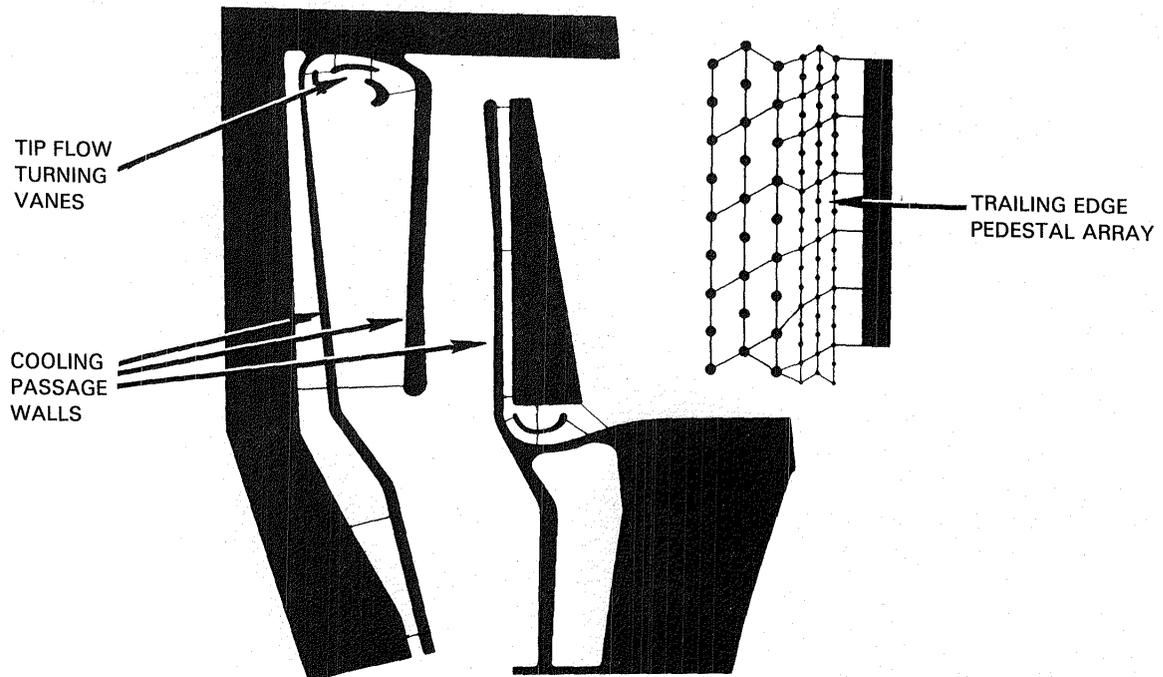
Figure 57   Three-Piece Blade Transient Liquid Phase Foil Preforms

The optimum method of applying the transient liquid phase interlayer to the bond joint is by preplacing a 100 percent dense foil to the mating surface. Boron, as stated earlier, is added to the interlayer as a melting point depressant. In bulk form, however, the boron can cause these compositions to become extremely brittle. To combat this, a method was developed at Pratt & Whitney Aircraft for producing the transient liquid phase interlayer alloys in the form of ductile, all metal foils without boron content. Boron is then added to provide the necessary melting point depressant. These ductile borided foils can be readily cut, punched or photo-etched to any required preform shape.

5.3 Pre-Bond Processing

Pre-bond processing encompasses the activities required to prepare the castings and bond tool assemblies for the bonding process. As suitable castings are received from the casting trials, they are assembled into the tooling dies for a preliminary bond line fit-up inspection. This is accomplished through a method that utilizes carbon paper tracings.

The carbon paper trace method gives a qualitative indication of bond fit-up between the mating component halves. The two mating component halves are placed together and loaded in the bonding dies prior to final assembly with a piece of carbon and plain white paper replacing the transient liquid phase foil. When loaded in the die, contact areas between the two halves leave an indication on the paper while uncontacted areas leave no mark. Examples of carbon paper tracings of blades with poor and good fit-up are shown in Figure 58. Some qualitative degree of contact can be interpreted from these tracings, although they are used primarily to give a first order indication of potential fit-up problem areas, and to characterize fit-up reproducibility.

After carbon paper tracing was completed, the castings and preforms were subjected to a cleaning process aimed at removing surface impurities and providing a "clean" bonding surface. The basic pre-bond cleaning operation involves anodic pre-cleaning in an alkali solution followed by anodic etch cleaning in a muriatic acid solution and careful drying to preclude surface stains.

All acid and alkali operations are separated by rinsing steps in clean water. All of the water used for these operations is demineralized to less than 5 ppm ion impurities. The alkali process is used to clean the surface prior to anodic etching to enhance etching uniformity. It is also used after etching to remove surface smut created by the etching. Two graphite slabs are employed in the solution as cathodes, while the parts themselves are anodes for both the alkali and acid treatments.

Preforms were cleaned by standard methods. The preforms were carefully tack welded to the convex airfoil half with a capacitor discharge welder. Weld parameters, weld locations and contact methods were established for each component.
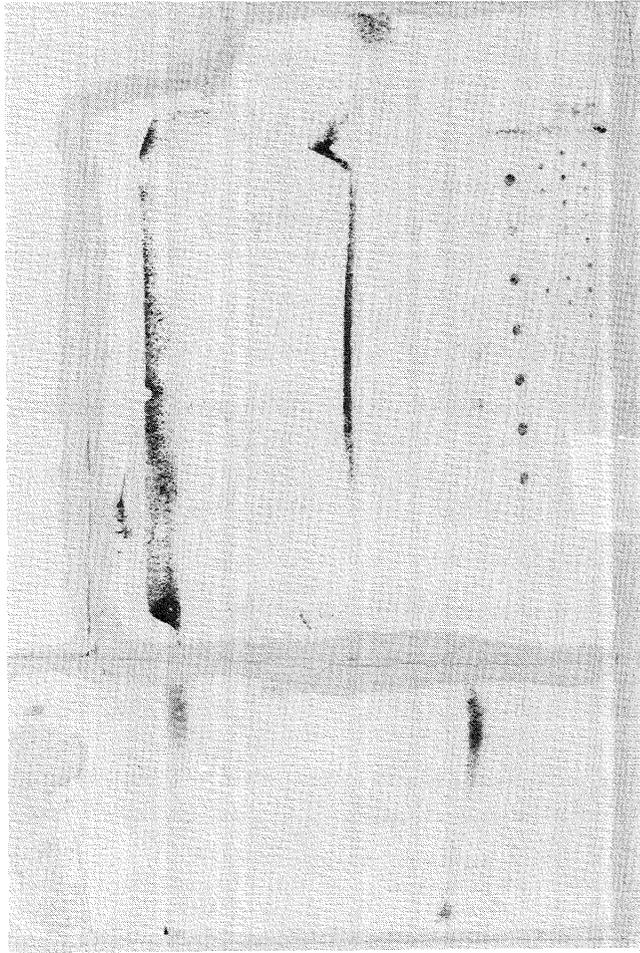
POOR FIT-UP
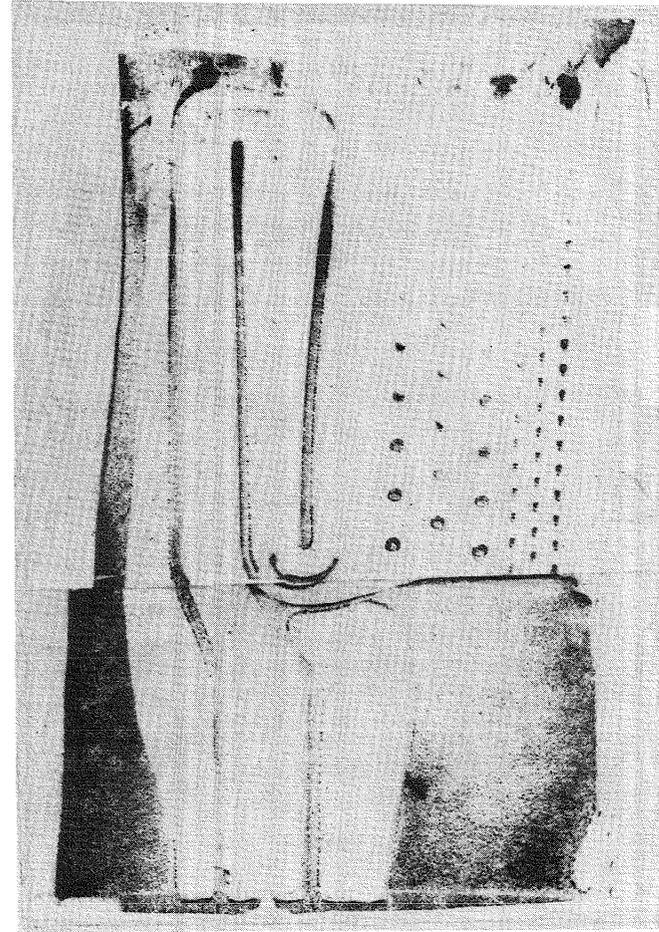
GOOD FIT-UP

Figure 58   Carbon Paper Trace of Blade Bond Plane
(Dark Areas Indicate Contact)

Pre-bond cleaning trials concentrated on establishing the required process combinations (wet blast, grit blast, anodic etching) and optimizing parameters such as clamping position, current density and cleaning cycle limits for the anodic etch procedure. Reproducibility and uniformity of surface cleaning was also evaluated. Other pre-bond activities included optimizing flash trimming methods and dimensions as well as the coordination of pre-bond procedures to preclude recrystallization of the PWA 1480 single crystal alloy. These are discussed in the following paragraphs.

The surface condition of the trial castings, after completion of all post-cast processing operations, was generally unsuitable for bonding due to surface contamination and local areas of cold work from previous operations. In order to prepare the cast surfaces for bonding, an alkali/anodic etch sequence was established. Prior to this sequence, however, it was found necessary to condition the surface mechanically to enhance the alkali/acid cleaning and to improve uniformity. Wet abrasive blasting was found capable of preparing the cast surfaces, but control and uniformity were difficult due to the low metal removal rate. Alumina blasting was subsequently found to be more reliable in producing a uniform surface for the cleaning operations. Alumina grit sizes and pressures were established to minimize working of the cast surfaces and metal removal.

The alkali/anodic etch cleaning sequence in conjunction with the alumina blasting, effectively prepared the cast surfaces for bonding without surface recrystallization of the PWA 1480. Successive alkali/anodic etch treatments were performed, as necessary, to ensure adequate cleaning and sufficient metal removal to reliably prevent recrystallization. Measurement showed a metal removal of approximately 0.0012 cm (0.0005 in.) from each surface. A pressurized water rinse was also introduced after anodic etching steps to remove the smut residue from the etching operation. While the sequence of operations was the same for both the vane and the blade, specific current densities, etching times and clamping positions were required for each component.

The effectiveness of this established pre-bond cleaning procedure is demonstrated in Figures 59 and 60 with respect to both the prevention of surface recrystallization and joint cleanliness. Figure 59 shows two identically treated cast surfaces, except that one sample has been exposed to the pre-bond cleaning process (right) and the other has not (left). After exposure to the bonding thermal cycle, surface recrystallization is evident on the untreated surface, while no recrystallization was found on a properly cleaned surface. Figure 60 illustrates blade root bonds during initial bond trails (left) and after final cleaning procedures were established (right). As shown, the introduction of alumina blast surface conditioning and optimized alkali/anodic etch techniques has totally eliminated the occurrence of bond defects related to surface contamination.

RECRYSTALLIZATION

No RECRYSTALLIZATION
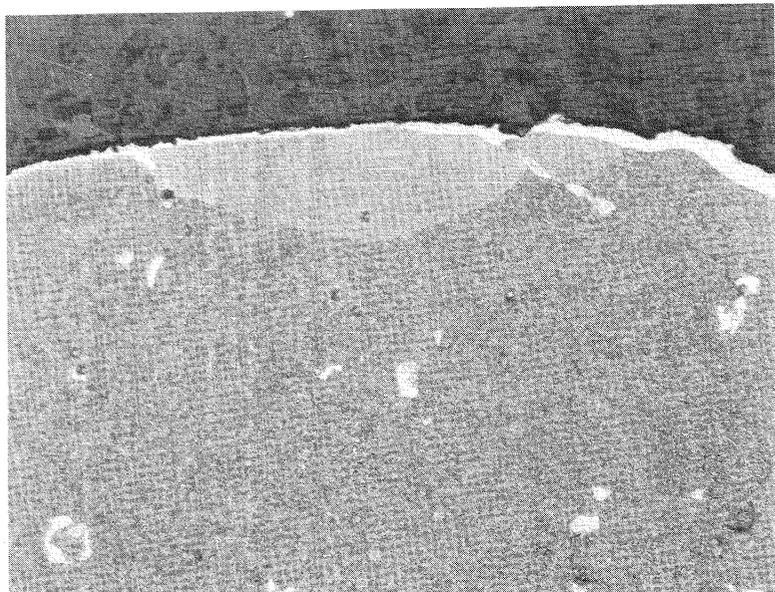
No PRE-BOND CLEANING
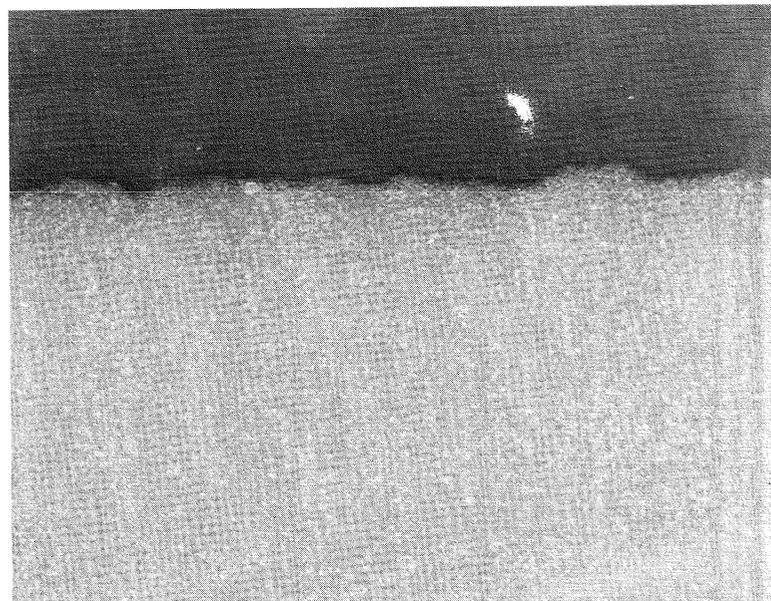
ANODIC ETCH CLEANED

Figure 59   Comparison of PWA 1480 Cast Surfaces Showing How Recrystallization
was Eliminated through Use of Established Pre-bond Cleaning Methods

CLEANING DEFECT
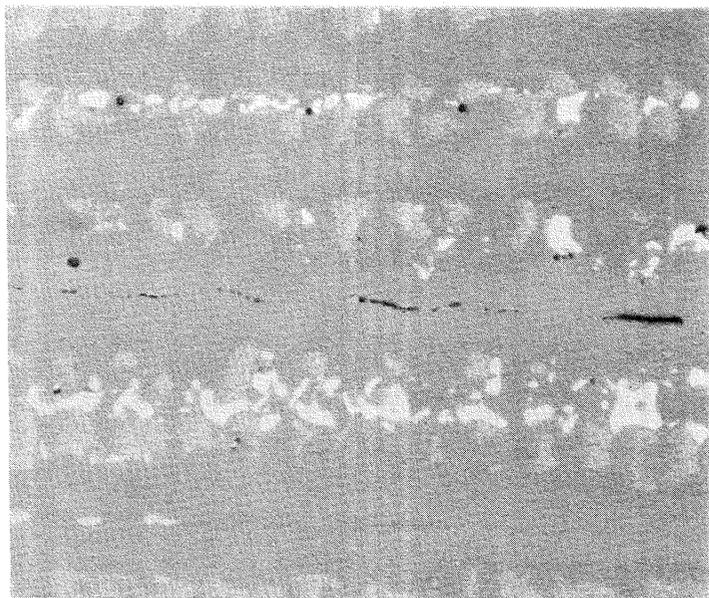
PROPER CLEANING
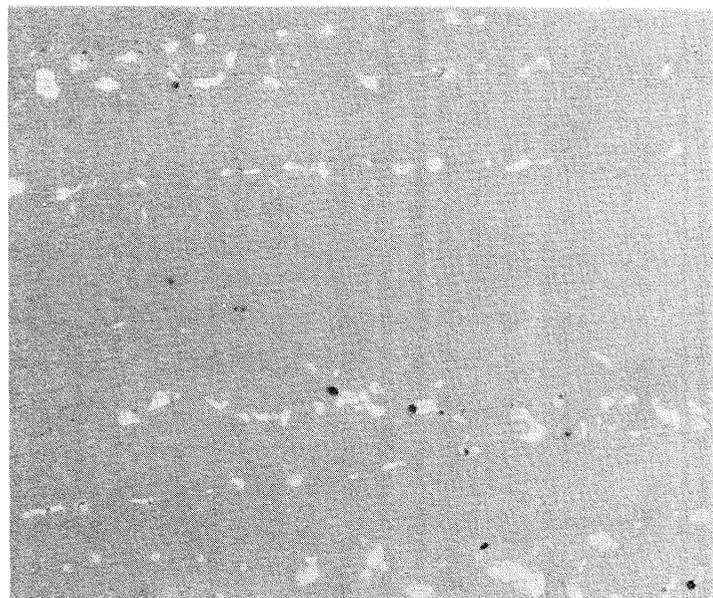
Figure 60   Comparison of Blade Root Bonds Showing Improved Bonding Following
Establishment of Final Pre-bond Cleaning Procedures

Mechanical blending and grinding operations were also established to further improve the contact between the bonding die and external component surface. The vane and blade leading edge flash are blended to not less than 0.31 cm (0.125 in.) of the airfoil to prevent interference with the airfoil dies. Controlling the flash blend limit effectively eliminated flash recrystalliza- tion. Any excess metal on the casting bond surface due to strongback defects in the casting trials was mechanically blended prior to cleaning. Grinding methods were established to improve the die contact on the vane platform and the blade root when these do not meet the wax blueprint dimensions due to casting shrinkage of the large mass.

5.4 Bonding

5.4.1 Process Description

After the cast parts had completed pre-bond processing, they were assembled in the bond tooling assembly for bonding. A parting agent was utilized between the die and castings to preclude any adhesion between the castings and tooling dies during the bonding cycle. Actual bonding was conducted in either of the two cold wall vacuum furnaces shown in Figure 61 using standard vacuum heat treating and bonding procedures previously established at Pratt & Whitney Aircraft for nickel-base superalloys. After bonding, the assemblies were cooled using recirculated argon. Immediately, the parts were removed from the bonding dies and solution heat treated in the same furnaces.
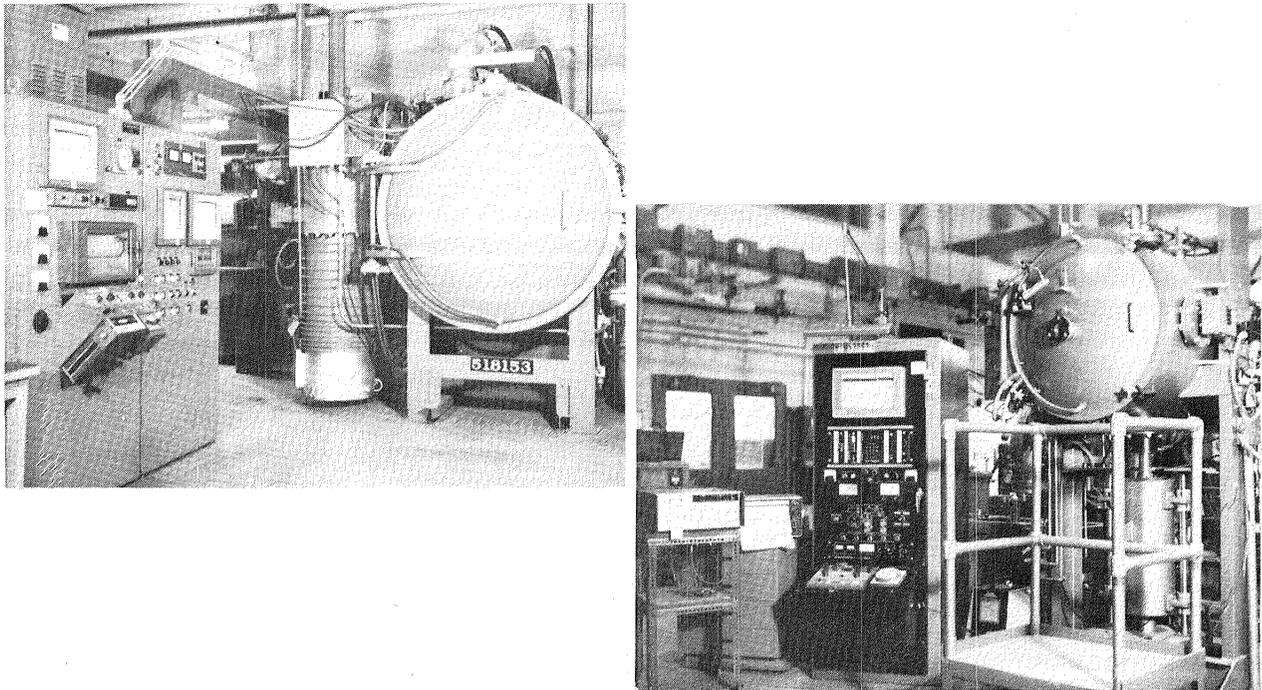
Figure 61   Cold Wall Vacuum Furnaces Utilized for Bonding Energy Efficient Engine Vanes and Blades

After disassembly from the bonding dies, a qualitative assessment was made of the coverage of the die contact area on the component. A trace of the contacted areas is left on the component surface due to the parting agent used between the part and the dies.

Subsequent to blending and polishing, the leading edge was etched electrolytically with a phosphoric acid solution and examined visually for unbond and microstructural defects. This etch/visual inspection procedure allows the inspection of athermally solidified (A/S) microstructure in the bond, a defect not discernable by standard methods.

Final evaluation of the vanes and blades involved visual and metallographic evaluation of bond quality. The vanes and blades were sectioned near engineering machine drawings sections, and visually examined for unbonded regions. Unbonded areas were mapped for each vane and blade. Selected sections were metallographically prepared and examined.

5.4.2 Bonding Trials

Like casting, defining an acceptable bonding procedure is an iterative process; the techniques depending to a great extent on empirical information and trial-and-error methods. Consequently, this effort comprised a total of 10 vanes and 22 blades which were bonded and subsequently examined visually and metallographically for bond quality. Due to the complexity of the bonding process, several unanticipated problems arose during the bonding trials. Most of these problems were dimensional in nature and affected the fit-up between the mating halves and consequently affected bond quality. These fit-up problems were generally interrelated with casting quality. Some deviations from perfect bond fit-up could be corrected by modifications to tooling design and materials, assembly methods and in-process inspection. Other dimensional defects, however, could not be overcome by bond tooling and must be corrected by improving casting quality. Some of these dimensional problems were identified during the fabrication trials but correction of these problems was not within the scope of this program. These fit-up related dimensional problems included airfoil to root transition match-up of the blade bond surfaces and rib interference near the tip of the blade, along with rib and pedestal chordal mismatch in the vane.

The entire process by which each component was transient liquid phase bonded was controlled through detailed operations sheets in which each particular operation was itemized. During the bonding trails, any anomalies in the component or the process were recorded. The effect of each operation on the transient liquid phase bond quality on each component fabricated was determined using the information from these detailed operations sheets.

5.4.2.1 Bond Tooling Assembly

The objective of this task was to establish a specific bond tooling assembly sequence to ensure consistent bonding of vanes and blades. During the determination of this sequence, several problems were encountered. These are discussed in the following paragraphs.

Initial estimated shrinkage factors used to design casting tooling for the vane halves were incorrect and the vane did not meet blueprint dimensions. Consequently, the original vane transient liquid phase foil preform, designed to meet the vane blueprint dimensions, did not fit the actual bond plane. Subsequent modifications to the preform resolved this problem.

The original blade leading edge transient liquid phase foil preform also did not fit the bond surface of the blade, primarily due to the compound curvature of this surface. An iterative hand fitting preform design technique was employed and this, plus the establishment of a specific lay-on sequence, resulted in an accurate fit of the blade preform to the bond surface. The original blade leading edge transient liquid phase preform is compared with the final preform design in Figure 62.

ORIGINAL PREFORM SHAPE

MODIFIED PREFORM SHAPE
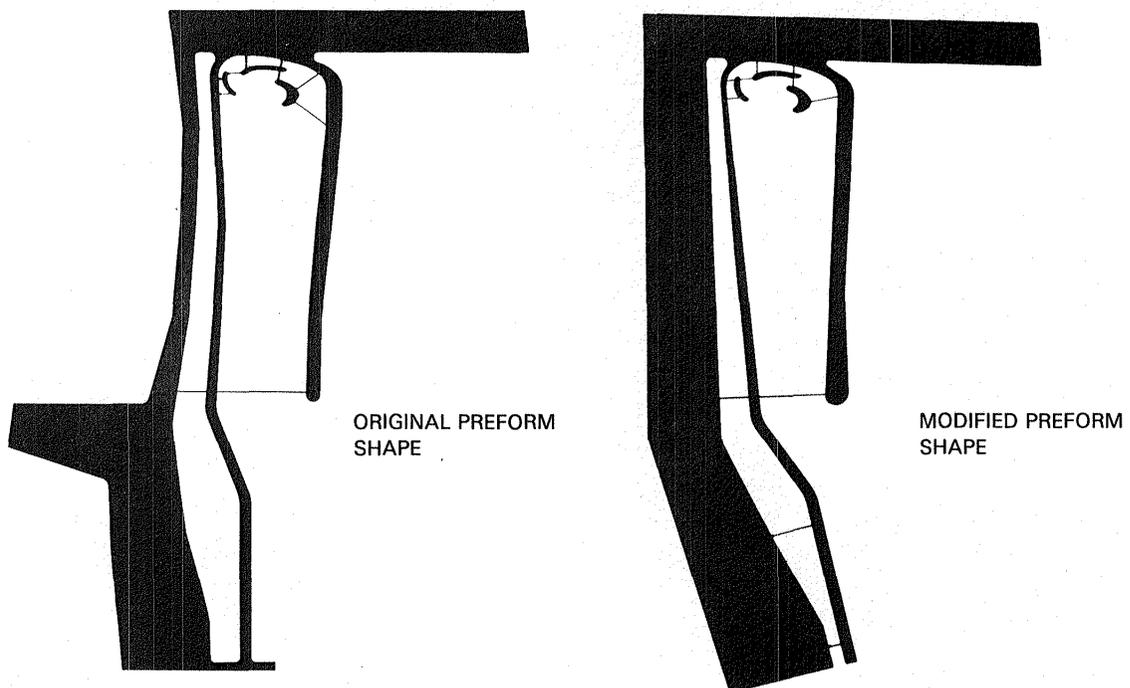
Figure 62   Blade Leading Edge Transient Liquid Phase Preforms Showing Modifications Necessary to Achieve Acceptable Bond Surface Fit-Up

Properly fitted preforms were tack welded to the bonding surface to hold them in place during bond tool assembly. Weld parameters and contact locations were established which ensured consistent preform tack welds and precluded any effect of the tack weld on the transient liquid phase bond.

An yttrium oxide (Y_2O_3) slurry parting agent was utilized to prevent bonding of the castings to the dies. This parting agent was removed when vane and blade castings were heat treated after disassembly from the dies.

The bonding yokes, fabricated from a molybdenum alloy, sporadically cracked during the assembly of the castings into the bond tooling. This occurred because assembly was accomplished at room temperature, which is below the ductile-to-brittle transition of the molybdenum alloy at the pre-load conditions utilized. The assembly pre-load was reduced and this prevented any further cracking of the yokes.

5.4.2.2 Vane Bonding Trials

Initial vane bonding trials indicated poor bond quality in the vane first rib. This was traced to the use of AISI Type 330 deformable spacers in the bond tool assembly which were found to yield at a stress too low to provide the load required to successfully bond the cast halves. This problem was solved by changing the spacer material to DA-25 alloy, the same as that used in the tooling dies themselves. The improvement in bond quality is illustrated in Figure 63.

The achievement of complete platform bonding and good bond microstructure in the platofrm was found to be just as dependent on the number and proper location of the deformable spacers in the final tooling configuration as on the selection of DA-25 as the spacer material. Originally, two deformable spacers were used on each platform. The resultant bonds were of poor quality with large voids in some areas. By using three spacers on both platforms, one located at each platform edge and one placed at each platform center, complete shroud bonding was achieved. The improvement in bond quality is illustrated in Figure 64.

Vane trailing edge pedestal bonding was initially poor due to insufficient bond line loading caused by inadequate airfoil-to-airfoil die contour fit-up in the trailing edge area. The problem resulted because the vane airfoil external contour did not meet the wax blueprint specifications. This was caused by casting mold dimensional instability in the casting process. To compensate for this fit-up problem, shims were placed at the vane leading edge flash and trailing edge as shown in Figure 65. This effectively solved the pedestal bond problem.

Upon sectioning bonded vane castings, a chordwise mismatch between the cast halves at the bond plane was observed. This mismatch averaged a nominal 0.04 cm (0.017 in.) and is illustrated in Figure 66. It was found to be the result of an offset in the strongback alignment pin during the casting process due to an error in the wax pattern tooling. The problem could be easily eliminated by correcting that tooling.

The vane tooling configuration which evolved out of the bonding trials is illustrated in Figure 67. The extent to which bonding improvement was achieved is shown in Figure 68.
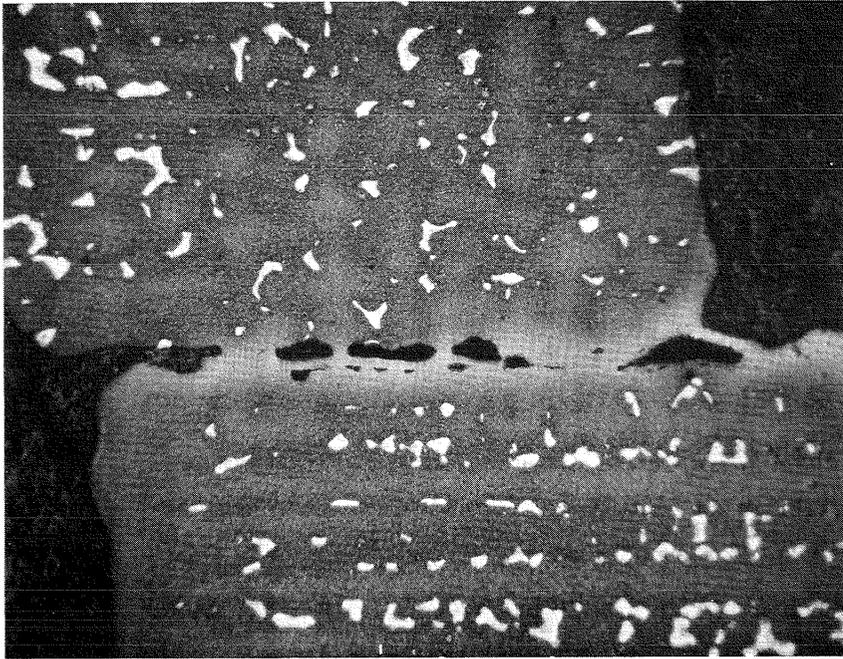
POOR QUALITY BOND JOINT USING TOOL DESIGN
WITH STAINLESS STEEL SPACERS
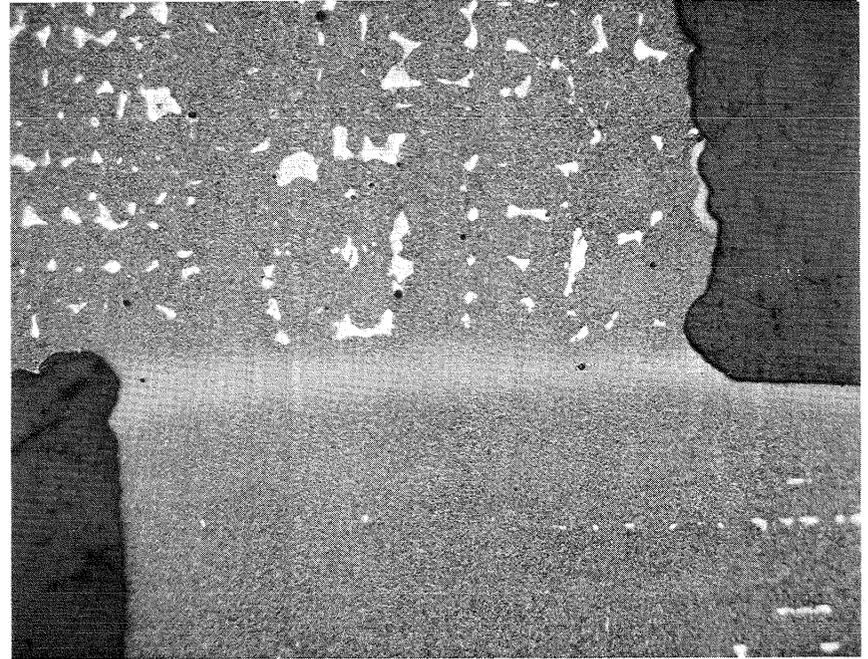
ACCEPTABLE QUALITY BOND JOINT USING TOOL
DESIGN WITH DA-25 SPACERS

Figure 63   Energy Efficient Engine Vane First Rib Bond Microstructure
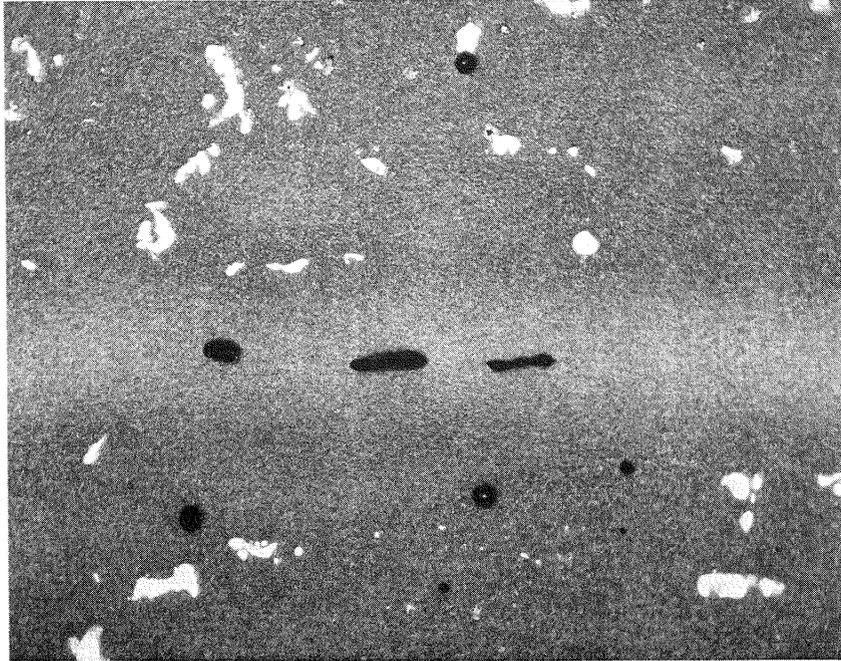
POOR QUALITY BOND USING TWO DEFORMABLE
SPACERS IN EACH PLATFORM (DARK AREAS ARE VOIDS)
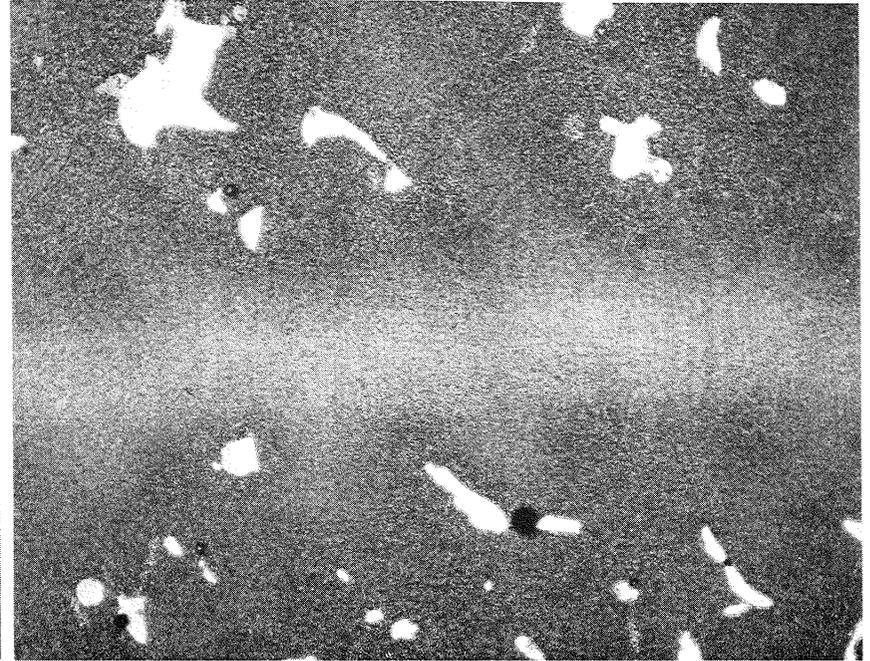
ACCEPTABLE BOND QUALITY ACHIEVED WITH
THREE DEFORMABLE SPACERS

Figure 64   Energy Efficient Engine Vane Platform Bond Microstructures
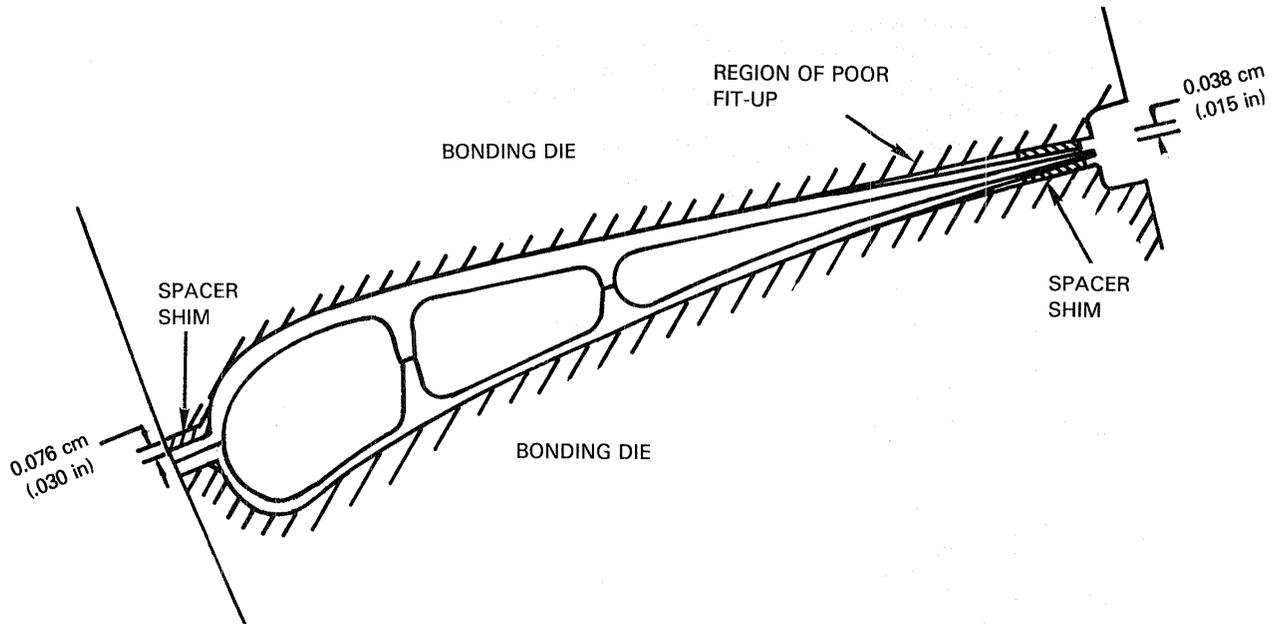
Figure 65   Location of Spacer Shims on Energy Efficient Engine Vane Airfoil
             to Correct Inadequate Airfoil-to-Airfoil Die Contour Fit-Up
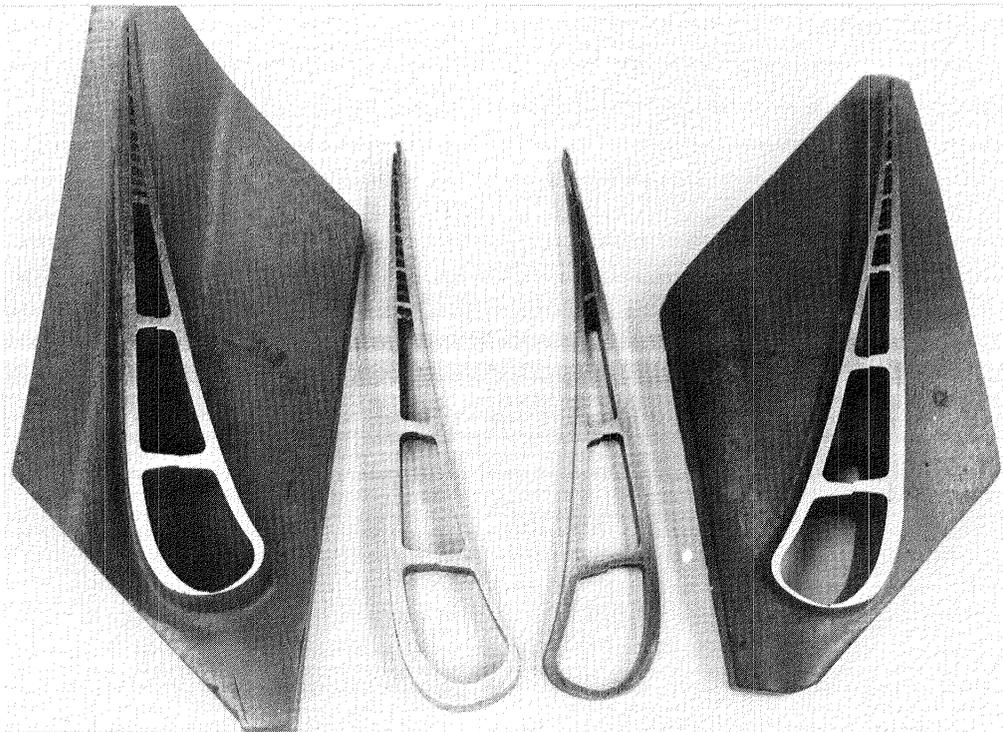
Figure 66   Energy Efficient Engine Vane Chordwise Mismatch due to Strongback
             Misalignment

VANE TIP SECTION
TOOLING

VANE AIRFOIL
SECTION TOOLING

VANE ROOT
SECTION TOOLING
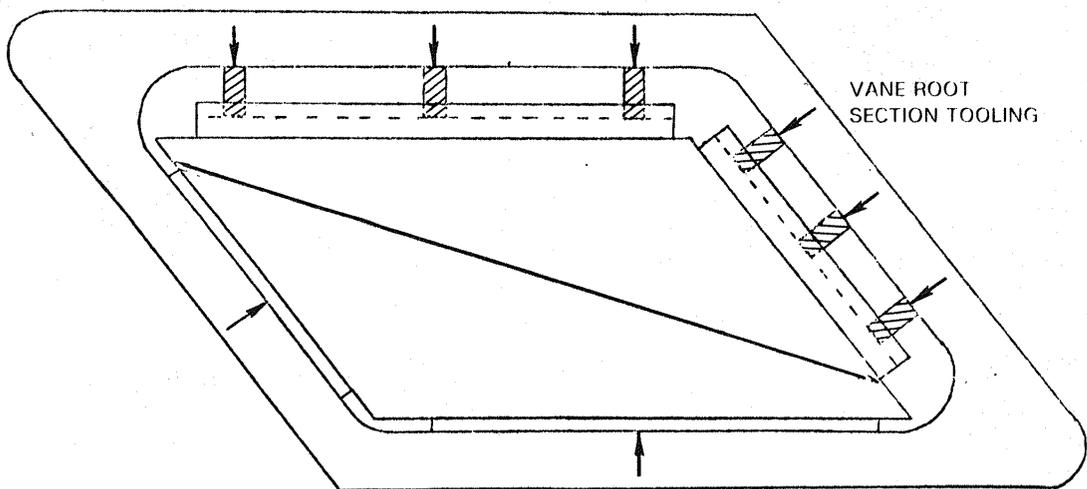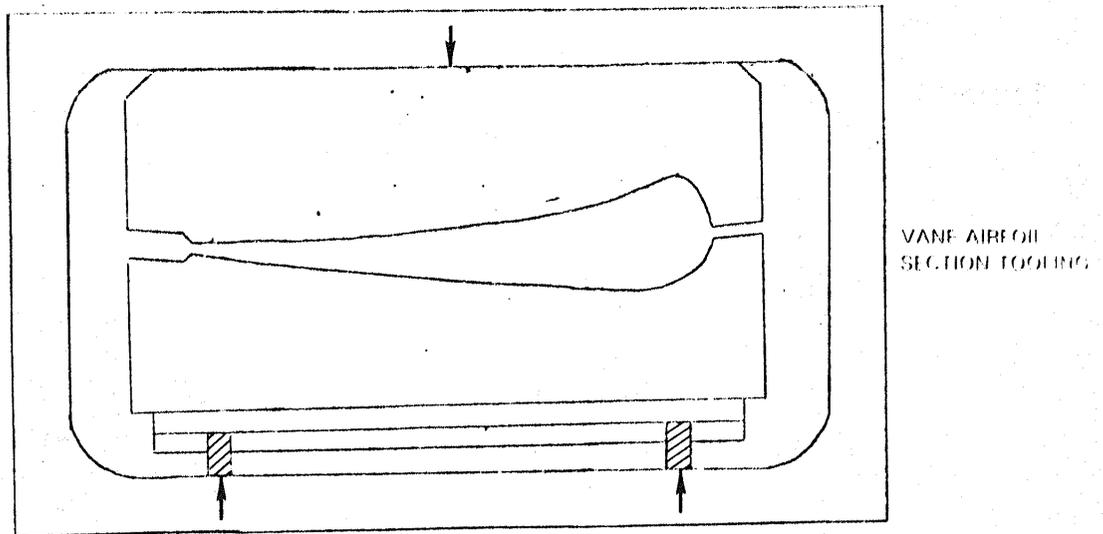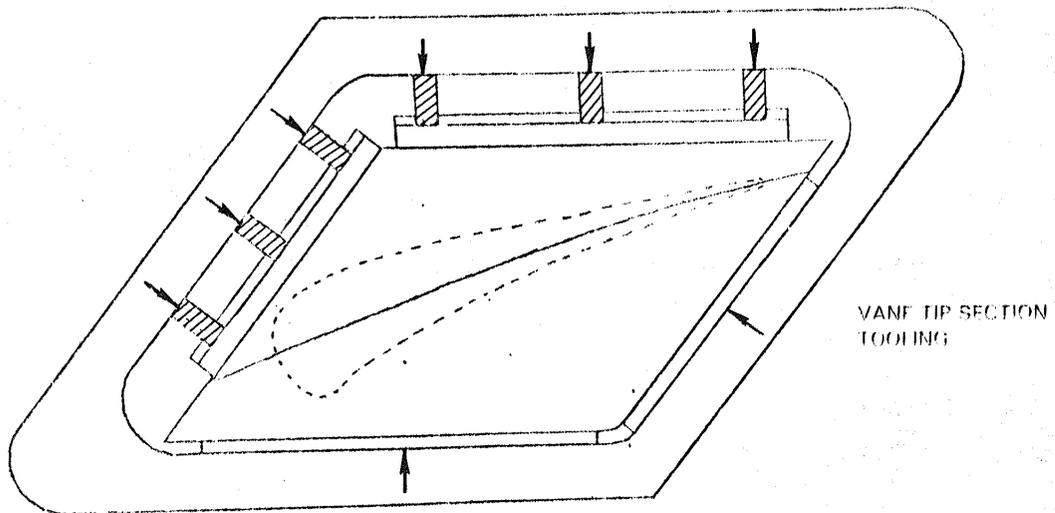
Figure 67   Energy Efficient Engine Vane Final Design Tooling
(Arrows Indicate Direction of Loads)
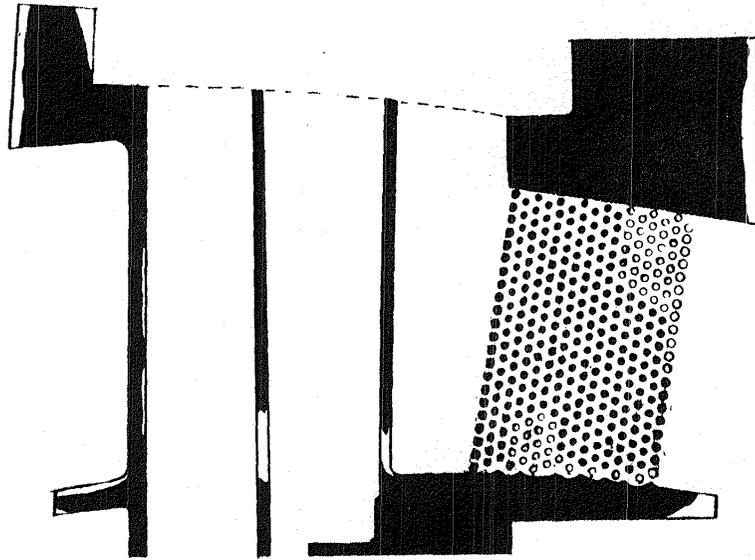
ORIGINAL DESIGN TOOLING
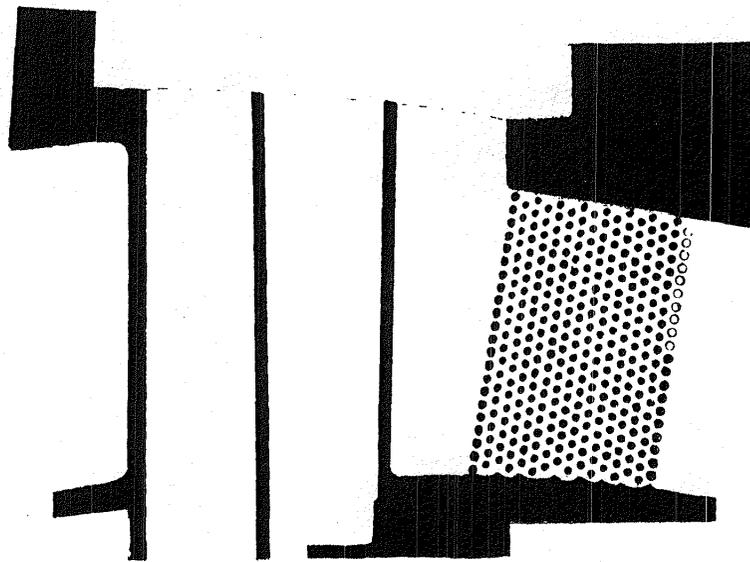
FINAL DESIGN TOOLING

Figure 68   Improvements in Vane Bonding (Shaded Areas Indicate Bond)

5.4.2.3 Blade Bonding Trials

As was noted earlier, blade bond tooling was divided into that associated with bonding the blade airfoil sections and that associated with bonding the blade root section. This was required due to the complex geometry of the blade castings. As with the vane, the initial material chosen for the blade airfoil tooling and root tooling deformable spacers was AISI Type 330 stainless steel. After several blade bonding trials, it was found necessary to change to spacers using DA-25 material because of the low yield strength of the stainless steel at bonding temperatures.

Airfoil Bonding Trials

The initial tooling design for the airfoil trials incorporated a loading plane which was rotated 19 degrees counterclockwise to the rib axis as shown in Figure 69(a). This loading plane had been defined through the use of finite element analysis when the tool was designed and was thought to be acceptable. Examination of the first rib bond joint microstructure, following bonding, indicated a poor quality bond as shown in Figure 69(b). The dies were subsequently modified so that loading was applied parallel to the rib axis (i.e., 0 degrees rotation in Figure 70(a)), which significantly improved both the quality of the bond and its microstructure as shown in Figure 70(b).

The initial bond tooling configuration was a single-direction loading system with the loads applied to the blade castings as shown in Figures 69(a) and 70(a). Although the modified version of this configuration improved the first rib bond joint, it was inadequate to consistently provide good quality bonds at the trailing edge pedestals. Consequently, a multi-direction loading system (shown in Figure 71) was implemented. This system consistently produced high quality pedestal bonds as shown in Figure 72.

Metallographic examination of the tip end of the third rib revealed that the rib was crushed during bonding (Figure 73). This deformation was the result of a misalignment in the y plane of the strongback tool which caused interference between the mating halves of the third rib. A schematic of this problem is illustrated in Figure 74. This bonding problem could be easily remedied by correcting the misalignment in the strongback tool.

The remaining bonding fit-up related bond defects were a result of casting dimensional problems. The first blades available for bonding were warped in the tip area, prohibiting complete tip bonding. The warpage problem was corrected by pinning the tip area during casting, and this, in conjunction with the improved airfoil die system, produced high quality bonds at the tip.

Blade Root Bonding Trials

The original blade root bond tool design is shown in Figure 75(a) and employed a single direction loading system. Bonding achieved with this system was poor as evidenced by the wide gap bonds and voids in Figure 75(b).

RIB AXIS

19°
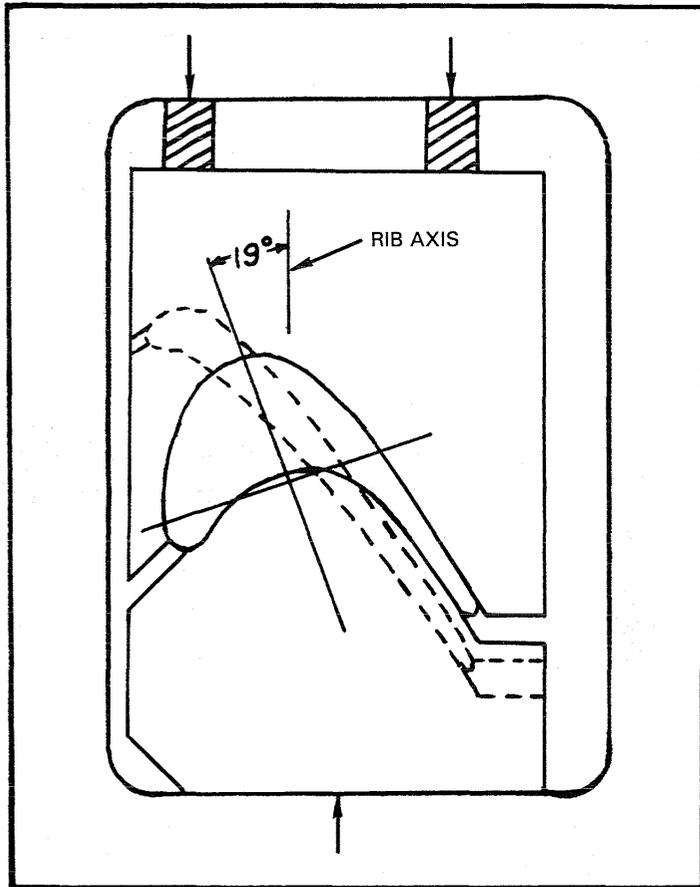
ORIGINAL DESIGN
(ARROWS INDICATE DIRECTION OF LOADS)
(a)
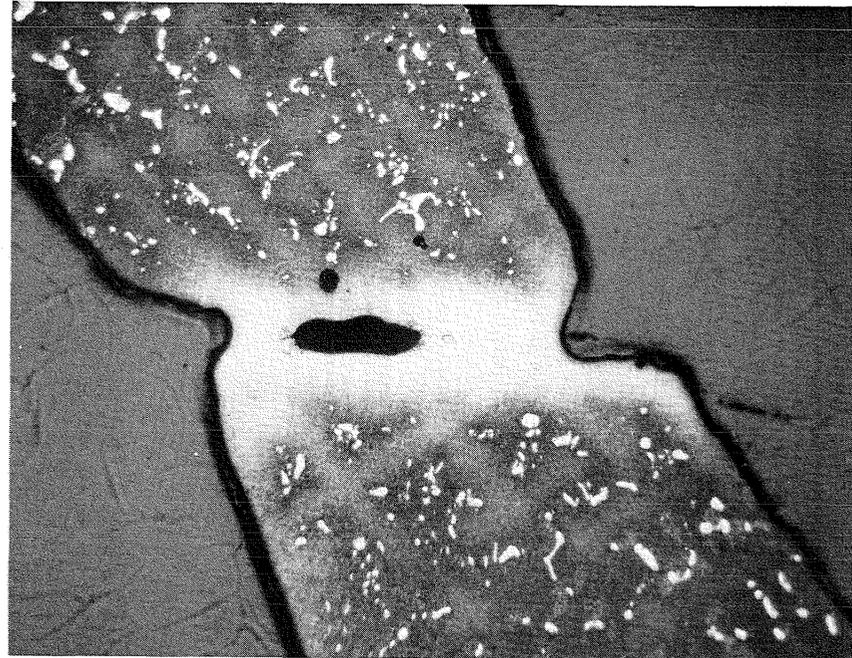
BOND JOINT
(b)

Figure 69   Initial Blade Airfoil Bond Tool Design and Poor Quality First
Rib Bond Joint Resulting from Its Use

75
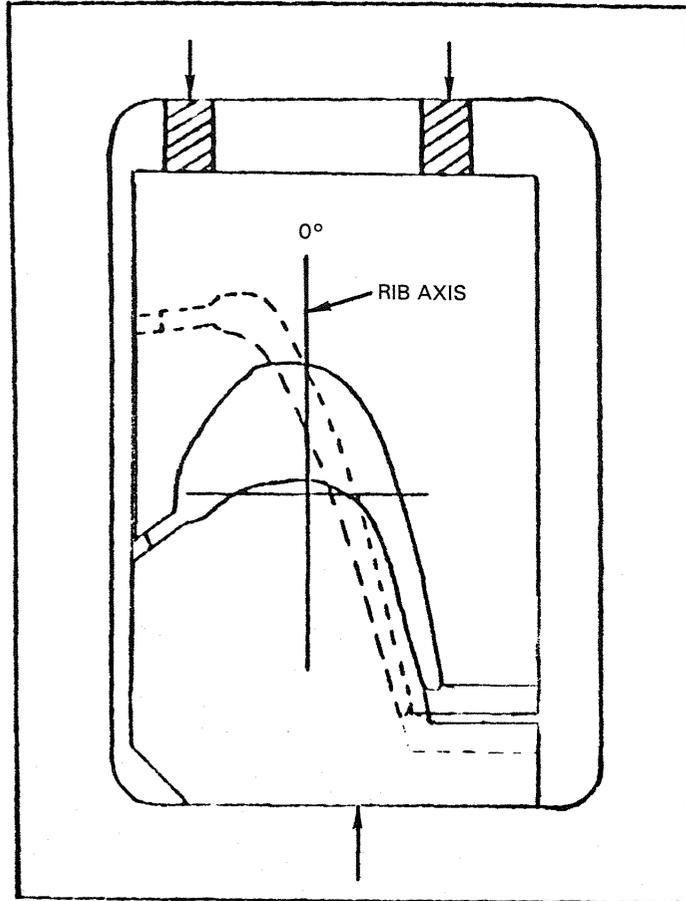
MODIFIED DESIGN
(ARROWS INDICATE DIRECTION OF LOADS)
(a)
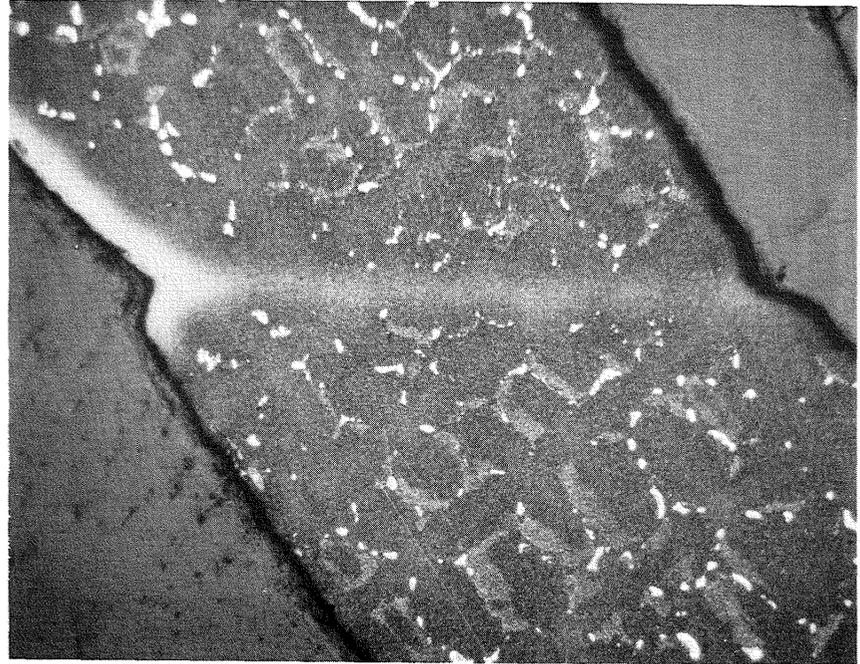
BOND JOINT
(b)

Figure 70   Modified Blade Airfoil Bond Tool Design (Loading Parallel to Rib Axis) and Good Quality First Rib Bond Joint Resulting from Its Use
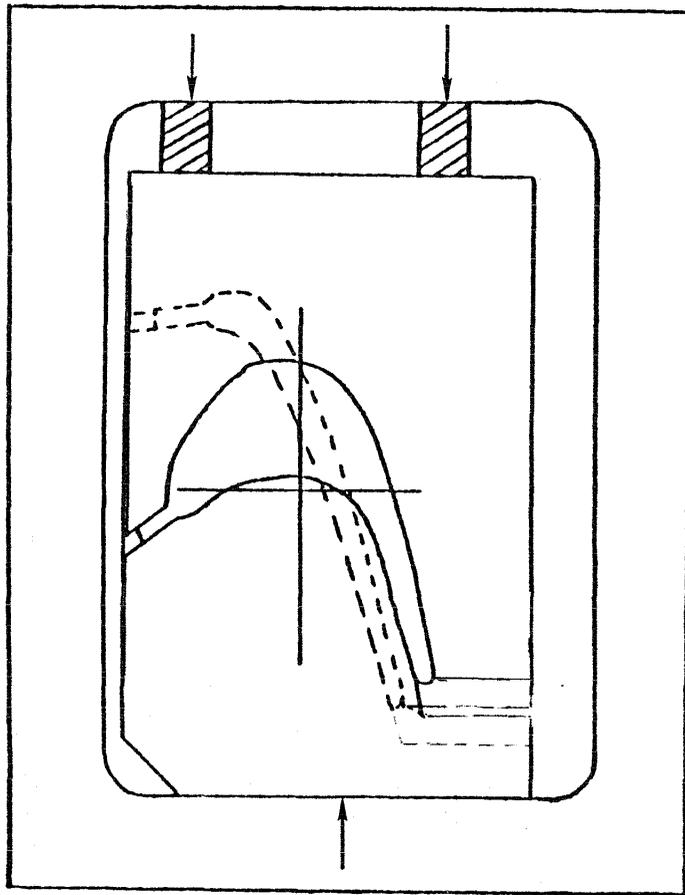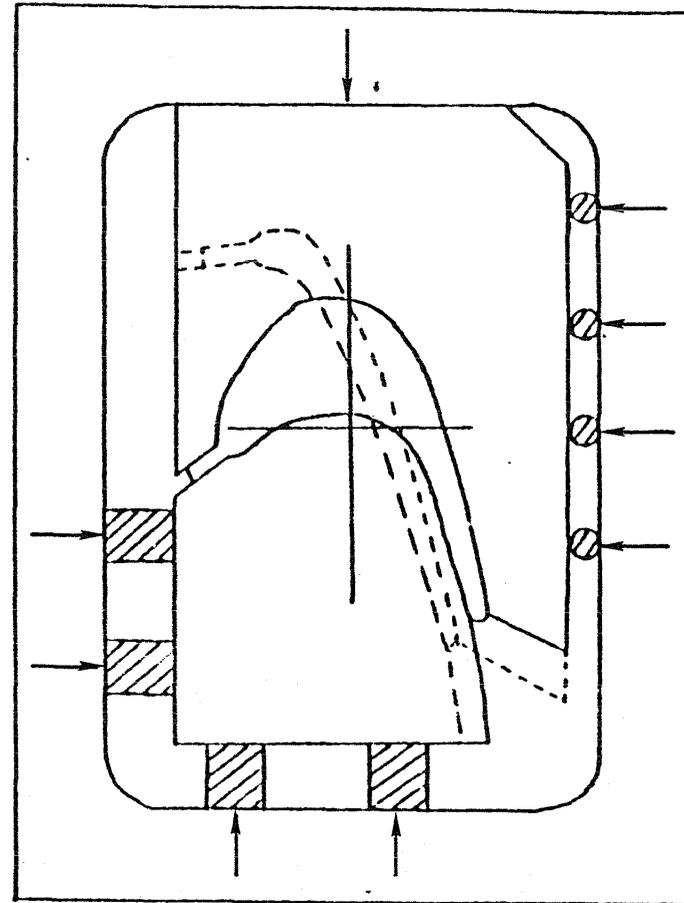
ORIGINAL DESIGN

FINAL DESIGN

Figure 71   Energy Efficient Engine Blade Airfoil Tooling Modification
Showing Multi-directional Loading System
(Arrows Indicate Direction of Loads)
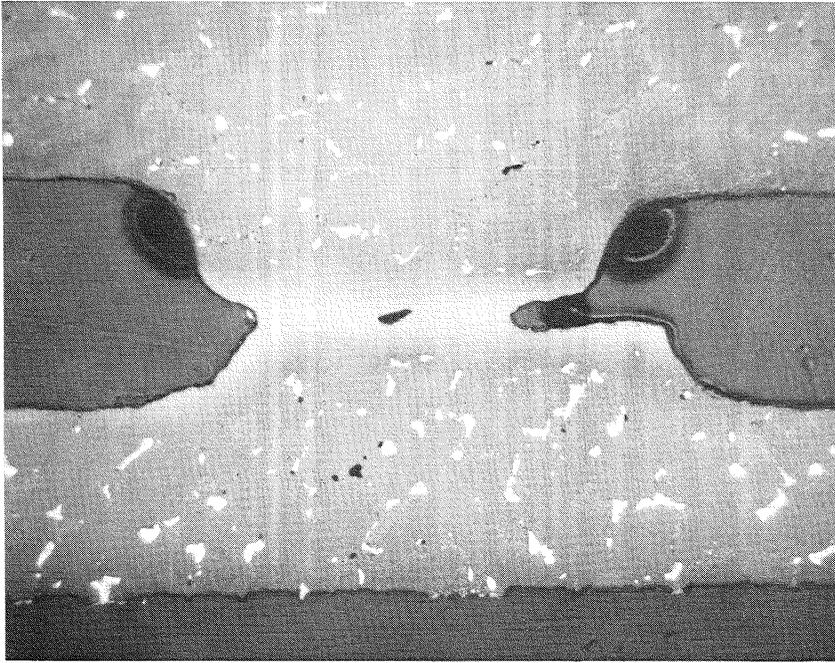
PRELIMINARY TOOL DESIGN WITH
SINGLE DIRECTION LOADING
(a)

50X
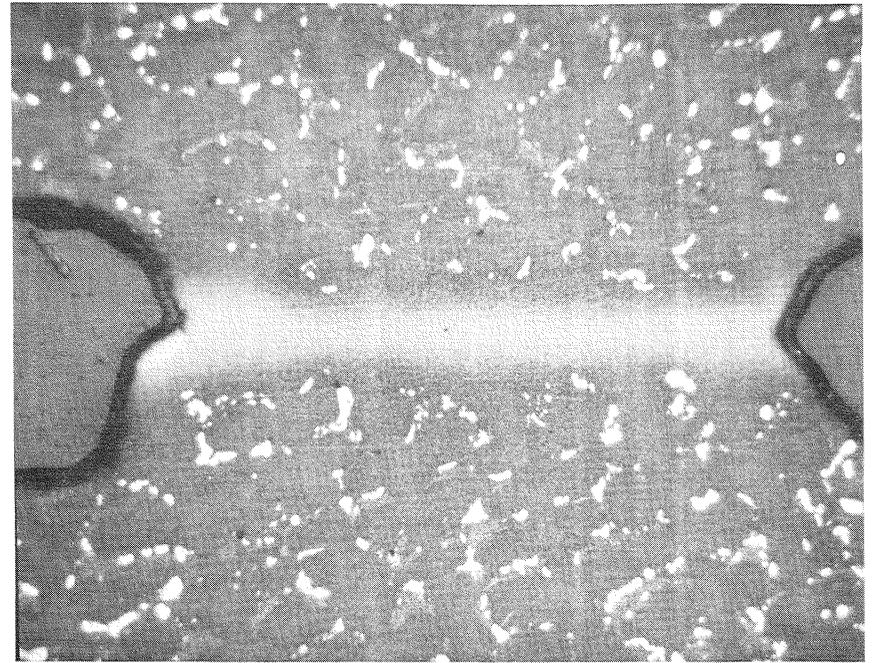
FINAL TOOL DESIGN WITH
MULTI-DIRECTIONAL LOADING
(b)

Figure 72   Energy Efficient Engine Blade Multi-direction Loading Systems
Applies Load to Produce High Quality Pedestal Bonds
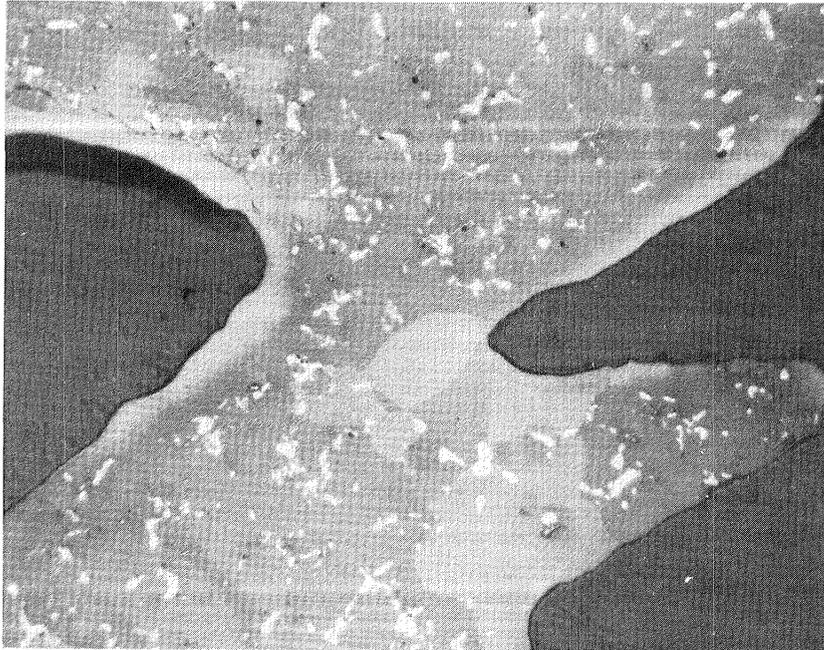
Figure 73   Energy Efficient Engine Blade Third Rib Interference Showing
             Deformation Due to Strongback Tool Misalignment

Large areas of unbond were noticeable at the blade root leading edge, first
rib, and trailing edge. These problems were attributable to fit-up problems
caused by the high degree of curvature and camber in the blade root bond
plane. The tooling die was therefore modified to incorporate the multi-direct-
ional loading system illustrated in Figure 76(a). This system significantly
improved the quality of the bond joints where contact between mating parts was
good (as shown in Figure 76(b)). However, unbonded areas persisted and selec-
tive bond plane rework of the mating surfaces was required to correct this
problem. This selective rework was done with a co-electrical discharge machin-
ing technique which provided excellent intimate contact between mating sur-
faces at the bond plane.

The extent to which bonding was improved in the blade due to modifications in
the airfoil and root dies is shown in Figure 77. Although some small areas of
unbond are evident in Figure 77(b), these were subsequently eliminated by
extending the multi-directional root dies to the blade platform.

5.4.2.4 Bonding Evaluations

As bonding trials progressed, the bonded parts were subjected to a rigorous
evaluation, which included die contact assessment, destructive metallographic
bond characterization, and non-destructive inspection. Results of these eval-
uations were used to modify the bonding process, where required, to achieve
the desired bonding results. These evaluation steps are described as follows:

BLADE STRONGBACK TOOL

BONDED BLADE

Y PLANE

BOND
PLANE

X PLANE

Y PLANE
MISALIGNMENT

0.50 cm
(0.200 in)

PEDESTAL
DRAW

Y PLANE

X PLANE

RIB INTERFERENCE

BOND PLANE
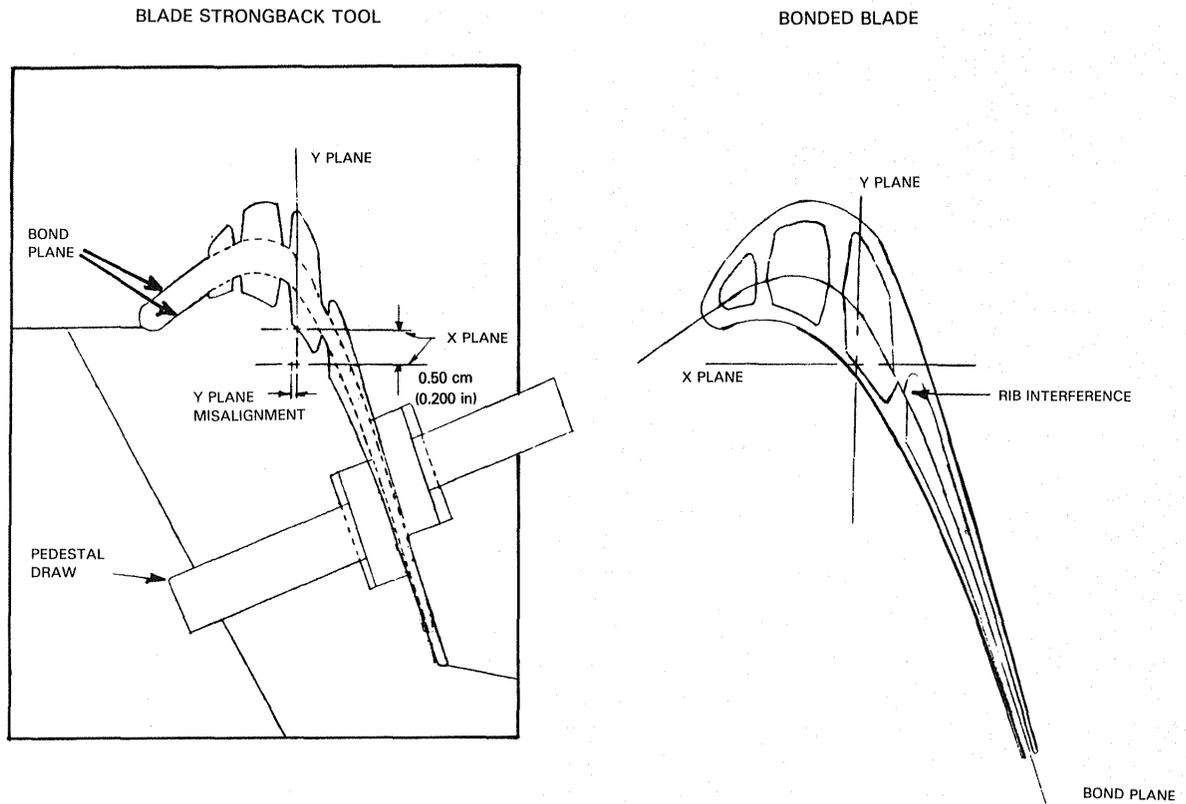
Figure 74   Interference of Blade Rib Due to Misalignment of Strongback Tool

(ARROWS INDICATE DIRECTION OF LOADS)
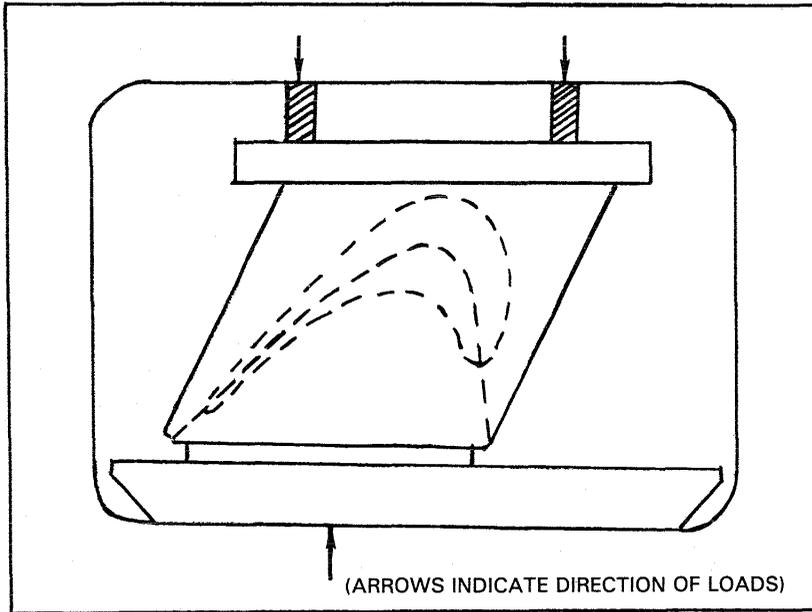
ORIGINAL DESIGN
(a)
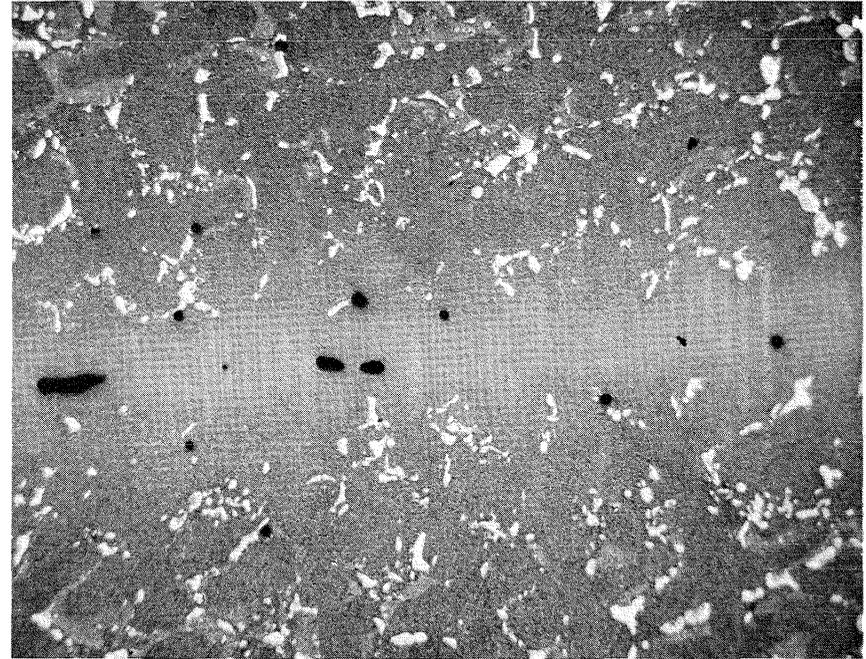
BOND JOINT   50X
(b)

Figure 75   Initial Blade Root Bond Tool Design and Poor Quality Bond
Resulting from Its Use
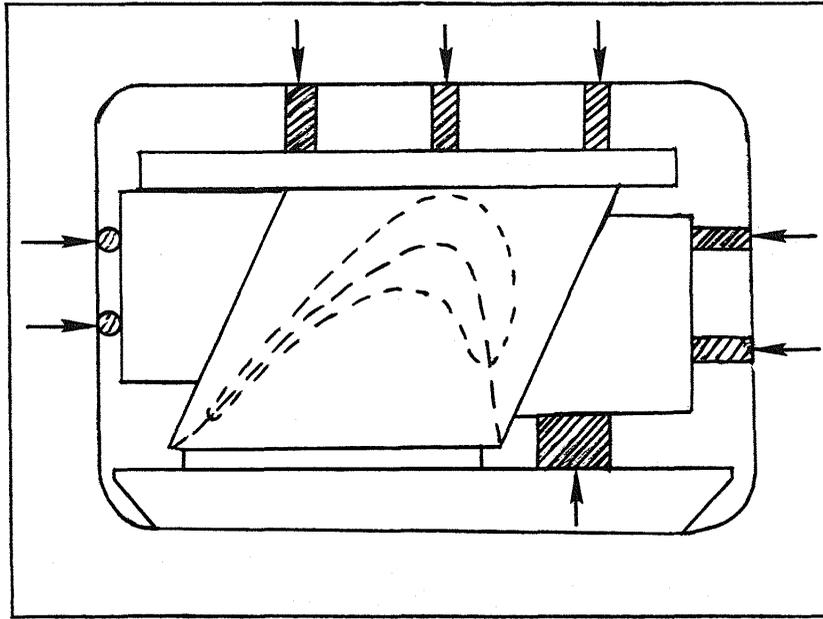
MODIFIED DESIGN
(ARROWS INDICATE DIRECTION OF LOADS) ·

(a)

BOND JOINT   50X

(b)

Figure 76   Modified Multi-Directional Load Blade Root Bond Tool Design and
Good Quality Bond Resulting from its Use
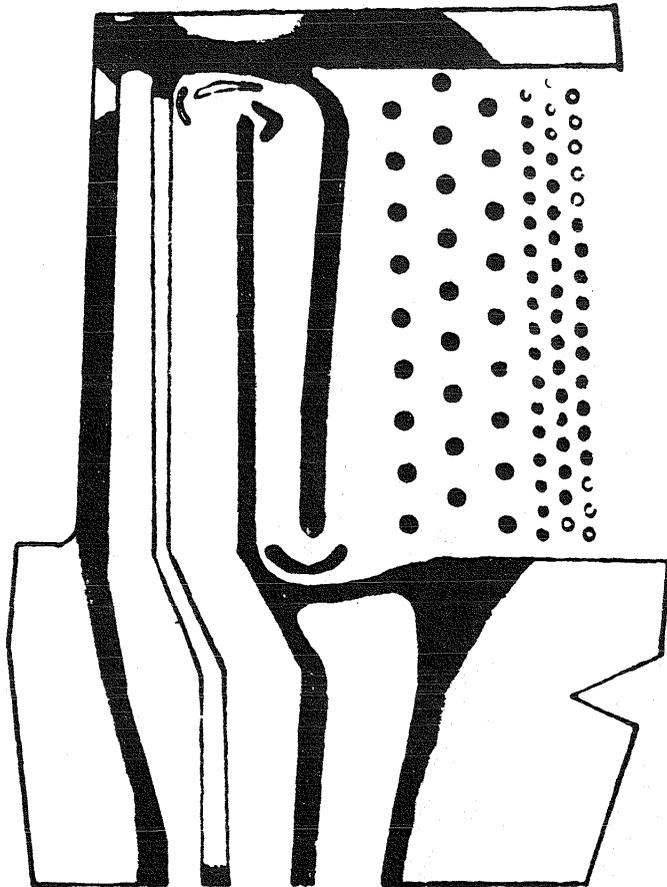
ORIGINAL DESIGN TOOLING
(a)
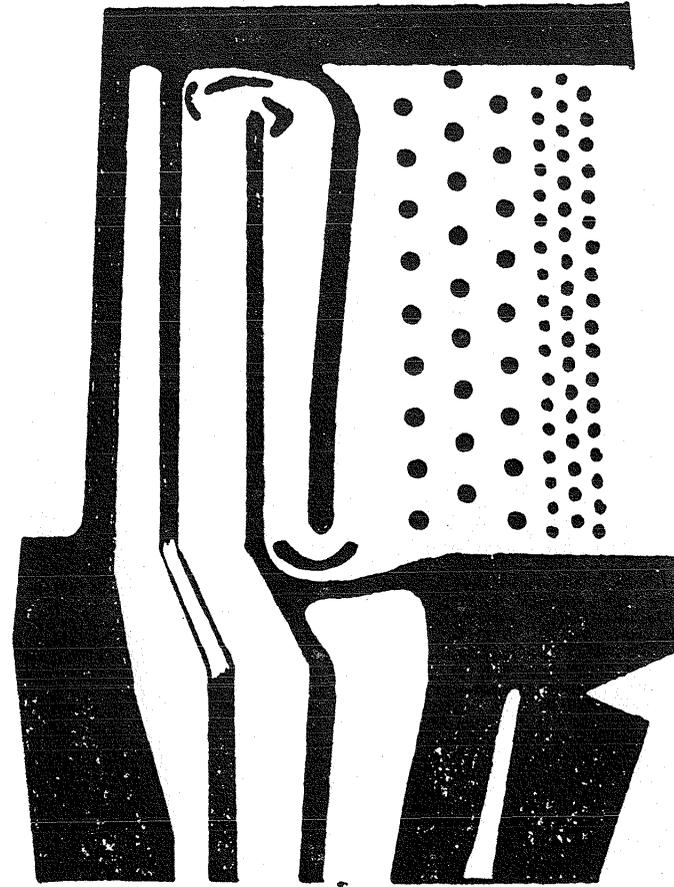
FINAL DESIGN TOOLING
(b)
CORRECTED BY SELECTIVE BOND
PLANE REWORK

Figure 77   Improvements in Blade Bonding (Dark areas indicate bond)

Die Contact Assessment

The extent to which the tooling dies fit the external contours of the parts being bonded can influence the quality of the bond. The more complete the contact, the higher the probability of good bonds. The yttrium oxide parting agent adheres to the vane or blade casting surfaces where the die has made contact with the part and is absent from those surfaces where contact has not been made. The technique used was to visually examine the external surfaces of the castings after bonding but prior to solution heat treatment in order to assess the extent to which the parting agent was adhering to the surfaces. Potential unbonded areas requiring more thorough examination were identified and bond tooling was modified as necessary to provide complete contact. Examples of poor and good contact indicated by this technique are shown in Figure 78.
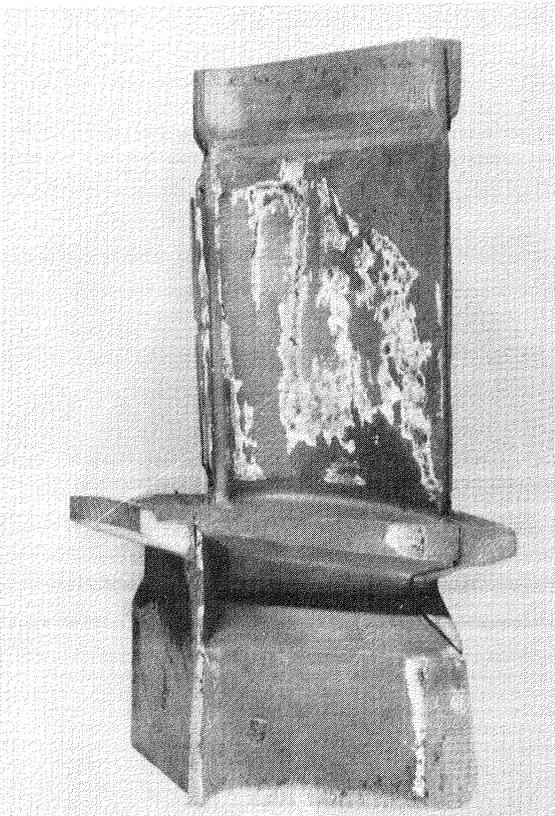
POOR DIE CONTACT   GOOD DIE CONTACT

Figure 78   Die Contact Assessment (Light areas indicate good
             die-to-casting contact)

84

Destructive Metallographic Bond Characterization

Destructive metallographic bond characterization was the most thorough bond evaluation method. After sectioning the component, the internal details were visually examined for the first time and any unbonded areas were recorded. Although the extent of the bond area noted visually correlated well with the subsequent metallographic investigation, the quality of the bonds could only be evaluated metallographically. This metallographic investigation involved a detailed assessment of the sectioned parts to determine areas where voids, contamination, recrystallization, or undesirable grain structure existed in the material microstructure. Metallographic results from sample vane and blade bond evaluations are shown in Figures 79 and 80.

BOND QUALITY

V — VOID
G — GRAIN
C — CONTAMINATION
Rx — RECRYSTALLIZATION

AREA INVESTIGATED

■ ISOTHERMALLY SOLIDIFIED BOND
☐ NO BOND
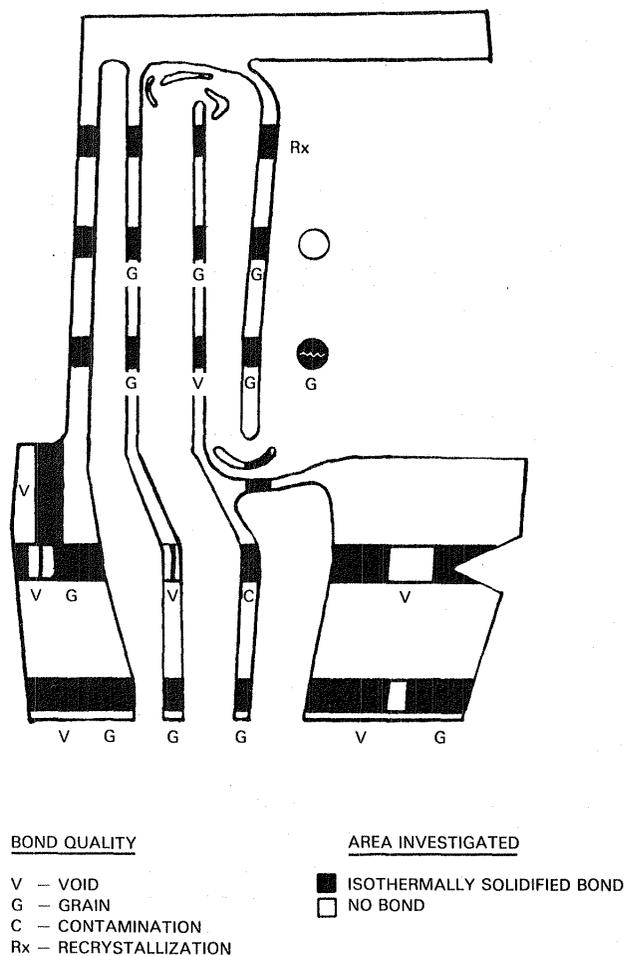
Figure 79   Typical Blade Metallographic Record
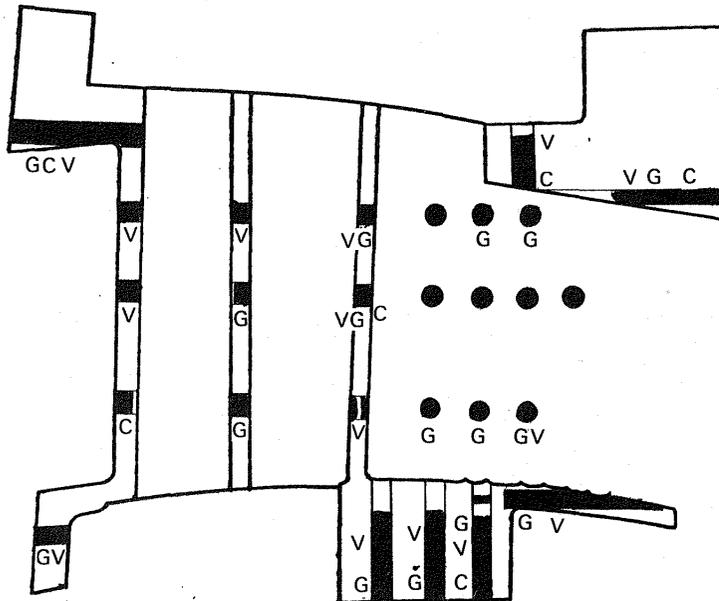
BOND QUALITY

V — VOID
G — GRAIN
C — CONTAMINATION
Rx — RECRYSTALLIZATION

AREA INVESTIGATED

■ ISOTHERMALLY SOLIDIFIED BOND
☐ NO BOND

Figure 80   Typical Vane Metallographic Record

Non-Destructive Inspection

Two existing non-destructive inspection methods were evaluated on Energy
Efficient Engine hardware: etch/visual and fluorescent penetrant. Both tech-
niques successfully revealed linear and pinpoint defects in the vane and blade
leading edge bonds. Fluorescent penetrant also revealed defects in accessible
bonds. No athermally solidified material was found in the leading edge of any
vane or blade. The correlation between each inspection method and the quality
of the bond determined metallographically was excellent. A record of the etch/-
visual inspection of a poor blade leading edge bond is shown in Figure 81.
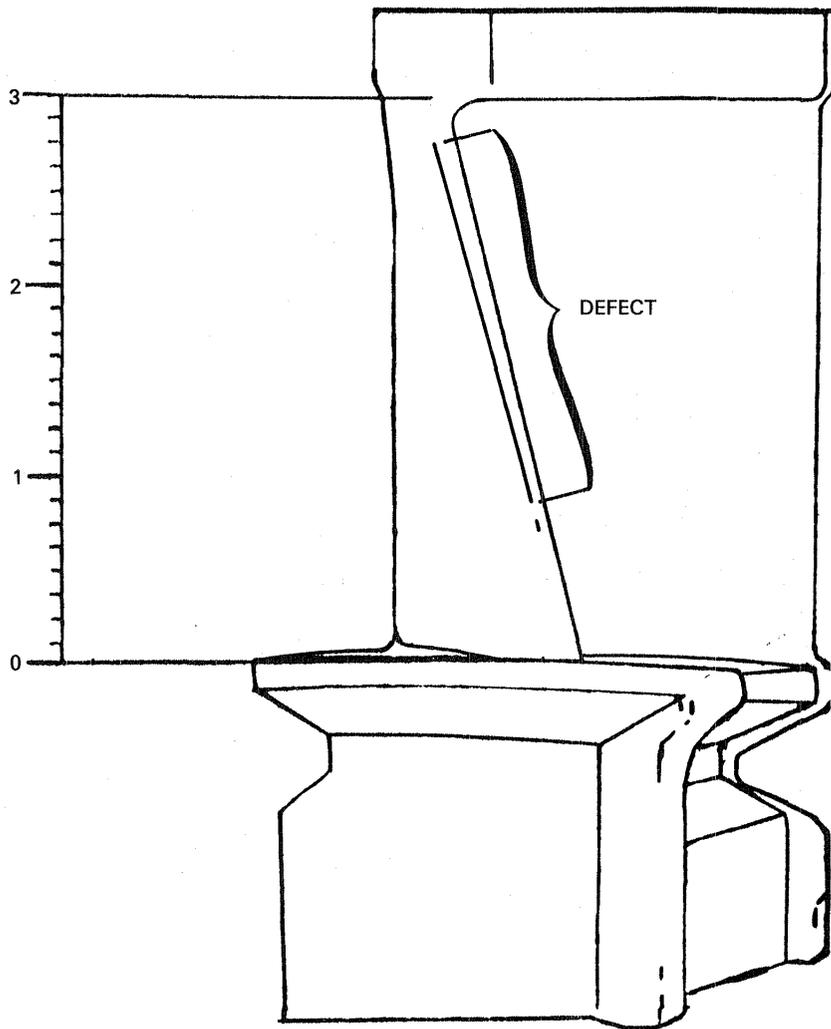
Figure 81   Record of Etch and Visual Inspection of Poor Blade Leading
             Edge Transient Liquid Phase Bond

5.5 Bonding Reproducibility Assessment

After the optimization of the bonding process for both the vane and blade,
additional bonding trials were conducted to verify the reproducibility of
acceptable bonds using the established procedures and tooling. Four blades and
four vanes were bonded as part of this effort, all using the tooling pro-
cedures optimized for each component. Three of each component were sectioned
and evaluated metallographically.

5.5.1 Vane Bond Reproducibility

The results of the vane bonding reproducibility trials are summarized in Figure 82 and Table VI. Fit-up and bond quality were generally good in all three vanes, particularly at the leading edge bond. All bonding defects were fit-up related and were noted in three distinct regions of the vane: (1) the leading edge outer buttress, (2) the trailing edge pedestals, and (3) the trailing edge inner buttress below the second rib. All vanes exhibited some degree of chordwise mismatch at the bond plane interface as discussed previously.

LEADING EDGE OUTER DIAMETER DEFECTS

TRAILING EDGE PEDESTAL DEFECTS

TRAILING EDGE BUTRESS DEFECTS
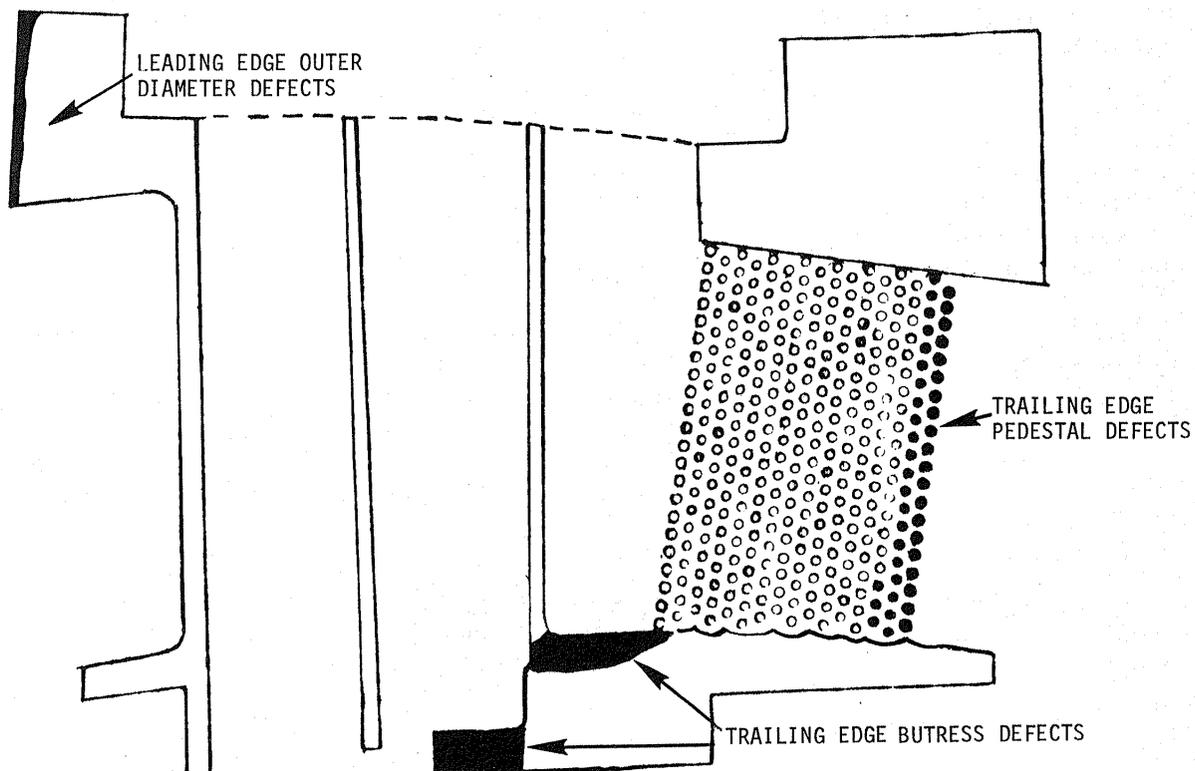
Figure 82   Summary of Energy Efficient Engine Vane Bonding in Reproducibility Trials

Defects in the outer buttress appeared to be outside of the final part dimensions. These were attributable to lack of die contact in that region. Die contact was prohibited by interference with the leading edge flash. This can be readily eliminated by removing the flash completely prior to assembly.

88

TABLE VI
VANE BONDING REPRODUCIBILITY - SUMMARY OF RESULTS
(3 Vanes Evaluated)

	Vane Identification Number		
Defect Location	V-013	V-014	V-015
Leading Edge Outer Buttress	X	-	X
Trailing Edge Pedestals	X	X	X
Inner Buttress	-	X	X

Unbonding of trailing edge pedestals, as observed on all vanes, was generally less severe than had been found using previous fabrication trial hardware. The earlier problem appeared to be a result of poor matching of the airfoil die contour with the vane airfoil surfaces due to midchord bulging of the vane suction side surface. This mismatch was resolved by employing leading edge and trailing edge spacer shims which resulted in consistent leading edge flash loading and reproducible bond quality at the leading edge. The trailing edge shims were not totally successful due to inadequate spacer thickness and inconsistent positioning. Better control of airfoil contour both in the vane and bond tooling should resolve this problem.

Defects in the inner buttress just beyond the second rib are not full unbond defects, but existed as a line of porosity in the bond as shown in Figure 83. This porosity resulted from marginal fit-up in this region along with a transient liquid phase foil liquidation effect caused by the marginal bond gaps being partially starved for liquid due to a slow response to heat-up in this heavy section. A potential solution to this problem is faster and more uniform overall heat-up to the bonding temperature.

← LINE OF POROSITY
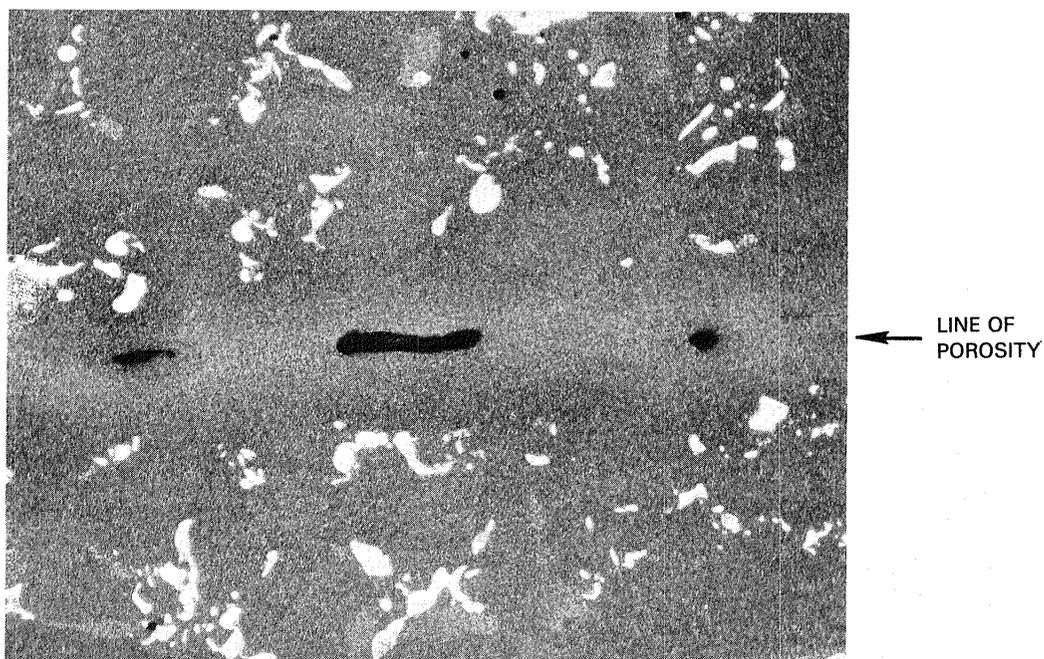
Figure 83   Vane Inner Buttress Bond Showing Porosity

Based on these results and minor processing improvements, bonding yields on the order of 75 percent should be reasonable for the vane. In order to achieve full bonding in the pedestals, improvements are required in the contour fit-up between the airfoil bonding die and the vane airfoil.

5.5.2 Blade Bond Reproducibility

Blade reproducibility results are summarized in Figure 84 and Table VII. Overall blade airfoil bond quality was somewhat inconsistent, particularly at the leading edge bond. This was attributed to bond die-to-blade airfoil contour mismatch along with poor contact at the leading edge flash. In reviewing die contact area results, blade B-027, with full leading edge bonding, indicated good contact over the entire length of the leading edge flash, while the two blades with bond defects showed leading edge flash contact interruptions in the region of the defects. As with the vane, contour conformity between the blade airfoil and bonding die is critical, but in this case, the fit-up was aggravated even more by the extreme camber and twist of the airfoil. In order to achieve more reproducible airfoil bonding, additional methods of improving airfoil bond reproduciblity are required. These include positive positioning of the deformable spacers, calibrated preload of the deformable spacers and improved in-process inspection during assembly.
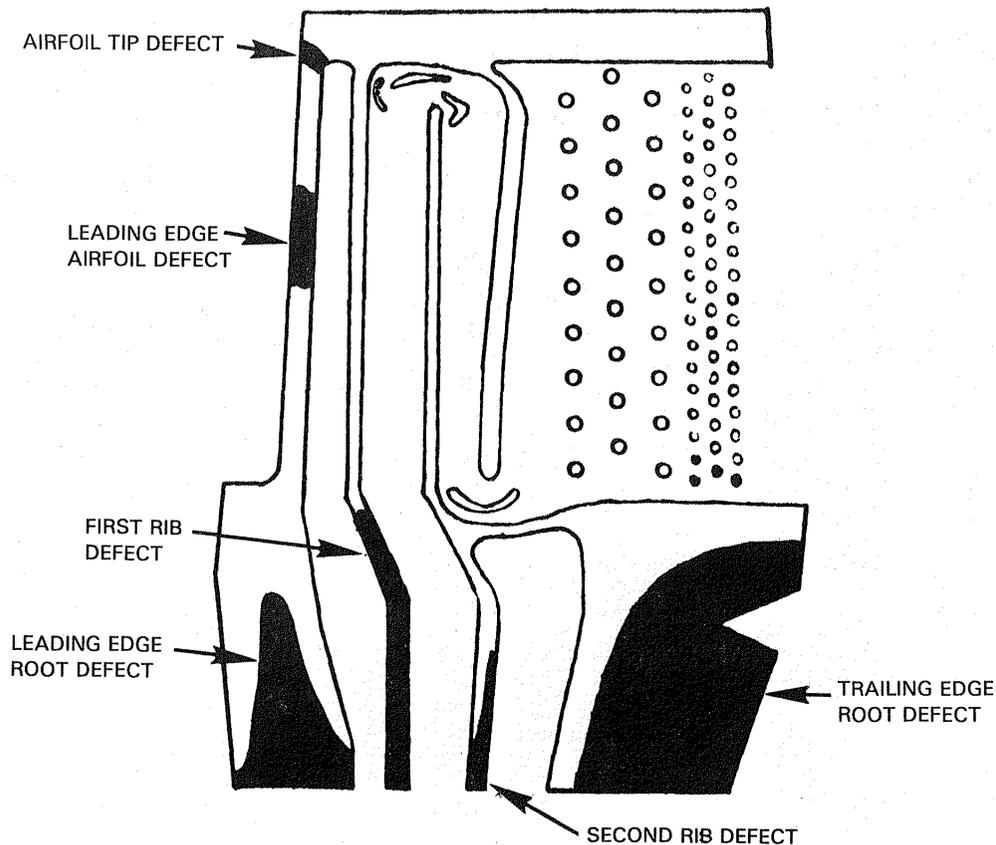
Figure 84   Summary of Energy Efficient Engine Blade Bonding in
             Reproducibility Trials

90

TABLE VII

BLADE BONDING REPRODUCIBILITY - SUMMARY OF RESULTS
(3 blades evaluated)

Defect Location	Blade Identification Number		
	B-027	B-028	B-030
Leading edge - airfoil		X	X
- root	X	X	
Trailing edge - root	X	X	X
1st Rib - airfoil			X
- root	X	X	X
2nd Rib - root		X	
Airfoil - tip			X

The same problems occurred with the blade root as has occurred during the feasibility fabrication trials. Unbonded areas in all three blades were noted in both the leading edge and trailing edge joint extremities and in the first rib. One blade also indicated some unbonded areas on the root end of the second rib. All of these defects were bond fit-up related.

Based on these observations, blade airfoil bonding yields will be low, about 30 percent, at the existing state of bonding process refinement. In order to achieve more reproducible airfoil bonding, additional methods of improving airfoil bond reproducibility will be required, such as, positive positioning of the deformable spacers, calibrated preload of the deformable spacers, and improved in-process inspection during assembly. Modifications to improve root bond quality might include reduced camber and lower mass in the root section as well as local bond surface matching by electro-discharge machining. The program was terminated before these modifications could be effected.

5.6 Bonding Results and Conclusions

During the bonding phase of this effort, bonding feasibility was demonstrated and bonding yields of 75 percent were shown to be reasonable for the vane, and yields of 30 percent for the blade at the existing state of bonding process refinement. Methods for improving on these yield percentages were identified. A bond process was established for PWA 1480 single crystal material which incorporated a transient liquid phase (TLP®) interlayer, 1232°C (2250°F) bond temperature, and full heat treatment after bonding. Bond properties (i.e., stress-rupture, isothermal low cycle fatigue equivalent to parent metal) were substantiated and bond sensitivity to crystallographic misorientation was determined. Bond tooling die materials compatible with casting materials were identified and an advanced differential thermal expansion tooling concept utilizing multi-directional loading was incorporated into the process. During the bonding effort, several significant problems were addressed and corrected. These are summarized in Tables VIII, IX and X according to the steps in the process where they occurred.

91

TABLE VIII

PRE-BOND HANDLING AND CLEANING

Problems	Corrective Action
o Surface recrystallization after pre-bond handling processes	o Controlled operations and anodic etch cleaning preclude recrystallization
o Bond surface contamination after post-cast processing	o Two-cycle alkali clean/anodic etch sequence established
o Incomplete cleaning of bond area - microstructural defects	o 275 kPa (40 psi) alumina blast pre-treatment
o Surface smut during anodic etch clean	o Water blast included in operation
o Flash interference with bonding dies	o Selective leading edge flash removal
o Recrystallization at flash	o Flash bend limits controlled
o Positive metal on bond surface due to strongback defects	o Mechanical blending on bond surface only, prior to cleaning
o Incomplete die contact on blade root and vane platforms due to casting shrinkage	o Grinding methods established - not required

TABLE IX

BOND ASSEMBLY

Problems	Corrective Action
o Improper fit of vane foil preform	o Shrinkage factor corrected
o Improper fit of blade foil preform due to compound curve	o Iterative hand fitting preform design and specific lay-on sequence to assure proper fit
o Inconsistent foil preform tack welds	o Weld parameters and contact locations established to preclude weld effect after bond
o Cracking of yoke during assembly	o Reduced assembly pre-load
o Inconsistent bond fit-up	o Specific bond tooling assembly sequence identified

TABLE X

BOND TRIALS

Problems	Corrective Action

Vane

o Incomplete platform bond cover-
   age and poor microstructural
   quality

o a) Proper location of deform-
      able spacers
   b) DA-25 deformable spacers

o Incomplete airfoil bond

o DA-25 airfoil dies and deformable
   spacers

o Poor trailing edge pedestal
   bonding (poor airfoil die
   contour fit-up)

o Adjust assembly sequence

o Rib and pedestal mismatch

o Change casting tooling

Blade

o Incomplete airfoil bond coverage
   and poor microstructural

o a) Tooling modification
      - load parallel to ribs
      - load leading edge flash
   b) Tooling materials selected
      - DA-25 airfoil dies
      - DA-25 deformable spacers

o Poor trailing edge pedestal
   bonding

o Implement multi-directional
   loading die

o Incomplete platform bond
   coverage

o Multi-directional root dies
   extended to platform

o Incomplete tip bonding

o Casting warpage corrected

o Interference of 3rd rib
   (tip end)

o Strongback tool problem
   identified

o Incomplete root bond

o a) Multi-directional die load
   b) DA-25 dies and deformable
      spacers
   c) Casting modification
   d) Selective bond plane rework

6.0 MATERIALS EVALUATION

6.1 Overview

As part of the overall fabrication development program, mechanical properties testing was conducted on cast Energy Efficient Engine vanes and blades to verify the PWA 1480 material properties cast in the Energy Efficient Engine geometry. Specimens were machined from solid (no strongback) vane and blade castings and tensile and creep-rupture tested at PWA 1480 specification conditions and key design conditions. Prior to machining the specimens, the vane and blade castings received the full PWA 1480 heat treatments according to standard Pratt & Whitney Aircraft heat treating practices. These included solution heat treatment (1287°C (2350°F)/4 hours), a simulated coating diffusion cycle (1079°C (1975°F)/4 hours), and material aging heat treatment (904°C (1660°F)/32 hours).

6.2 Test Procedures

Tensile and creep-rupture specimens were machined from the vanes and blades in two specific orientations: (1) longitudinal, or in the growth direction, and (2) transverse, or perpendicular to the growth axis. Slugs were electro-discharge machined from the component; these slugs were then electro-chemically ground to meet the specimen requirements. The tensile and creep-rupture specimens used are similar to those shown in Figures 85 and 86, respectively.

L ref	Gs	Dg	D thd.
4.597 cm (1.810 in)	2.870 cm (1.130 in) 2.971 cm (1.170 in)	0.314 cm (0.124 in) 0.317 cm (0.125 in)	0.635 cm (0.250 in) - 28 UNS
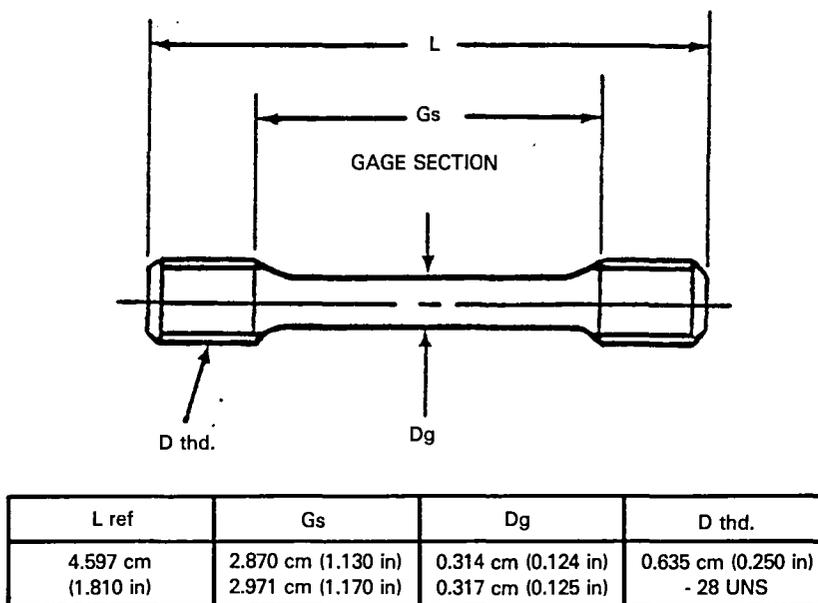
Figure 85   Standard Smooth Round Tensile and Stress Rupture Specimen

L ref	GI	Ds	Dg	Dthd
5.003 cm	1.016 cm	0.449 cm	0.254 cm	0.482 cm
(1.970 in)	(0.400 in)	(0.177 in)	(0.100 in)	(0.190 in) - 32N5
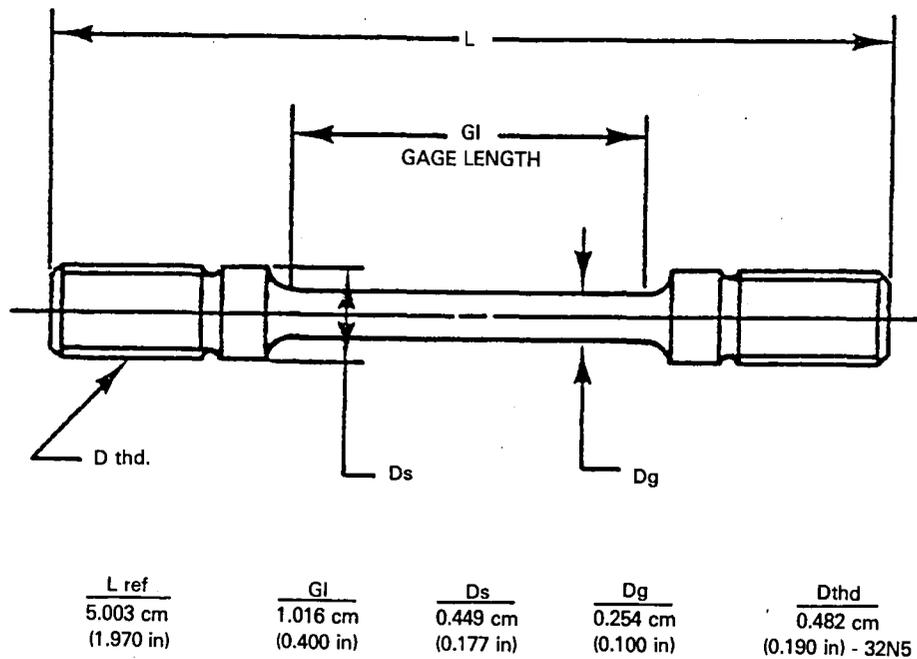
Figure 86   Standard Smooth Round Creep Specimen

Tensile tests were performed at 593°C (1100°F) and 704°C (1300°F). Creep-rupture tests were conducted under five sets of conditions ranging from 760°C (1400°F)/896 kPa (130 ksi) to 1176°C (2150°F)/82 kPa (12 ksi) in accordance with the ASTM standard E-139. Results from this testing were then evaluated and compared to specification requirements and available design data for the alloy.

The crystallographic orientation was determined on all specimens after testing. One end of the specimen was electro-chemically polished and a back reflection Laue pattern was taken from which the crystallographic orientation was determined.

6.3   Results and Conclusions

The tensile and stress-rupture data generated on specimens machined from solid cast components is tabulated in Table XI and XII, respectively. Crystallographic orientation data are also included.

Blade longitudinal tensile properties exceeded the 593°C (1100°F) PWA 1480 specification 0.2 percent yield strength requirements. However, the ultimate tensile strength in one instance was lower than the requirement. This parti-cular specimen was machined from blade No. 3 and found to be misoriented 10° from the <001> crystallographic orientation, which may account for this debit. The remaining tensile test specimens were machined from blades No. 1 and 2 and tested at 704°C (1300°F). The axes of the specimens were oriented closer to the <001> direction (6.0° - 6.5°) and results exceeded both 0.2 percent yield strength and ultimate tensile strength design minimum levels.

TABLE XI
ENERGY EFFICIENT ENGINE BLADE AND VANE TENSILE PROPERTIES

Condition	Component ID No.	Crystallo-graphic Orientation[1]	Test Temperature °C (°F)	UTS kPa (ksi)	0.2% YS kPa (ksi)	% Elongation
Blade Airfoil (Longitudinal)	1	6.0	704 (1300)	1,332 (193.3)	1,195 (173.4)	4.5
	2	6.5	704 (1300)	1,302 (188.9)	1,202 (174.4)	1.2
	3	10.0	593 (1100)	1,094 (158.7)	1,050 (152.4)	4.2
Vane Buttress (Transverse)	1	8.5	704 (1300)	1,182 (171.5)	1,123 (163.0)	1.4
	1	15.5	704 (1300)	1,203 (174.5)	1,134 (164.5)	2.6
Vane Airfoil (Longitudinal)	1	5.0	704 (1300)	1,346 (195.3)	1,288 (186.9)	5.8
	1	6.5	704 (1300)	1,359 (197.2)	1,276 (185.2)	6.1
	2	31.5	593 (1100)	1,010 (146.6)	976 (141.7)	1.8
Test Goals (min.)		≤10.0	593 (1100)	1,089 (158.0)	965 (140.0)	2.0

[1] Listed as degrees between specimen axis and <001> crystallographic direction

96

TABLE XII
ENERGY EFFICIENT ENGINE BLADE AND VANE CREEP-RUPTURE PROPERTIES

Condition	Compo-nent ID No.	Crystallo-graphic Orientation*	Condition (1) 760°C [1400°F] 896 kPa [130 ksi]	Condition (2) 954°C [1750°F] 303 kPa [44 ksi]	Condition (3) 982°C [1800°F] 248 kPa [36 ksi]	Condition (4) 1,093°C [2000°F] 137 kPa [20 ksi]	Condition (5) 1,176°C [2150°F] 68 kPa [10 ksi]
				Time to Rupture, Hours (% Elongation)			
Blade Airfoil	1	NA	24.6[7.6]				
(Longitudinal)	1	4.0		88.3[32]			
	1	2.0				46.8[33.7]	
	3	11.5			87.1[33.1]		
Vane Airfoil	1	4.5	26.5[11.3]				
(Longitudinal)	1	4.0		28.8[30.2]			
	1	5.5					5.6[26.1]
	1	5.0	5.3[11.0]				
	2	5.0	8.3[10.7]				
	2	20.0		23.5[6.6]			
	2	3.0			61.3[18.1]		
	2	45.0		25.7[NA]			
Vane Buttress	1	16.5	Ruptured on Loading				
(Transverse)	1	19.0	0.1(-)				
	2	NA	Ruptured on Loading				
Test goals (min.)		≤10.0			40.0[2.0]		

(NA)   not available

(*)   Listed as degrees between specimen axis and <001> crystallographic
       direction

97

The 982°C (1800°F) blade longitudinal creep-rupture properties exceeded the specification requirement even though the specimen machined from blade No. 3 was misoriented 11.5° from the <001> direction. All other machined from blade specimen tests showed acceptable values at 760°C (1400°F) 954°C (1750°F) and 1093°C (2000°F) and were consistent with previous data generated at Pratt & Whitney Aircraft.

Vane longitudinal tensile properties for the specimen machined from Vane No. 2 did not satisfy specification 593°C (1100°F) tensile requirements. Subsequent Laue x-ray analysis showed the specimen to be misoriented 31° from the <001> crystallographic direction, accounting for the property debit. The value, however, is comparable to previous Pratt & Whitney Aircraft data generated on specimens similarily misoriented from the <001> direction. As with the blade, tests conducted at 704°C (1300°F) using specimens with less misorientation exceeded design minimum values.

The 982°C (1800°F) vane longitudinal creep-rupture properties exceeded the PWA 1480 specifications requirements. The specimen from vane No. 2 was properly oriented with respect to the <001> direction. All of the vane stress-rupture lives were lower than typical PWA 1480 data at all test conditions, but are expected to improve with improved casting quality.

7.0 CONCLUSIONS

o   Single crystal casting and bonding feasibility was successfully demonstrated for both the blade and vane configurations.

o   Seeded single crystal casting of complex shaped hardware was demonstrated for both the blade and vane airfoil designs.

o   A suitable TLP® bond process, tooling system, and processing sequence was identified and demonstrated for both the vane and blade.

o   Several casting and bond process modifications were identified capable of significantly improving bonding yields.

o   Vane and blade tensile properties met or exceeded design minimum levels with proper crystallographic orientation.

REFERENCES

1. Giamei, A. F. and Brody, H. D., "Effect of Hafnium Additions on the Solidification Behavior of Directionally Solidified Superalloys", Interim Technical Report, Contract F33615-75-C-5204, August 1976.

2. Cullity, B. D., Elements of X-Ray Diffraction, Addison-Wesley Publishing Company, Inc. Reading, Massachusetts, 1959

LIST OF SYMBOLS

A	annulus, area, cm^2 in^2
Cx	axial flow velocity, m/sec.
G/R	ratio of casting furnace hot zone temperature gradient to the withdrawl rate of the filled mold from the casting furnace
h/t	ratio of height to thickness
N	mechanical speed, RPM
ppm	parts per million
<001>	primary crystalline orientation in the cubic system (radial)
<110>	desired chordwise crystalline orientation in the cubic system
<100>, <010>	secondary crystalline orientations in the cubic system
α	rate of thermal expansion
γ'	material phase

GOVERNMENT AGENCIES

NASA Headquarters
600 Independence Ave., SW
Washington, D.C. 20546
Attention: RTP-6/R.S. Colladay
        RRP-6/J. Facey
        Library

NASA-Lewis Research Center
21000 Brookpark Road
Cleveland, OH 44135
Attention: D. L. Nored   MS 301-2
        C. C. Ciepluch   MS 301-4 (20 copies)
        J. W. Schaefer   MS 301-4
        G. K. Sievers   MS 301-2
        Library   MS 60-3 (2 copies)
        Report Control Office MS 5-5
        Tech Utilization Office MS 3-19
        M. A. Beheim   MS 3-5
        M. J. Hartmann   MS 5-3
        R. A. Rudey   MS 60-4
        R. A. Weber   MS 500-127
        N. T. Saunders   MS 49-1
        T. P. Moffitt   MS 77-2
        J. E. Rohde   MS 77--2
        R. Purgert   MS 500-305
        R. L. Davies   MS 106-1
        R. H. Johns   MS 49-6
        J. O. VanVleet   MS 86-2
        R. L. Dreshfield   MS 105-1
        AFSC Liaison Office   MS 501-3
        Army R&T Propulsion Lab MS 302-2

NASA Ames Research Center
Moffett Field, CA 94035
Attention: 202-7/M. H. Waters
          202-7/L. J. Williams
          Library

NASA Langley Research Center
Langley Field, VA 23365
Attention: R. Leonard
          D. Maiden
          Library

NASA Dryden Flight Research Center
P.O. Box 273
Edwards, CA 93523
Attention: J. A. Albers
          Library

NASA Scientific and Technical Information
     Facility   P.O. Box 8757
B.W.I. Airport, MD 21240
Attention: Acquisition Branch (10 copies)

Department of Defense
Washington, D.C. 20301
Attention: R. Standahar 3D1089 Pentagon

Wright-Patterson Air Force Base
Dayton, Ohio 45433
Attention: APL Chief Scientist AFWAL/PS

Wright-Patterson Air Force Base
Dayton, Ohio 45433
Attention: E.E. Abell ASD/YZE

Wright-Patterson Air Force Base
Dayton, Ohio 45433
Attention: H.I. Bush AFWAL/POT

Wright-Patterson Air Force Base
Dayton, Ohio 45433
Attention: E.E. Bailey (NASA Liaison)
                    AFWAL/NASA

Wright-Patterson Air Force Base
Dayton, Ohio 45433
Attention: R.P. Carmichael ASD/XRHI

Wright-Patterson Air Force Base
Dayton, Ohio 45433
Attention: R. Ellis ASD/YZN

Wright-Patterson Air Force Base
Dayton, Ohio 45433
Attention: W.H. Austin, Jr. ASD/ENF

Eustis Directorate
U.S. Army Air Mobility
R&D Laboratory
Fort Eustis, VA 23604
Attention: J. Lane, SAVDL-EU-Tapp

Navy Department
Naval Air Systems Command
Washington, D. C. 20361
Attention: W. Koven AIR-03E

Navy Department
Naval Air Systems Command
Washington, D. C. 20361
Attention: J.L. Byers AIR-53602

Navy Department
Naval Air Systems Command
Washington, D. C. 20361
Attention: E.A. Lichtman AIR-330E

Navy Department
Naval Air Systems Command
Washington, D. C. 20361
Attention: G. Derderian AIR-5362C

NAVAL AIR Propulsion Test Center
Trenton, NJ 08628
Attention: J. J. Curry
          A. A. Martino

U.S. Naval Air Test Center
Code SY-53
Patuxent River, MD 20670
Attention: E. A. Lynch

USAVRAD Command
PO Box 209
St. Louis, MO 63166
Attention: Ropbert M. Titus (ASTIO)

Department of Transportation
NASA/DOT Joint Office of Noise Abatement
Washington, D.C. 20590
Attention: C. Foster

Federal Aviation Administration
Noise Abatement Division
Washington, D.C. 20590
Attention: E. Sellman AEE-120

Environmental Protection Agency
1835 K Street, NW
Washington, D.C. 20460
Attention: J. Schettino
           J. Tyler

Environmental Protection Agency
2565 Plymouth Road
Ann Arbor, MI 48105
Attention: R. Munt

Federal Aviation Administration
12 New England Executive Park
Burlington, MA 18083
Attention: Jack A. Sain, ANE-200

ENGINE MANUFACTURERS

Curtiss Wright Corporation
Woodridge, NJ 07075
Attention: S. Lombardo
           S. Moskowitz

Detroit Diesel Allison Div. G.M.C.
P.O. Box 894
Indianapolis, IN 46206
Attention: W. L. McIntire

Cummins Engine Co.
Technical Center
500 S. Poplar
Columbus, IN 47201
Attention: J. R. Drake

AVCO/Lycoming
550 S. Main Street
Stratford, CT 06497
Attention: H. Moellmann

Detroit Diesel Allison Div. G.M.C.
333 West First Street
Dayton, Ohio 45402
Attention: F. H. Walters

The Garrett Corporation
AIResearch Manufacturing Co.
Torrance, CA 90509
Attention: F. E. Faulkner

The Garrettt Corportion
AIResearch Manufacturing Co.
402 S. 36 Street
Phoenix, AZ 85034
Attention: F. B. Wallace

General Electric Co./AEG
One Jimson Road
Evendale, Ohio 45215
Attention: T. Hampton (3 copies)
           T. F. Donohue

Pratt & Whitney Aircraft Group/UTC
Government Products Division
P.O. Box 2691
West Palm Beach, Fl 33402
Attention: B. A. Jones

The Garrettt Corportion
AIResearch Aviation Co.
19201 Susana Road
Compton, CA 90221
Attention: N. J. Palmer

AIResearch Manufacturing Co.
111 South 34th Street
P.O. Box 5217
Phoenix, AZ 85010
Attention: C. E. Corrigan
           (93-120/503-4F)

Williams Research Co.
2280 W. Maple Road
Walled Lake, MI 48088
Attention: R. VanNimwegen
           R. Horn

Teledyne CAE, Turbine Engines
1330 Laskey Road
Tolendo, Ohio 43612
Attention: W. Q. Wagner

General Electric Co./AEG
1000 Western Ave.
Lynn, MA 01910
Attention: R. E. Neitzel

Pratt & Whitney Aircraft Group/UTC
Commercial Products Division
East Hartford, CT 06108
Attention: W. Gardner
           M. E. Brazier

AIRFRAME MANUFACTURERS

Boeing Commercial Airplane Co.
P.O. Box 3707
Seattle, WA 98124
Attention: P. E. Johnson MS 9H-46
           D. C. Nordstrom MS 73-01

Boeing Aerospace Co.
P.O. Box 3999
Seattle, Wa 98124
Attention: D. S. Miller MS 40-26
           H. Higgins

The Boeing Co., Wichita Division
Wichita, KS 67210
Attention: D. Tarkelson

Douglas Aircraft Company
McDonnell Douglas Corp.
3855 Lakewood Boulevard
Long Beach, CA 90846
Attention: R. T. Kawai Code 36-41
           M. Klotzsche

Lockheed California Co.
Burbank, CA 91502
Attention: J. F. Stroud, Dept. 75-42
           R. Tullis, Dept. 75-21
           J. I. Benson

General Dynamics Convair
P. O. Box 80847
San Diego, CA 92138
Attention: S. Campbell, MZ 632-00

Rockwell International
International Airport
Los Angeles Division
Los Angeles, CA 90009
Attention: A. W. Martin

Gates Learjet Corp.
P. O. Box 7707
Wichita, KS 67277
Attention: E. Schiller

McDonnell Aircraft Co.
McDonnell Douglas Corp.
P. O. Box 516
St. Louis, MO 63166
Attention: F. C. Claser Dept. 243

Lockheed Georgia Co.
Marietta, GA 30060
Attention: H. S. Sweet

Grumman Aerospace Corp.
South Oyster Bay Road
Bethpage, New York 11714
Attention: C. Hoeltzer

Airlines

American Airlines
Maint. & Engr. Center
Tulsa, OK 74151
Attention: W. R. Neeley

Eastern Airlines
International Airport
Miami, FL 33148
Attention: A. E. Fishbein

Delta Airlines, Inc.
Hartsfield-Atlanta International Airport
Atlanta, GA 30320
Attention: C. C. Davis

TransWorld Airlines
605 Third Avenue
New York, NY 10016
Attention: A. E. Carrol

Pan American World Airways, Inc.
JFK International Airport
Jamica, NY 11430
Attention: J. G. Borger
        A. MacLarty

United Airlines
San Francisco International Airport
Maint. Operations Center
San Francisco, CA 94128
Attention: J. J. Overton

Others

Hamilton Standard
Bradley Field
Windsor Locks, CT 06096
Attention: P. J. Dumais, MS 1A-3-1
        A. T. Reiff, MS 1-2-2

FluiDyne Engineering Corp.
5900 Olson Memorial Highway
Minneapolis, MN 55422
Attention: J. S. Holdhusen

Rohr Corporation
P.O. Box 878
Foot & H Street
Chula Vista, CA 92012
Attention: Library

Solar Division
International Harvester
2200 Pacific Highway
San Diego, CA 92112
Attention: Library

Gas Dynamics Laboratories
Aerospace Engineering Building
University of Michigan
Ann Arbor, MI 48109
Attention: Dr. C. W. Kaufmann

Massachusetts Inst. of Technology
Dept. of Astronautics & Aeronautics
Cambridge, MA 02139
Attention: Jack Kerrebrock

Massachusetts Inst. of Technology
Dept. of Structural Mechanics
Cambridege, MA 02139
Attention: James Mar

Westinghouse Electric Corp.
P.O. Box 5837
Beulah Road
Pittsburgh, PA 15236
Attention: Library

University of Tennessee
        Space Institute
Tullahoma, TN 37388
Attention: Dr. V. Smith

TRW Equipment Group
TRW Inc.
23555 Euclid Ave.
Cleveland, OH 44117
Attention: I. Toth

Aerospace Corporation
R & D Center
Los Angeles, CA 90045
Attention: Library

George Shevlin
P.O. Box 1925
Washington, D.C. 20013

Brunswick Corporation
2000 Brunswick Lane
Deland, Fl 32720
Attention: A. Erickson

Pennsylvania State University
Department of Aerospace Engineering
233 Hammond Building
University Park, Pennsylvania 16802
Attention: Dr. B. Lakshminarayana

Iowa State University
Department ;of Mechanical Engineering
Ames, Iowa 50011
Attention: Dr. Patrick Kavanagh

Detroit Diesel Allison
P.O. Box 894
Indianapolos, Indiana 46206
Attention: Mr. Robert Delanie
              Speed Code U29A

Howmet Trubine Components Corporation
Austenal Dover Division
Roy Street
Dover, New Jersey 07801

Attn: Mr. C. Caccavale
       R. E. Miller

Jetshapes, Inc.
Rockleigh Industrial Park
Valvo Drive
Rockleigh, New Jersy 07647

Misco
One Nusco Drive
Whitehall, Michigan   49461

End of Document